NTNU – Trondheim
Norwegian University of
Science and Technology

Optimization of FLNG liquefaction processes

Eirik Rødstøl

Mechanical Engineering
Submission date: June 2015
Supervisor: Jostein Pettersen, EPT

Norwegian University of Science and Technology
Department of Energy and Process Engineering

NTNU
Norwegian University
of Science and Technology

Department of Energy
and Process Engineering

EPT-M-2015-75

MASTER THESIS

for

Student Eirik Rødstøl

Spring 2015

Optimization of FLNG liquefaction processes

Optimalisering av prosesser for naturgasskondensering i FLNG-anlegg

Background and objective

Optimization of the process for natural gas liquefaction will be essential for both the design and operation of floating LNG (FLNG) installations. Various liquefaction processes are being considered as candidates for FLNG, and these generally differ from the well proven processes for base-load onshore gas liquefaction. There is then a need for improved capabilities for design and operational optimization of FLNG liquefaction processes, preferably using built-in functions in "standard" process modelling software.

In the fall 2014 specialization project, various built-in optimizers in Aspentech HYSYS were tested and evaluated for relatively simple FLNG processes based on gas expansion and single mixed refrigerant (SMR). A conclusion from this work was that the "Hyprotech SQP" optimizer offered the by far best performance and capabilities. Further work should then focus on more advanced and realistic process configurations, as well as more challenging conditions in terms of setting initial values, variable boundaries, constraints and tolerances. The selection of variables for optimization also needs further exploration. A Dual Mixed Refrigerant (DMR) process is currently an attractive and realistic option for FLNG, with quite some challenges regarding optimization. The optimization can be focused on design aspects, but operational optimization scenarios are also quite relevant. Models for heat exchangers, compressors, drivers and utility systems can be varied in complexity depending on the direction of results.

The objective of this Master thesis will be to further explore the capabilities of the Hyprotech SQP optimizer for FLNG process optimization, using more advanced liquefaction process models as a basis, e.g. DMR and/or SMR. The evaluation need to identify issues, limitations, any remedial actions and provide an assessment of the potential of using the built-in function for design and/or operational optimization.

The following tasks are to be considered:

1. Review and summary of results from the Specialization Project and review of other relevant input and updated basis information.

2. Establishment of updated process model(s) and a good basis for optimization studies and testing, focusing on DMR and SMR processes and relevant scenarios/cases and principles for testing.

3. Optimizer testing, including exploration of capabilities, limitations and issues that are discovered during the work.

4. Analysis and review of results and experience, and presentation of results in a report with complete, understandable, reproducible and relevant information from the testing and case studies.

5. Conclusions and recommendations regarding use of the built-in Hyprotech SQP optimizer for FLNG processes.

-- " --

Within 14 days of receiving the written text on the master thesis, the candidate shall submit a research plan for his project to the department.

When the thesis is evaluated, emphasis is put on processing of the results, and that they are presented in tabular and/or graphic form in a clear manner, and that they are analyzed carefully.

The thesis should be formulated as a research report with summary both in English and Norwegian, conclusion, literature references, table of contents etc. During the preparation of the text, the candidate should make an effort to produce a well-structured and easily readable report. In order to ease the evaluation of the thesis, it is important that the cross-references are correct. In the making of the report, strong emphasis should be placed on both a thorough discussion of the results and an orderly presentation.

The candidate is requested to initiate and keep close contact with his/her academic supervisor(s) throughout the working period. The candidate must follow the rules and regulations of NTNU as well as passive directions given by the Department of Energy and Process Engineering.

Risk assessment of the candidate's work shall be carried out according to the department's procedures. The risk assessment must be documented and included as part of the final report. Events related to the candidate's work adversely affecting the health, safety or security, must be documented and included as part of the final report. If the documentation on risk assessment represents a large number of pages, the full version is to be submitted electronically to the supervisor and an excerpt is included in the report.

Pursuant to "Regulations concerning the supplementary provisions to the technology study program/Master of Science" at NTNU §20, the Department reserves the permission to utilize all the results and data for teaching and research purposes as well as in future publications.

The final report is to be submitted digitally in DAIM. An executive summary of the thesis including title, student's name, supervisor's name, year, department name, and NTNU's logo and name, shall be submitted to the department as a separate pdf file. Based on an agreement with the supervisor, the final report and other material and documents may be given to the supervisor in digital format.

☐ Work to be done in lab (Water power lab, Fluids engineering lab, Thermal engineering lab)
☐ Field work

Department of Energy and Process Engineering, 14. January 2015

Olav Bolland
Department Head

Jostein Pettersen
Academic Supervisor

Preface

This master thesis has been written at the Department of Energy and Process Engineering, Norwegian University of Science and Technology (NTNU) during the fall 2015, and completes the final semester in the master program of mechanical engineering.

First, I would like to thank my supervisor Jostein Pettersen at Statoil ASA for his dedicated support through frequent meetings and by being available at all time through email. His assistance through this project is greatly appreciated.

Second, I would like to thank the following:
Lorenz T. Biegler for personally providing me with information in regards to optimization, Nontas Voutsas for discussions concerning optimization and equations of state, Donghoi Kim and Bjørn Austbø for great discussions regarding optimization.

Finally, I would like to thank my friends that have supported me through these incredible years of study.

Trondheim, 10th June, 2015

Eirik Rødstøl

Summary

As the development of FLNG is on the rise, improvements in liquefaction process design and operation is of high priority. The liquefaction processes utilized for FLNG vary in complexity and efficiency. Space requirement and efficiency are high priorities for FLNG and mixed refrigerant processes such as Prico and DMR are suitable processes. In order to improve the liquefaction processes in terms of energy use, many factors needs to be considered and the task can be challenging. A specialization project carried out in the fall of 2014 (Rødstøl 2014) concluded that amongst the built-in optimizers in Hysys, the Hyprotech SQP optimizer is the most suitable optimizer when dealing with advanced liquefaction processes. The purpose of this thesis is to explore the Hyprotech SQP optimizer in terms of its applicability to mixed refrigerant liquefaction processes and challenges it may come across.

Prico and DMR liquefaction processes were modelled and described as a base for several case studies that were carried out in order to challenge the optimizer. The optimizer was challenged in regards to process design, process modifications, initial variable values, variable boundaries and constraints. Studies in relation to the different optimizer parameters were carried out in both models with setup recommendations for the parameters. The Prico process was modified in regards to process temperatures, pressure levels, initial variable values, initial variable boundaries and process constraints. The DMR process was modified in regards to three different constraint conditions in the Warm Mixed Refrigerant (WMR) circuit that was used to investigate whether the optimizer provided logical decisions to uphold the given constraints. Additionally, the DMR process was optimized in regards to different pressure levels, process constraints and process temperatures.
The final case study was carried out in order to improve an earlier optimized DMR process in regards of energy usage. As the study progressed, more and more constraints were put on the process to make the optimization more challenging.

The studies in the modelled Prico and DMR process showed that the optimizer was able to adapt to process modifications by small adjustments in either the Flowsheet, derivative utility or the optimizer parameters, which were carried out in terms of analyses. As different process modifications were carried out, the optimizer provided logical decisions in regards to the refrigerant composition and pressure levels.

In the final study, the optimizer improved an earlier optimized DMR process provided by Kusmaya (2012). The improvements were carried out with the process being constrained further as the study progressed. The Hyprotech SQP optimizer was able to reduce the energy consumption by 17%, and by utilizing same compressor drivers as Kusmaya (2012); the optimizer was able to provide a model that had 17% higher LNG production.

Results from the studies show that the Hyprotech SQP optimizer may be challenging to adjust, and simplifications in the Flowsheet may be carried out in order to assist the optimizer. By adjusting the derivative and the optimizer parameters, the Hyprotech SQP optimizer is able to provide good objective values that upholds the given constraints.

Sammendrag

Utviklingen av FLNG er på vei framover, og i den sammenheng har forbedring av prosessdesign og drift fått en høy prioritet. Ved FLNG benytter man seg av flytendegjøringsprosesser som varierer både i kompleksitet og effektivitet. Det er særskilt plassbehovet og effektiviteten som er essensielt, noe som gjør det aktuelt å benytte seg av kjøleprosessene Prico og DMR. For å forbedre energibruken av flytendegjøringsprosessene må flere faktorer tas i betraktning, noe som gjør oppgaven mer kompleks.

Prosjektoppgaven (Rødstøl 2014) konkluderte med at blant de innebygde optimaliseringsverktøyene i Hysys, framstod Hyprotech SQP som det meste egnede optimaliseringsverktøyet for å håndtere avanserte kjøleprosesser. Formålet med denne masteroppgaven er å undersøke hvor anvendelig Hyprotech SQP optimaliseringsverktøyet er ved bruk på flytendegjøringsprosesser som benytter seg av blandede kjølemedier, samt overfor de komplikasjoner og utfordringer som kan oppstått i den regi.

I oppgaven ble flytendegjøringsprosessene Prico og DMR modellert og benyttet som grunnlag for videre studier av optimaliseringsverktøyet. Ved å anvende de modellerte prosessene, oppnådde man å utfordre optimaliseringsverktøyet i forhold til prosessdesign, prosessmodifikasjoner, variabel grenser, opprinnelige variabel verdier og pålagte restriksjoner. Utredning av de forskjellige optimaliseringsparameterne ble gjennomført i begge modellene med anbefalt oppsett og justeringer for å oppnå best mulig resultat. Prico-prosessen ble modifisert i henhold til prosesstemperatur, trykknivå, opprinnelige variabelverdier, variabel grenser og pålagte restriksjoner. I den varme kjølemediekretsen i DMR-prosessen ble det gjennomført tre ulike restriksjonsmodifikasjoner, som ble brukt til å kartlegge hvorvidt optimaliseringsverktøyet var i stand til å ta logiske avgjørelser for å oppholde de pålagte restriksjonene. I tillegg ble DMR-prosessen optimalisert i henhold til forskjellige trykknivåer, prosessrestriksjoner og prosesstemperaturer.

Resultatene fra DMR- og Prico-forsøkene viste at optimaliseringsverktøyet var tilbøyelig til prosessmodifikasjoner ved små justeringer som ble utført i enten «*Flowsheet*», «*derivative*» eller optimaliseringsparameterne, justeringene ble utført ved sensitivitetsanalyser. Etter hvert som ulike prosessmodifikasjoner ble utført, klarte optimaliseringsverktøyet å konkludere med logiske beslutninger i henhold til kjølemediekomposisjon og trykknivåer.

Avslutningsvis ble en tidligere optimalisert DMR prosess av Kusmaya (2012) forbedret ved bruk av Hyprotech SQP optimaliseringsverktøyet. Forbedringsprosessen ble stadig mer utfordrende etter hvert som ytterligere begrensninger ble innlagt slik at man stadig stilte høyere krav til optimaliseringen. Hyprotech SQP optimaliseringsverktøyet klarte å redusere energiforbruket med 17 %, og ved å utnytte samme kompressordrivere som Kusmaya (2012) oppnådde optimaliseringsverktøyet å øke produksjonen av LNG med 17 %.

Resultater fra studiene viser at Hyprotech SQP optimaliseringsverktøyet kan være utfordrende å innstille, og at det kan være nødvendig å benytte seg av forenklinger i «*Flowsheet*» for å assistere optimaliseringsverktøyet. Ved å justere «*derivative*» og optimaliseringsparameterne er Hyprotech SQP optimaliseringsverktøyet i stand til å regne ut gode resultater med spesifikasjoner som holdes innenfor de gitte begrensningene.

Table of Contents

List of Figures

List of Tables

Nomenclature

Abbreviations

APCI	Air Products and Chemicals Inc
BAL	Balance function
BFGS	Broyden, Fletcher, Goldfarb and Shanno
CMR	Cold Mixed Refrigerant
DMR	Dual Mixed Refrigerant
DP	Dew Point
FLNG	Floating Liquefied Natural Gas
GT	Gas Turbine
LMTD	Logarithmic Mean Temperature Difference
LPG	Liquefied Petroleum Gas
MR	Mixed Refrigerant
MTPA	Million Ton per Annum
NGL	Natural Gas Liquid
P-F HX	Plate and Fin Heat Exchanger
PR	Peng Robinson
SET	Set function
SMR	Single Mixed Refrigerant
SQP	Sequential Quadratic Programing
SRK	Soave-Redlich-Kwong
SWHE	Spiral Wound Heat Exchanger
WMR	Warm Mixed Refrigerant

Symbols

A	Surface Area
c	Constraints
$\dot{m}$	Mass flow
N_F	Degrees of freedom
N_V	Total Number of Variables involved
N_E	Number of Independent equations
Q	Heat Transfer
U	Heat Transfer Coefficient
$\dot{W}$	Power
x	Adjustable Variables
ϕ	Merit Function
ΔT_{LM}	Logarithmic Mean Temperature Difference

1 Introduction

This Master thesis explores use of optimization within liquefaction process in the LNG production chain, applicable to FLNG units. The optimizer in focus is the Hyprotech SQP optimizer, which is a built-in optimizer in the well-known simulation software: Hysys version 8.3, provided by Aspentech. By optimizing liquefaction processes, is it possible to explore the capabilities and restrictions in the Hyprotech SQP optimizer.

1.1 Motivation

Liquefaction of natural gas has been growing rapidly during the past decades and the liquefaction processes has developed, as new technologies has entered the market. The growth of FLNG production has forced the liquefaction processes to be more compact and efficient as the space requirement is a significant factor at an FLNG unit compared to onshore facilities. Considering the liquefaction process of natural gas is the main expenditure of the process of converting natural gas to LNG and account for 30 – 40% of the total cost (Rangaiah 2009), improvements of these processes are considered of great importance in both an energy and capital saving manner.

1.2 Background

In the fall of 2014, Rødstøl (2014) carried out a specialization project that studied the different optimizers in the well-known simulation program Aspentech Hysys version 8.3. The optimizers in scope were the ones that managed to optimize within non-linear constraints. Two different liquefaction processes were in focus, in which one of them was a SMR process and the other was an expander process. The two processes were:

- PRICO single mixed refrigerant process (SMR) by Black and Veatch
- NICHE dual expander process by CB&I – Randall gas Technology

Among the optimizers that were studied, the Hyprotech SQP optimizer provided best objective values with respect to constraints, and is also recommended by Aspentech as the best optimizer to utilize when optimizing complex process models. Therefore, this thesis focus on further exploration of the Hyprotech SQP optimizer in terms of its capabilities and limitations within process optimization of liquefaction processes relevant to FLNG.

1.3 Objectives

The main objective in this thesis is to further explore the Hyprotech SQP optimizer and gain knowledge in regards to its capabilities, in addition to explore the impact different process modification has on optimization and the process itself.

1.4 Scope

The following tasks were in scope when writing the master thesis:

1. Review and summary of the Specialization project by Rødstøl (2014) and review of other relevant input and updated basis information.
2. Establishment of updated process models and a good basis for optimization studies and testing, focusing on DMR and SMR processes and relevant scenarios/modifications and principles for optimizer setup and testing.
3. Optimizer testing, including exploration of capabilities, limitations and issues that are discovered during work.
4. Analysis and review of results and experience, and presentation of results with complete, understandable, reproducible and relevant information from the testing and case studies.
5. Conclusion and recommendations regarding the use of the built-in Hyprotech SQP optimizer for FLNG processes.

1.5 Thesis structure

This thesis consists of ten chapters including the introduction.

Chapter 2 Process Basis

Contain explanations of the liquefaction processes utilized in the thesis and general theory behind different aspects in regards to the processes.

Chapter 3 Optimization

Contain a study of general optimization and in depth theory in regards to the Hyprotech SQP optimizer.

Chapter 4 Earlier Work

Contain a small literature study in regards of studies that has utilized Hysys optimizers. There is also a summary of the project performed by Rødstøl (2014) of the built-in Hysys optimizers in Aspentech Hysys version 8.3.

Chapter 5 Hysys Process Models and Optimizer Setup

Considers the DMR and Prico process in terms of design and conditions. There are also brief explanations of the variables involved in each process followed up by optimizer configurations.

Chapter 6 Case Study Prico process

Concerns the Prico process and contain a study on how the different optimizer parameters affects the optimization results concerning its ability to converge to a minimum objective value that is upholding the given process constraints. Several different studies in regards to different process modifications such as process temperatures and fixed or adjustable pressure values in regards to objective and UA values.

Chapter 7 Case Study DMR process

Contain a study of the DMR process and similar to Chapter 6, this chapter contain a study on how the different optimizer parameters affects the optimization results concerning the optimizers ability to obtain a minimum objective value that upholds the given constraints. This chapter also contain three modifications in the WMR circuit that are analyzed in order to see if the optimizer is making logical decisions in regards of the Nitrogen component in the WMR circuit. Studies in regards of different process temperatures and fixed or adjustable pressure values in regards to objective and UA values are also considered.

Chapter 8 Improvement of existing Liquefaction Models by Optimization

Contain necessary information in regards to a DMR process optimized by Kusmaya (2012) and modelled in regards of APCI design. The model is improved in regards of several modifications and limitations. The Chapter also contain a comparison between the geometric mean pressure ratio and the pressure ratio optimized by the Hyprotech SQP optimizer.

Chapter 9 Conclusion and Recommendations

Contain findings through the study relevant to the Hyprotech SQP optimizer and recommendations concerning the use of the Hyprotech SQP optimizer.

Chapter 10 Further Work

Provides information concerning further studies in regarding the Hyprotech SQP optimizer.

2 Process Basis

Based on their application to FLNG and potential complexity in regards to optimization, the SMR and DMR processes are good candidates for optimization. The Prico process is the simplest liquefaction process that utilize mixed refrigerant, while the DMR process consists of several units that can influence the efficiency. Depending on the gas composition and LNG requirements, NGL extraction can be integrated in the LNG processes, or take place upstream. Whether the NGL extraction is integrated or not will influence the processes in regards of optimization.

In this thesis, the NGL extraction process itself is not considered, but the influence it has on the natural gas stream in regards of component change throughout the process is considered by utilization of component change in the stream throughout the DMR model.

2.1 Prico Process (SMR)

The Prico process is the simplest kind of the single mixed refrigerant processes. The process utilizes the evaporation principle to cool both the natural gas stream and to condense its own inlet stream tube side, which is in a state between vapor and liquid phase before it enters the plate fin heat exchanger. Compression of the mixed refrigerant can be split into several stages, in the process that can be seen from Figure 1**,** the refrigerant that exits the heat exchanger first is compressed before it enters a cooler and is separated from its liquid and vapor state in a separator. After the separator, the refrigerants pressure is further increased in the second stage, a pump is utilized to increase the pressure of the liquid part, and a compressor is used to increase the pressure of the vapor part. After the second stage, the refrigerant is in 100% vapor state before it enters the second cooler. After the second cooler, the refrigerant is in a mixed state of both liquid and vapor before it is further cooled in the heat exchanger. In some cases, the compression stages consists only of compressors and not a pump. If that is the case, either the composition or the cooling capacity of the intermediate cooler after the first compressor needs to be changed in order to avoid two phase inlet into the second compressor.

Integrated NGL extraction is possible in the Prico process, in case of integrated NGL extraction, the natural gas stream will be cooled to the desired temperature (around -48°C) and extracted before the stream will be further cooled to LNG temperature. However, in this thesis, NGL extraction is not be considered in the Prico process.

The Prico process is suitable for FLNG because of its low complexity and low amount of equipment. In regards of its efficiency, the DMR process is a better option.

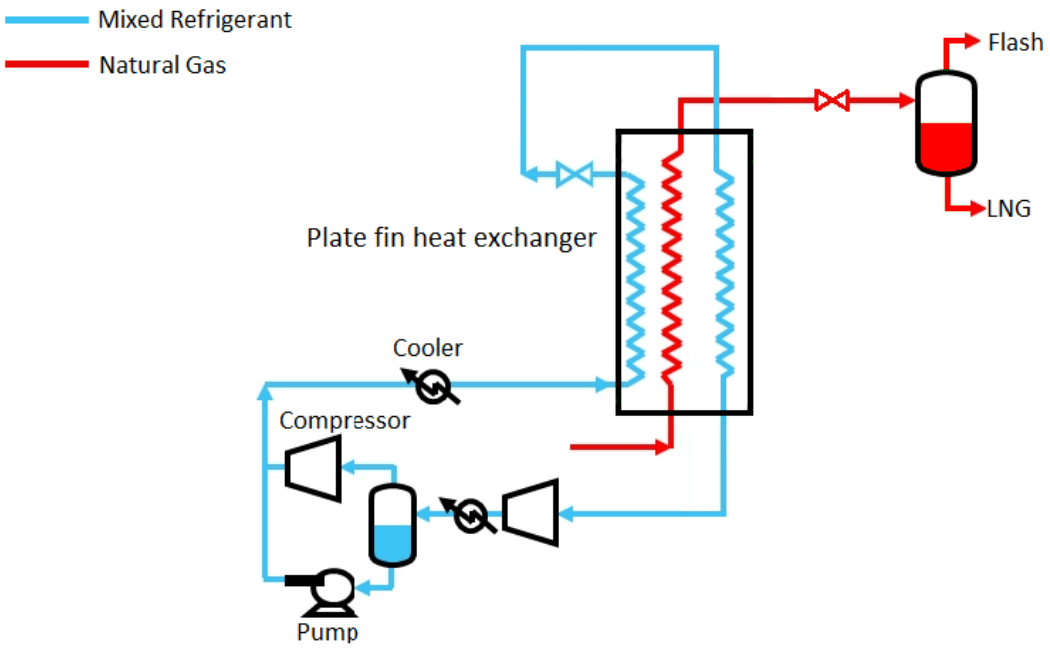

Figure 1: Illustration of a Prico liquefaction process

2.2 DMR Process

It can be seen from Figure 2 that in order to cool the NG stream to the desired temperature, the DMR process utilize two mixed refrigerant (MR) cycles, in which the warm MR is utilized for pre-cooling and the cold MR is used to further cool the natural gas (NG) to its desired temperature before throttling and separation. The warm MR stream pre-cools the warm MR stream in liquid phase, the NG and the cold MR stream in SWHE-1, while the cold MR stream is utilized to further cool the NG stream to its desired temperature.

The warm MR cycle consists of two compressors, one pump, one separator, one JT valve, SWHE-1 and two heat exchangers. The compressors and the pump increases the pressure, the separator separates the vapor from the liquid before the pump and the second compressor, and the coolers are used for intercooling. The JT valve is used to expand the warm MR in order to utilize the evaporation principles that allows it to cool the three streams in SWHE-1.

The cold MR cycle consists of SWHE-1, SWHE-2, compressor arrangements with intercoolers, two valves and one separator. Both valves are utilized to lower the pressure in both the MR-Vapor and MR-Liquid stream before they cool the Natural Gas stream at two different temperature levels.

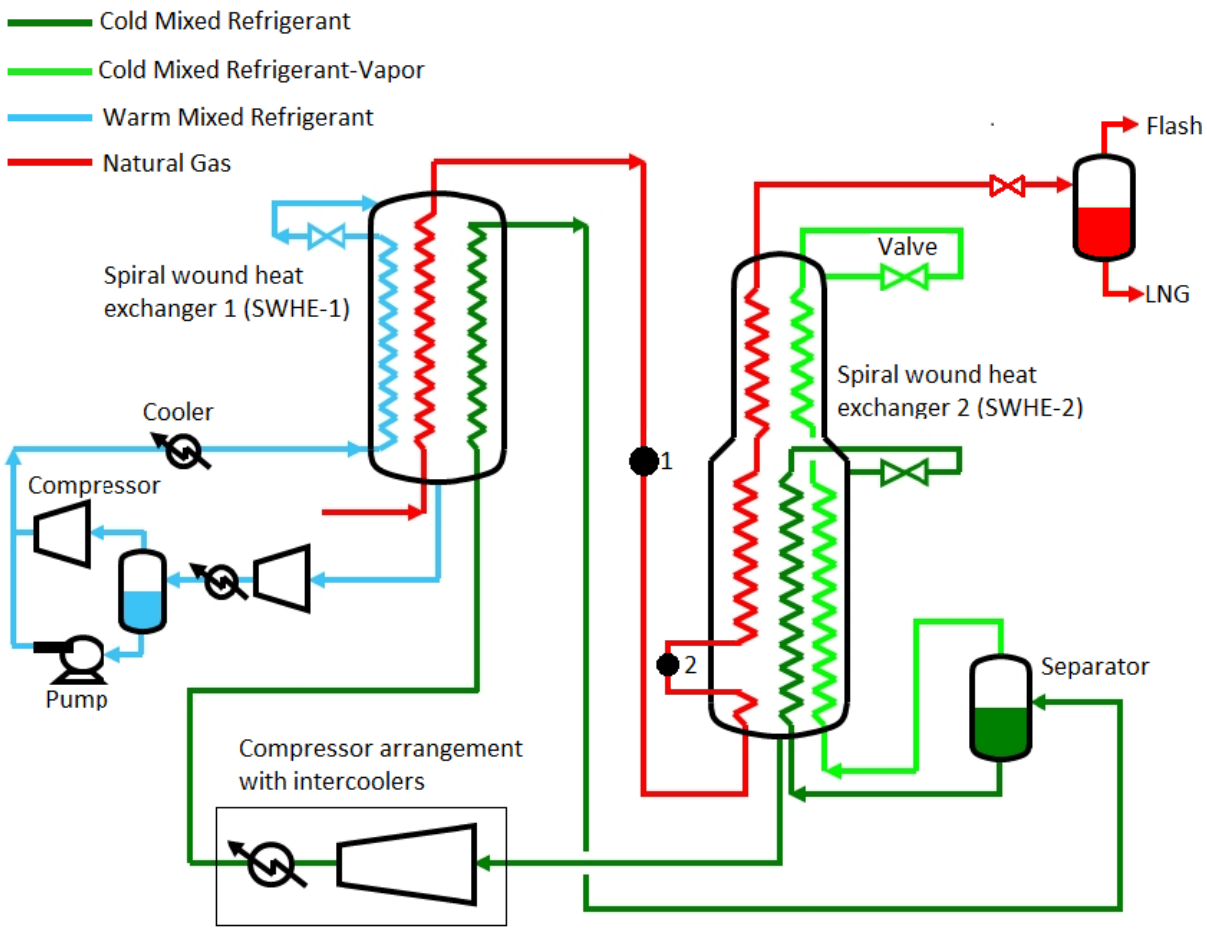

Figure 2: DMR process with numbers that illustrates where integrated NGL extraction would take place according to APCI design (an eventual reflux stream will be necessary if integrated NGL extraction is taking place).

The warm and cold MR circuits consists of different mixtures that are designed to liquefy at different conditions in order to deliver energy to the other streams by using evaporation. The refrigerant properties are determined by the amount of different components. Components relevant for the refrigeration stream have their properties listed in Table 1. The refrigerant composition are affected by the process temperature.

In the case of integrated NGL extraction, a composition change in the natural gas stream will occur at the LPG extraction point (1) between SWHE-1 and SWHE-2 and at the reflux process (2) in the SWHE-2 heat exchanger. The LPG extraction and reflux process will affect the temperature and pressure requirements at each of the two points in order to extract the necessary amount of NGL.

Considering the compressor arrangements with intercoolers in the cold MR circuit, there are both advantages and disadvantages with several compressors and intercoolers. By utilizing multistage compression with intercooling, the theoretical compressor work will be decreased, and it makes possibilities for distribution on several drivers. But at one point, the theoretical advantage with extra compression steps disappears either in pressure loss in the intercooler, regularity losses, maintenance etc.

Table 1: List of components that are utilized in both the Prico and DMR process. The list contain properties that are relevant in order to select a composition for the refrigeration streams (Pettersen 2012) (Aspentech Hysys software v8.3).

Component	Mole weight	Liquid density at std. cond	Normal boiling point	Critical Temperature	Critical Pressure
	[kg/mole]	[kg/m^3]	[°C]	[°C]	[Bar]
Nitrogen	28.01	807.31	-195.80	-146.90	33.94
Methane	16.04	299.70	-161.49	-82.60	46.00
Ethane	30.07	355.68	-88.60	32.28	48.84
Ethylene	28.05	383.23	-103.77	9.20	50.32
Propane	44.10	507.20	-42.07	96.67	42.50
i-Butane	58.12	562.00	-11.73	134.94	36.48
n-Butane	58.12	583.22	-0.50	152.04	37.97
IsoPentane	72.15	623.44	36.07	196.50	33.69

2.3 Mixed refrigerant

Mixed refrigerant processes consists of a multi-component mixture. The objective is to utilize the temperature glide that occurs in the heat exchanger upon evaporation of the refrigerant to match the condensing temperature curve of the natural gas stream in order to reduce exergy losses in the process. An illustration of the temperature glide can be seen in Figure 3.

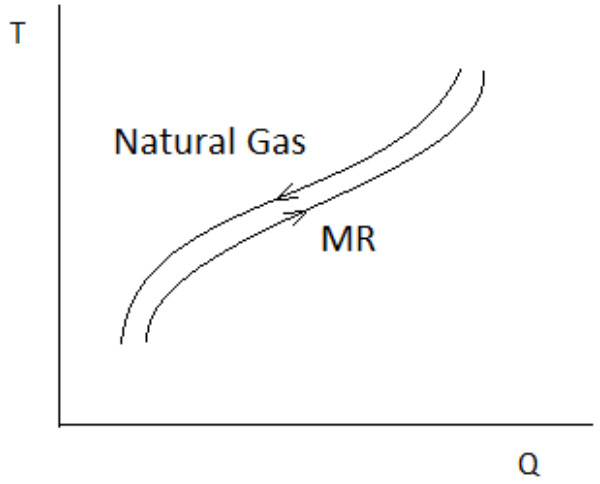

Figure 3: Illustration of temperature glide in an heat exchanger with an inlet natural gas stream and a mixed refrigeratn stream, which cools the natural gas stream.

In order for the temperature glide of the refrigerant to match the temperature glide of the objective stream, the component composition of the stream has to be evaluated according to boiling points, which can be seen from Table 1, and gas constant.

For a DMR process, different refrigerants are utilized for the two refrigeration streams. For the Warm MR, methane, ethylene / ethane, propane, i-butane, n-butane and pentane may be utilized (Bukowski et.al 2011). The main reason that ethylene is utilized instead of ethane is because the normal boiling point of ethane is too far away from the normal boiling point of methane, making it harder to find a good mixture (Pettersen 2012), also, Ethane is expensive and hard to extract, so it is both cheaper and easier to buy ethylene.

The cold refrigeration stream, only the components with boiling points below -40°C is considered because of the low temperature of the NG stream after the first Spiral Wound Heat Exchanger. The Natural Freezing points should also be considered.

Since the Prico process only consists of one refrigeration circuit, components that are able to cool the natural gas stream in its entire range are needed. An overview of the different components in regards to which process that is being utilized can be seen in Table 2.

Table 2: Overview over the refrigerants utilized in the Prico and DMR process.

DMR		Prico
WMR	**CMR**	**MR**
Methane	Nitrogen	Nitrogen
Ethylene / Ethane	Methane	Methane
Propane	Ethylene	Ethylene
n-Butane	Propane	Propane
i-Butane		i-Butane
		n-Butane

2.4 Compressor arrangements

The optimum pressure ratio between the different stages depends on several factors, such as the refrigerant composition, the compressor efficiency, the minimum and maximum pressure etc. This is hard to determine in an optimization process as the inlet temperature to each of the compressor may vary. In this thesis, polytropic efficiency are utilized in all of the compressors. When operating with constant polytropic efficiency, the isentropic efficiency of the compressor will decrease as the pressure ratio increase, which will make the optimal pressure ratio shift closer to the geometric mean (Austbø 2015), which can be seen in Eq. 1.

According to Koelet & Gray (1992) The geometric mean is optimal for the following assumptions:

- The temperature of the gases are cooled between each step back to the process temperature (this happens in the model)
- The temperature drop is equal for every stage

$$Pressure\ ratio = \sqrt[compression\ stages]{\frac{High\ Pressure}{Low\ Pressure}} \qquad \text{Eq. 1}$$

When Austbø (2015) studied the geometric pressure ratio, he concluded that the geometric mean could be used as an estimate in the initial phase of an optimization search. However, in LNG processes, the inlet temperature to the first compressor in a compressor arrangement with intercoolers will most likely have a lower temperature than the process temperature, the process may benefit from having a high-pressure ratio in the first compression stage.

Even though the low pressure compressor may benefit from a higher pressure ratio because of the low inlet temperature, the initial, non-optimized models in Chapter 6 and Chapter 7 are designed according to the geometric mean pressure ratio.

2.5 Natural gas

Natural gases are classified in different terms according to their compositions. A natural gas is considered “lean” if the composition consists of almost pure methane, “rich” when other hydrocarbons are present to a greater extent, such as ethane and heavier hydrocarbons. The gas is considered as condensate if the gas consists of a high content of hydrocarbon liquid and form a liquid phase during production (Mkhatab & Poe 2012).

Before the natural gas stream enter the liquefaction facility, removal of acid gases, removal of mercury and dehydration is necessary. Whether upstream NGL-extraction has been performed or not will affect the gas composition. In the Prico process in this thesis, both the lean gas will be studied, while in the DMR, the lean gas will be studied in an upstream DMR process, while the other compositions will be included in a DMR process that contain an integrated NGL extraction process.

The compositions displayed in Table 3 show a lean dry feed gas utilized in the Prico and DMR process with upstream NGL extraction and a rich wet feed gas with the following development of the gas after each step of the NGL-extraction in a DMR process (the extraction and reflux stream with natural gas and LPG).

Table 3: Natural gas composition of the natural gases utilized in both the Prico and DMR processes provided by Kusmaya (2012)

Natural Gas Composition				
Upstream		Integrated		
	NG Feed (Lean Dry Gas)	NG Feed (Rich Feed Gas)	NG-SWHE2-1 (Gas after extraction)	NG+LPG (LPG injection)
Component	Mole Fraction			
C1	0.9800	0.8250	0.9208	0.8632
C2	0.0086	0.0830	0.0572	0.0829
C3	0.0039	0.0360	0.0066	0.0269
iC4	0.0007	0.0116	0.0004	0.0053
n-C4	0.0008	0.0137	0.0002	0.0061
iC5	0.0000	0.0050	0.0000	0.0000
n-C5	0.0000	0.0040	0.0000	0.0000
n-C6	0.0000	0.0030	0.0000	0.0000
n-C7	0.0000	0.0010	0.0000	0.0000
n-C8	0.0000	0.0020	0.0000	0.0000
n-C9	0.0000	0.0001	0.0000	0.0000
n-C10	0.0000	0.0000	0.0000	0.0000
N2	0.0060	0.0149	0.0148	0.0156
CO2	0.0000	0.0000	0.0000	0.0000
Benzene	0.0000	0.0001	0.0000	0.0000
Toluene	0.0000	0.0005	0.0000	0.0000
M-Xylene	0.0000	0.0001	0.0000	0.0000
TOTAL	1	1	1	1

2.6 Energy losses in an NG liquefaction process

The two most important units in regards to energy losses in a liquefaction process are the compressors and the heat exchangers. By increasing the heat transfer area, the heat exchanger will be able to transfer more heat from the hot medium to the cold medium. In a case were a compressor is placed after an intercooler, the result will be a lower inlet temperature to the compressor, which will result in lower compressor work. One way to compensate for a small heat exchanger will be to increase the flowrate of the cold medium. The relationship between the heat transfer, heat transfer coefficient, surface area and logarithmic mean temperature difference in a heat exchanger can be seen in below.

$$Q = U \times A \times \Delta T_{LM} \qquad \text{Eq. 2}$$

In FLNG units, the availability of seawater is an important factor when cooling. Therefore, FLNG units that operate in colder climates have a high advantage in regards of the cold seawater.

Considering the liquefaction process, there will always be a trade-off between the heat exchanger size and the compressor duty (Aspelund et.al 2009). Throttling losses also plays an important role in energy losses.

3 Optimization

Optimization is a procedure that consists of several sub procedures that involves mathematical methods utilized to make a system as effective as possible within certain user or process defined limits and constraints. (Luenberger & Ye 2008).

There are many ways to categorize an optimization problem, but the two main categories are either linear or non-linear which means either that the problem is based on linear functions of the unknown or if it contains a non-linear objective function. Non-linear optimization is far more complex than linear optimization because it may contain several feasible regions, making it harder to find a global minima, and because it is harder to predict the outcome of an adjustment. (Chinneck 2012) & (Glandt et al. 1988).

To get an optimal solution the considerations should be the model representing the process and to choose a suitable objective criterion to guide the decision-making.

A typical optimization problem contains the following:

1. At least one objective function which is to be optimized (minimized or maximized)
2. Equality constraints or/and inequality constraints
3. Optimization Variables with boundaries

(Glandt et al. 1988) & (Luenberger & Ye 2008).

3.1 Degrees of freedom

When developing a model for optimization, the number of variables that can be manipulated to achieve the objective function is crucial. For a basic model with no independent equations, the degrees of freedom can be seen in Eq. 3.

$$N_F = N_V \qquad \text{Eq. 3}$$

Where: N_F = Degrees of freedom

N_V = Total number of variables involved in the problem.

In most processes, many independent equations, specifications, constraints and limits need to be adhered to. In a NG liquefaction process, these independencies can be molar rate, compressor and expander efficiencies, temperatures, pressures, flow composition etc. The equation used to evaluate the degrees of freedom considering these independencies can be seen in Eq. 4.

$$N_F = N_V - N_E \qquad \text{Eq. 4}$$

Where: N_E = Number of independent equations (including specifications)

By defining the degrees of freedom, a problem can be separated into three categories:

1. $N_F = 0$: The number of independent equations is equal to the number of process variables, this means that the problem is exactly determined, which makes this a non-optimization problem.
2. $N_F > 0$: The number of variables involved in the problem is higher than the number of independent equations and specifications. This means that problem is underdetermined. So in this case, at least one variable can be optimized.
3. $N_F < 0$: The number of independent equations and specifications is bigger than the number of variables involved in the problem. This means that the problem is overdetermined and that the set of equations cannot yield a solution. It should be mentioned that most optimization software use codes that permit the user to include all possible variables and constraints to prevent this problem from occurring (Glandt et al. 1988).

3.2 Equations of State

Equations of State models are accurate in predicting properties of most hydrocarbon based fluids over a wide range of operating conditions. Their application focuses on primarily non-polar or slightly polar components (Aspentech Hysys software v8.3).

Two equations of state have proven great success in applied thermodynamics. The equations are Peng-Robinson (PR) and Soave-Redlich-Kwong (SRK); both these equations descend from van der Waals equation of state (Ghosh 1999).

A Peng-Robinson model is ideal for VLE (vapor-liquid equilibrium) calculations and calculation of liquid densities for hydrocarbon systems. Several enhancements to the original model has been made to improve its predictions for some non-ideal systems. If highly non-ideal systems are being operated, the use of Activity Models is recommended.
SRK provides in many cases similar results to PR, but the range of application is more limited. In addition, SRK is not as reliable as PR for non-ideal systems (Aspentech Hysys software v8.3).
It is important to note that Hysys is not using the regular SRK or regular PR equations, but edited versions of these equations, which include volume shift (Professor Nontas Voutsas, Personal communication October 14, 2014). Volume shift is a parameter that supports the EOS in calculations for systems in near critical conditions where it is difficult to distinguish between gas and liquid phase. (Pedersen, Christensen & Shaikh 2015)

3.3 Non-linear optimization

Non-linear optimization is optimization with both linear and non-linear constraints with a non-linear objective function and n variables. Non-linear optimization is more complex than linear optimization because it is harder to predict the outcome of an adjustment (Glandt et al. 1988).

While there are few minimum points in a linear optimization, a non-linear optimization often consists of several local minima and only one global minimum. Because of the nature of non-linear optimization, the constraints can twist, curve, and create several feasible regions that all results in different local minimums. The problem with several feasible regions is that it is very common that an algorithm chooses a direction for search and finds the best value of the objective function in that particular direction. This means that if the starting point is at a feasible region where the local minimum is not the global minimum then the minimum point will have a poorer value than what it could have been if the chosen starting position were different. Because of the complexity of non-linear optimization, equality constraints are easily violated when the solver tries to move to another point to achieve a lower minimum (Chinneck 2012). A general mathematical formulation of constrained optimization problems can be seen in Eq. 5.

$$\min_{x \epsilon \mathbb{R}^n} f(x) \qquad \text{subject to} \begin{cases} c_i(x) = 0, & i \epsilon \mathcal{E} \\ c_i(x) \geq 0, & i \epsilon \mathrm{I} \\ x_l \leq x \leq x_h \end{cases} \qquad \text{Eq. 5}$$

In this case, f and the functions c_i are smooth, real valued functions on a subset of $\mathbb{R}^n$ and I and $\mathcal{E}$ are two finite index sets of inequality and equality constraints, respectively. The upper and lower boundaries of x represents the variable boundaries in which the search will take place.

3.4 SQP optimization

SQP optimization is a large subject, which includes a variety of different algorithms to fulfill different tasks. This subchapter explains the basic ideas behind SQP optimization and its challenges that can be encountered when operating the Hyprotech SQP optimizer.

For more information in regards to SQP optimization and optimization in general (Nocedal & Wright 1999) and (Biegler 2010) provides great information.

3.4.1 SQP – Sequential Quadratic Programming

In order of solving nonlinear constraint optimization problems, SQP is considered one of the most efficient methods. In order to solve a nonlinear-optimization problem, the SQP method creates a quadratic approximation of the nonlinear problem utilizing Karush-Kuhn-Tucker conditions of the original problem (Secanell & Suleman 2005).

A basic algorithm for the SQP method, in regards to Eq. 4 in addition to the parameter k, which represents each iteration and d represents the search direction:

1. Evaluate the objective function, $f(x_k)$, boundaries and constraints $c(x_k)$.
2. Solve a quadratic problem QP to determine a search direction, d_k for the variables, x_k. The process stops if a termination criterion is satisfied, i.e. the KKT conditions are fulfilled.
3. Find a steplength that leads to a sufficient improvement towards the solution and avoids the maratos effect. This can be done by utilizing either a trust region or a line search algorithm.
   For the line search, $x_{k+1} = x_k + \alpha_k \times d_k$ where α_k is a steplength parameter.
   For the trust region method, $d_k \in \Delta$, where Δ is adjusted and $x_{k+1} = x_k + d_k$.

(Alkaya, Vasantharajan & Biegler 2001)

3.4.2 Merit function

A merit function ϕ is a scalar-valued function of x. The values of the function indicates whether or not a new candidate iterate is better or worse than the current iterate. In optimization, the objective function f may be a merit function itself. Typically, algorithms that is utilized for minimizing the function f require a decrease in each iteration.

In nonlinear optimization, a widely used merit function is the ℓ_1 exact function, which is defined by Eq. 6.

$$\phi(x;\mu) = f(x) + \frac{1}{\mu}\sum_{i\in\mathcal{E}}|c_i(x)| + \frac{1}{\mu}\sum_{i\in\mathrm{I}}[c_i(x)]^- \qquad \text{Eq. 6}$$

The notation $[x]^- = \max\{0, -x\}$ indicates that the value needs to be lower than its original value. The scalar μ is the penalty parameter that determines the weight that is assigned to the constraint satisfaction relative to minimization of the objective (Nocedal & Wright 1999). An illustration of a Merit function can be seen in Figure 4.

The ℓ_1 merit functions are suitable for NLP problems that contain less than a few hundred variables (Biegler 2010).

3.4.3 Maratos effect

The Maratos effect is a phenomenon in which, steps that make a positive progress toward the objective function are being rejected because of an increasing merit function ϕ. The Maratos effect can cause the algorithm to reject steps that are taken in the right direction, and therefore causing difficulty and making the progress slow. It exists some nonmonotone algorithms that can do a certain extend override the increase or lack of decrease in f at every step, however, these algorithms will after a certain number of iterations require the function f to be decreased (Nocedal & Wright 1999). An example of Maratos effect can be seen in Figure 5.

The two fundamental strategies to avoid the maratos effect are line search and trust region. The Hyprotech SQP optimizer utilize the line search, therefore, the line search strategy will be in focus.

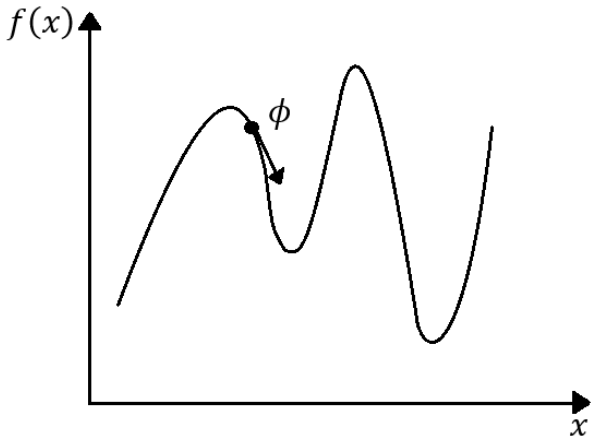

Figure 4: Illustration of a merit function

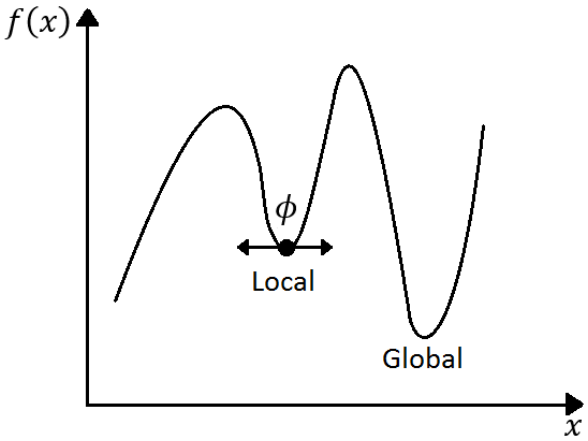

Figure 5: Illustration of the Maratos Effect

3.4.4 Watchdog (nonmonotone) line search strategy

By utilizing a nonmonotone strategy, a number of steps that increase the merit functions are accepted; these steps are called “relaxed steps”. However, if the set number have not reached a sufficient reduction, the process return to the point before the relaxed steps occurred, and thereafter perform a normal step by utilizing a line search or another technique in order to achieve a reduction in the ℓ_1 merit function. The Watchdog strategy is a technique that utilize these principles in finding the minimum (Nocedal & Wright 1999). An illustration of the Watchdog line search strategy can be seen in Figure 6.

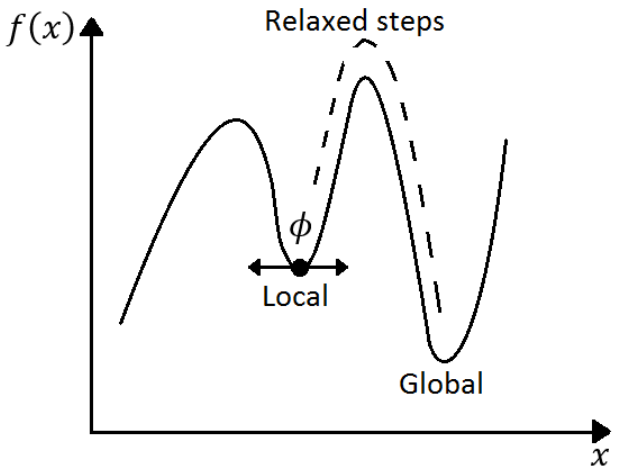

Figure 6: Illustration of the Watchdog line search strategy

3.4.5 The BFGS Method

The BFGS method is the most popular quasi-Newton algorithm. The algorithm is named after its discoverers, Broyden, Fletcher, Goldfarb and Shanno. Although this method is robust in practice, it cannot establish truly global convergence results for general nonlinear objective functions. (Nocedal & Wright 1999)

3.5 Hyprotech SQP

Concerning the Hyprotech SQP optimizer, several emails were sent to Aspentech through a paid license that involves customer support. Their unwillingness to cooperate with updated information concerning the Hyprotech SQP optimizer in terms of its parameters or the optimizer structure concerning mathematical iteration models was disappointing. Therefore, the information concerning the Hyprotech SQP optimizer is provided through several papers published by Aspentech, and some of the information may be outdated.

The Hyprotech SQP optimizer has embedded an L1-merit function and a BFGS approximation to the Hessian of the Lagrangian. Which are described in Chapter 3.4.2 and Chapter 3.4.5 respectively.
The Hyprotech SQP algorithm utilizes step size restriction, decision variable and objective function scaling, the watchdog line search strategy, and a problem-independent and scale-independent relative convergence test. The algorithm also ensures that the model is evaluated only within the variable boundaries (Aspen HYSYS petroleum Refining 2011).

Considering the Hyprotech SQP optimizer utilize the BFGS method means that it cannot be classified as a global optimizer as it can be seen in Chapter 3.4.5.

The Hyprotech SQP optimizer is recommended by Aspentech and studied in the project Rødstøl (2014) to be the most efficient and accurate optimizer in regards to complex process operations which may contain several independent variables and constraints.

In order to set up the Hyprotech SQP optimizer, a derivative utility is required.

3.5.1 Derivative utility

The derivative utility is used to set up proper variables, variable boundaries, constraint and the objective function. In addition, the derivative utility can be utilized to analyze results from the optimization, in terms of different conditions.

The optimizer manipulates the variable values in order to reach a good objective function. The variable boundaries need to be set up in a reasonable manner, which means that they cannot have to high maximum value or to low minimum value. This will lead to errors in the optimizer and the optimizer will not be able to converge to an objective value. The range of the variable boundaries can be user specified, or the optimizer can calculate them:

$$Range = Maximum - Minimum$$

The constraints are set up in order to assist the optimizer in not making calculations that does not correspond with functioning Flowsheet operations. The constraints can be set up according to both minimum and maximum values. The constraint boundaries can utilize the scale function, which in general relax the constraint boundaries to a certain value in order to reach an objective function.

$$(Minimum - Scale) \leq Current\ Value \leq (Maximum + Scale)$$

In certain problems, a scale value can assist in solving the problems by expanding the feasible region.

The objective function is the function that is supposed to be either maximized or minimized in regards to the variables and constraints, which can be seen in Eq. 7 from Chapter 4.

Derivative Analysis

Derivative analysis is carried out in order to observe different noise in the optimization. Noise can affect the Flowsheet and the gradient values, which can result in erroneous optimizer results. To reduce the noise, it is recommended to tighten the convergence tolerance in the units where the noise is occurring. By making the tolerance tighter, small changes are being applied to determine the direction, which may result in less noise.The number of maximum iterations should also be adjusted in order to deal with the noise (HYSYS RTO: Reference Guide). In simplicity, noise can be explained as inaccuracy in the function evaluation.

3.5.2 The optimizer set-up parameters

In the optimizer, several factors can be adjusted in order to affect the optimization process.

A. Maximum iterations

Maximum iterations is the number of major iterations the optimizer is allowed to perform in order to achieve a desired objective value. A major iteration consists of a sequence of minor iterations. The default value in the Hyprotech SQP optimizer is 50 iterations, which may be sufficient in some cases, but in cases that involves much noise, this number should be adjusted to a higher value.

B. Objective Scale factor

Scaling is an important issue in terms of optimization. Different parameters can be very sensitive to small changes. An example can be seen in this equation:

$$f(x) = 10^9 x_1^2 + x_2^2$$

It is easy to see that the function is very sensitive to small changes in the x_1 variable, but not so sensitive in the x_2 variable. In order to solve a complex optimization problem, scaling is necessary (Nocedal & Wright 1999). By adjusting the boundary values, the changes will differ when optimizing.

The Objective Scale Factor specifies the factor used for scaling the objective function. Positive values are used as-is. Negative values use the factor abs(scale*F) (where F is the initial objective function value) and a factor is generated automatically for zero values (Hysys V8.3). The objective scale factor gives a relative weight between the objective function and feasible search in an optimization process.

An important note is that in cases where the objective scale factor is 0.0, an objective scale factor will be automatically generated (Hysys V8.3).

C. Accuracy Tolerance

This factor is the relative accuracy tolerance of the objective function improvement and is used as a convergence test for the optimizer.

$$Convergence\ Sum \leq Accuracy\ Tolerance \times \max(|F(x)|, 1.0)$$

The Convergence Sum represents a weighted sum of all the possible objective function improvement and constraint violations, and it has the same units as the objective function. This test allows the same tolerance parameter to be used for different problems and it makes the convergence test independent of possible scaling of the objective function. By choosing a very low number, the objective function will be more accurate; however, a low number may result in step convergence, which indicates that the accuracy could not be achieved within the given number of iterations. The default value is 10^{-4} – 10^{-6}.

D. Step Restriction

The Step Restriction parameter is deciding the maximum value of each step the optimizer is during the first three iterations in a major iteration in order to reach the minimum objective value. This parameter is used to limit the overall step change. Step size greater than 1 will result in no step restriction. The default value is 0.2. (Hysys V8.3)

E. Perturbation

In general, Perturbation can be viewed as an influence on a system that modifies its behavior, such as a disturbance. In this optimization process with Hysys, the perturbation can be viewed as a change in the scaled variables during gradient evaluation. A lower value results in faster gradient calculations, however, by setting a lower value, the gradient is limited and therefore it may not give an accurate gradient in cases where there is significant noise in the simulation. The default value is 1e-03, but the typical range is 1e-02 to 1e-03. (Aspen HYSYS SQP Optimization: A practical guide) & (HYSYS.RTO: Reference Guide). The perturbation parameter is sensitive and may be challenging to adjust.

F. Max. Feasible points

This parameter decides the maximum number of iterations that the optimizer can utilize in the line search procedure. If the solver display the termination reason “Step Convergence” early in the optimization process, it may indicate that the initial variable values may be inappropriate, but step convergence can also be caused by other parameters (Hysys V8.3).

G. Gradient Calculations

Both one-sided and two-sided gradient calculations can be chosen in order to achieve an objective value. One-sided gradient calculations causes forward differences and can be written in the form:

$$\frac{dc}{dv} = \frac{c(v + \Delta v) - c(v)}{\Delta v}$$

While two-sided gradient calculations causes central differences can be written in the form:

$$\frac{dc}{dv} = \frac{c(v + 0.5\Delta v) - c(v - 0.5\Delta v)}{\Delta v}$$

Where v is an optimizer variable, and c is the objective function or constraint.

Two-sided gradient calculations use twice as many function evaluation as one-sided gradient calculations. The two-sided gradient calculations are recommended for highly non-linear problems or problems that contains a lot of noise. The formulas should be viewed with as very basic formulas in regards to the source from 2004 (HYSYS RTO: Reference Guide) & (Gibbons et. al 2006).

3.5.3 Running results

Result Analysis

When the optimizer has performed an optimization, the results can be analyzed in terms of several factors. The most important factors are the objective value and whether or not the constraints have been upheld, but aside from these factors, there are also total CPU time, gradient evaluations, model evaluations and feasible point iterations.

Total CPU Time

Total CPU time show the amount of time the optimizer use in order to converge to an objective value. This factor should only be considered if the deviation between the different tests are high. The reason for this is because this factor can be influenced by several factors:

- The computer specifications (CPU, Ram etc.)
- Background programs that run from time to time (windows updates, internet pages etc.)

Gradient and Model Evaluations

Gradient and Model Evaluations displays the number of gradient calculations and model evaluations that were performed in order to obtain the objective value.

Feasible Point Iterations

Feasible point iterations displays the amount of minor iterations since the last major iteration was performed.

4 Earlier Work

Optimization is a large and complex subject in which several books and studies have been written. In regards to the complexity, several optimization programs, which utilize different algorithms and techniques have been developed.

Aspentech Hysys is a commonly used simulation software and are utilized in several processes that contain natural gas treatment. However, the built-in optimizers in Hysys are not as commonly used as the simulation software itself. In regards to the Hyprotech SQP optimizer, it seems that there is no published research in regards to the optimizer itself or its application to process models. Considering that there may be no published work concerning the Hyprotech SQP optimizer, this project may be looked at as the first in-depth project concerning the Hyprotech SQP optimizer.

Earlier reports that has utilized Hysys built-in optimizer in order to analyze processes are the following:

Cao et. al (2005) Did a Parameter comparison of two small-scale natural gas liquefaction processes in skid-mounted packages. The two processes studied were a mixed refrigerant liquefaction process and a Nitrogen-Methane expander liquefaction process.
The fluid package utilized in the processes were the Peng Robinson equation of state and LKP equation. The optimization were based upon the power consumption divided by the produced LNG.
The optimizer utilized in these processes were the Original optimizer integrated in Hysys. As the result, the expander process were found to be the most energy efficient liquefaction process.

Hatcher et. al (2012) studied optimization of LNG mixed-refrigerant processes considering operation and design objectives. The paper focus on constructing and testing eight different objective functions in order to identify the most appropriate formulation. The liquefaction process utilized in this paper is a propane-precooled mixed refrigerant liquefaction process. Before optimization, reasonable starting variables were identified through sensitivity analysis. The optimizer utilized were the integrated BOX scheme within the Original optimizer in Hysys. Concerning the operation cost alone, the study concluded that minimizing the compressor power is the most effective operation objective. Concerning both CAPEX and OPEX, the objective function that involved minimization of a weighted sum of compressor power and UA provided the best result.

Mahabadipour & Ghaebi (2012) studied the development and comparison of two expander cycles used in refrigeration system of olefin plant based on exergy analysis. Two low temperature expander cycles were in focus for cold section of an olefin plant, in which one and two cooling stages were studied in regards to replacement of an ethylene refrigeration

cycle within the olefin plant. According to exergy analyses, results showed that the expander cycle that contained one stage cooling gave better results than the cooling cycle that had two cooling stages. Optimization with an optimizer that are integrated in Hysys were performed in order to minimize the power consumption. Which of the integrated optimizer in Hysys that were utilized is not mentioned in the paper.

Wang et al (2013) discussed operation optimization of propane precooled mixed refrigerant processes.
Two different propane-precooled mixed refrigerants processes were utilized in the optimization task; in which one of them were an ordinary C3MR process and the other were a C3MR with split propane process (C3MR-SP). The optimization task were to utilize four objective functions which included shaft work consumption, two different expressions of exergy efficiency and OPEX to identify improvements in the process performance. The models were simulated and optimized in Hysys using the Original optimizer with the BOX scheme. The best result for the two processes were obtained by utilizing different objective functions.

Three out of the four studies above utilized either the Original or BOX built-in optimizer in Hysys, while one of the studies did not mention which of the built-in optimizer that were utilized. Considering the project Rødstøl (2014) and Aspentech customer support, the Hyprotech SQP optimizer should be utilized when optimizing advanced process models. This should be taken into consideration when the analyzing results from the studies mentioned above.

Rødstøl (2014) studied the built-in optimization functions in Aspentech Hysys V8.3. The studies were carried out on two natural gas liquefaction processes:

- PRICO single mixed refrigerant process (SMR) by Black and Veatch
- NICHE dual expander process by CB&I – Randall Gas Technology

These processes were in focus because they both represent fundamentally different challenges in optimization, in which Prico is a mixed refrigerant process and NICHE is an expander process.

The optimizers and optimizer schemes studied through the report were the following:

- Original
    - SQP
    - Mixed
    - BOX
- Hyprotech SQP with one-sided and two-sided gradient calculations
- MDC Optim
    - SQP with one-sided and two-sided gradient calculations

- SLP with one-sided and two-sided gradient calculations

Some optimization schemes within the different optimizers were not tested because of their inabilities to handle non-linear optimization problems and constraints.

The main target of the optimization was to manipulate the independent free variables in the processes within certain boundaries and constraints in order to find a low objective value. The objective function were based upon the required power in order to produce LNG divided by the produced LNG, which can be seen from Eq. 7.

$$minf(x) = \frac{\dot{W}_{Comrpessors}}{\dot{m}_{LNG}} \qquad \text{Eq. 7}$$

The study was performed by first creating the process models in order to understand and analyze them in regards to calculations and independent variables. Matlab scripts were created for each study to calculate new variable boundaries or variable values. The different optimizers were provided with the same initial variable boundaries, constraints, variable values and working conditions for the optimizer. Four case studies were carried out in each model were the different criteria were tested:

- Expansion of the initial variable values in both minimum and maximum directions
- Narrowing of the initial variable boundaries in both minimum and maximum directions
- Expansion of the initial variable boundary in one direction
- Changing the initial variable values in one direction

The case studies were carried out to stress the optimizers in order to explore their capabilities and to find weaknesses or strengths within the different schemes and calculation methods.

The models were analyzed in different terms after every optimization too see if constraints had been violated or if errors within the model had occurred. In the Hyprotech SQP and MDC Optim optimizer, the time to converge to an objective value was compared within each of the optimizers to explore the differences between one-sided and two-sided gradient calculations.

The results indicated that the Original optimizer with its schemes were not suited for more advanced optimization models. Even though the MDC Optim optimizer were able to converge to an objective value in all of the studies, the objective values were poor in comparison to the Hyprotech SQP optimizer. The Hyprotech SQP optimizer was able to converge to an objective value with one exception through all of the studies by utilizing either one-sided or two-sided gradient calculations.

The Hyprotech SQP optimizer undoubtedly provided the best objective values, especially in the mixed refrigerant process, and should be considered as the default optimizer to utilize when the goal with the optimization is to achieve an optimum objective value at more advanced models.

For more information regarding the case studies, pre-conditions and results, see the project.

To challenge and obtain a better understanding in regards to the capabilities and limitations of the Hyprotech SQP optimizer, more advanced process models are necessary. By utilizing a Prico process, which will be studied in more depth, and a DMR process, the optimizer will be challenged and explored in different ways according to the optimizer parameters and the derivative utility. In addition, general modifications and simplifications on how the optimizer may provide an optimal objective value in regards to complex processes may be provided.

5 Hysys Process Models and Optimizer Setup

Since these processes are based on FLNG, the process temperature is calculated in regards to seawater cooling. The process temperatures affect the inlet natural gas stream and all the streams that are placed directly after a cooler. The default process temperature is set to be 15°C, but studies will be carried out at processes that have process temperatures at 5°C, 15°C, 25°C and 35°C.

5.1 Prico Hysys model

The Prico process will be studied in depth concerning process optimization and optimizer configuration. As mentioned in Chapter 2, the Prico process in this thesis will look very similar to the warm mixed refrigeration cycle in the DMR process. The Prico model can be seen in Appendix D.

5.1.1 Mixed Refrigerant Composition

The mixed refrigerant components are decided according to the boiling point values displayed in Table 1 and the composition for the Prico process is displayed in Table 2. There was an option to add Ethane and i-Pentane to the mix. Ethane would contribute by closing in the gap between the boiling point of Ethylene and Propane, while i-Pentane would work as a counterpart to the other refrigerants to increase the phase envelope and contribute to the equality constant in the mixture. However, if the mixed refrigerant composition provides difficulties in achieving the minimum temperature approach in the heat exchanger, more components may be added. It can be seen from Figure 7 how the mixing process in order to achieve the mixed refrigerant is fulfilled. The set (SET-1) and balance (BAL-1) functions are transporting the molar flow and pressure of the MR stream to the MR1 stream.

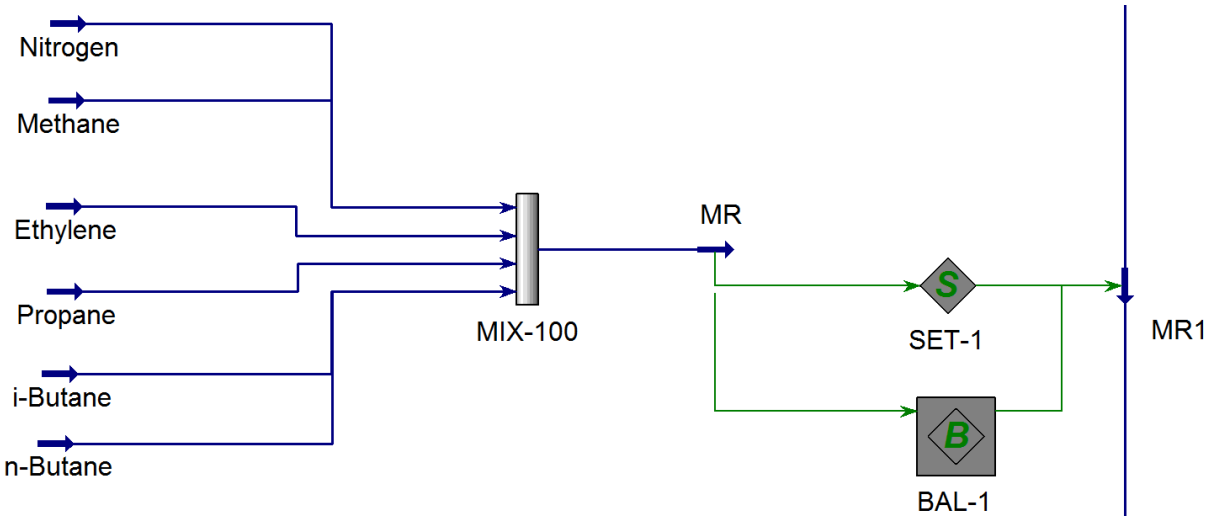

Figure 7: Mixing process of the different components which makes up for the composition in the MR stream.

5.1.2 Prico Refrigeration Circuit

The refrigeration circuit of the Prico process can be seen in Figure 8. At the MR1 stream, the initial pressure is set to be 45bar, and the temperature is set according to the process temperature, which can be either 5°C, 15°C, 25°C or 35°C. The stream (MR1) enters the plate-fin heat exchanger (P-F HX) and is cooled by stream MR3, which also cools the NG_Feed stream to a temperature of -153.4°C, which is selected according to the achieved conditions after VALVE2, which is a temperature of -160.1°C and a pressure of 1.2 Bara. These values are selected in order to flash off a sufficient amount of Nitrogen and to keep the gas above atmospheric pressure in order to store the LNG in tanks without air entering. The mixed refrigerant stream at MR2 is expanded through Valve1 to achieve the desired properties at MR3, which will vary in regards to the optimization. MR3 cools both the MR1 and NG_Feed streams by evaporation. The pressure drop in the P-F HX is set to be 2 bar at the warm side and 1.5 bar at the cold side. In order to change the variables when optimizing and still make sure that the heat exchanger is superheating the refrigerant stream 6K, the following flow sheet modification is made: at MR4, the stream is controlled through a dew point controller, which makes sure that the compressor K-100 does not receive a two-phase inlet stream. The dew point controller is utilizing a balance (BAL-2) and a set (SET-3) function to duplicate the composition and pressure from MR4 and export the values to MR4R. The MR4R stream get its temperature by manually setting the vapor phase of the stream to be at the dew point temperature. Both the temperatures at MR4 and MR4R are imported to the Dew point Controller spreadsheet, which calculates the difference between the temperatures and make it possible to utilize a temperature difference as a constraint in the optimizer. In this model, the constraint is making sure that MR4 have a temperature of 6K higher than the dew point temperature. After MR4, the stream enters a two-stage compression, which in the non-optimized model has fixed pressure ratios according to Eq. 1. The separator, SEP2, is used to separate the liquid and gas phase in order to avoid two-phase flow into the compressor. The SET-2 function is making sure that the pressure out of the compressor and pump are equal. All the coolers in the model have a pressure drop of 0.5 bar.

The process temperature affects all the streams connected to a cooler and the NG_Feed temperature.

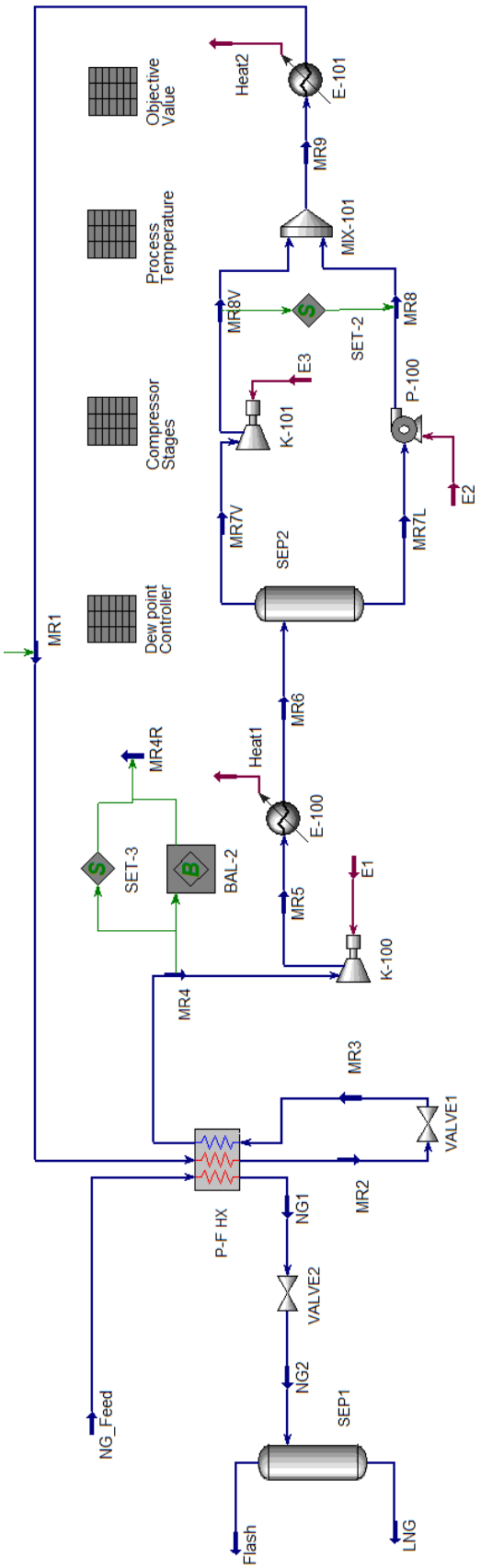

Figure 8: The refrigeration circuit of the Prico process

5.2 DMR Hysys model

Two different DMR processes are studied in this thesis in which, one of them has an integrated NGL extraction process, while in the other process, the NGL extraction takes place upstream and does not affect the DMR process itself. Both the upstream and integrated DMR processes can be seen in Appendix A and Appendix B respectively.

Considering their similarities, the DMR process that has an upstream extraction process will be divided into sub parts where each subpart will be explained. Thereafter, the modifications carried out on the DMR process in order to make a simplified NGL extraction will be illustrated and explained.

In the flow sheet explanation, only the simplest modifications in terms of free variables and constraints in both models will be explained.

5.2.1 Warm Mixed Refrigerant Components

The Warm Mixed Refrigerant components are decided according to the components boiling temperatures. In Table 2 from Chapter 2.3, can it be seen that the warm mixed refrigerant contain the following components: methane, ethylene, propane, i-butane and n-butane. In the Hysys model in Chapter 7, nitrogen will also be considered in the warm mixed refrigerant, nitrogen is included to observe if the optimizer will include it as a component of the WMR stream. The WMR mixing process without Nitrogen can be seen from Figure 9. As mentioned in Chapter 2.3**,** the main reason that ethylene is utilized instead of ethane is because of the difficulty to extract pure ethane and that ethylene are more available for import. When configuring the WMR composition, the molar flowrate of the pure component streams are adjusted in order to achieve a good composition in the WMR stream. The set (SET-3) and balance (BAL-3) functions are utilized to duplicate and export the composition and temperature of the WMR stream to the Warm Mixed Refrigerant Cycle. The WMR temperature is set as the process temperature, which varies between 5°C, 15°C, 25°C and 35°C.

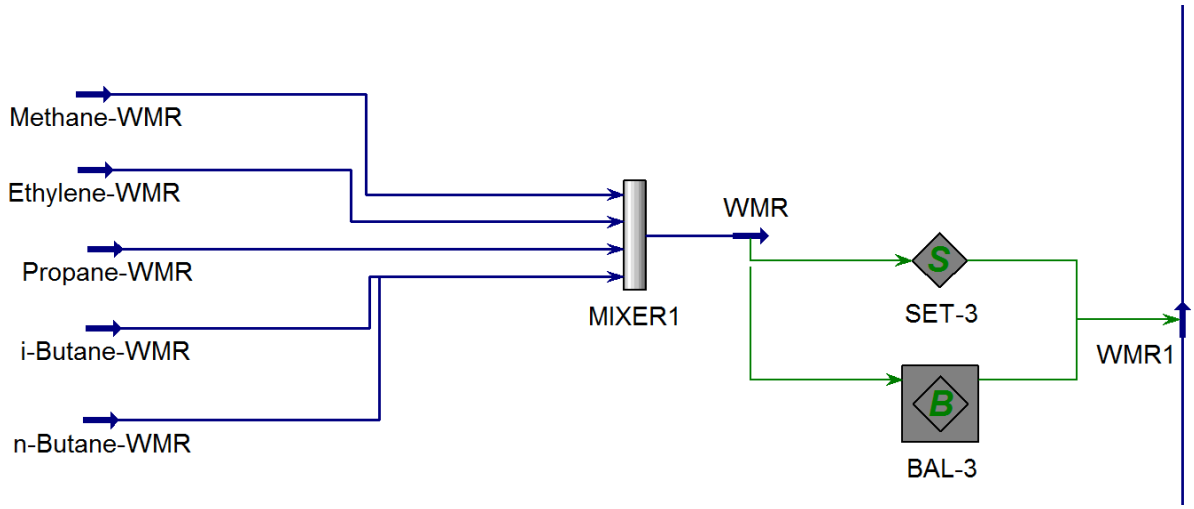

Figure 9: Mixing process of the different components that makes up for the composition in the WMR stream

5.2.2 Cold Mixed Refrigerant Components

Since the Cold Mixed Refrigerant is utilizing evaporation at a different temperature than the Warm Mixed Refrigerant, the components will differ, as can be seen in Chapter 2.3. The Cold Mixed Refrigerant will consist of components with lower boiling points. Therefore, a typical composition of Cold Mixed Refrigerant would naturally consist of lighter hydrocarbons and Nitrogen as it can be seen in Figure 10. A typical composition for a Cold Mixed Refrigerant would be Methane, Ethylene (or Ethane), Propane and Nitrogen. Some heavier hydrocarbons may provide a better mixture, but the freezing points also need to be taken into consideration (Mohd Shariq Khan et. al 2014). The balance "BAL-1" function is utilized to duplicate the composition and molar flow of the CMR stream and export it to the CMR1 stream. In the Warm Mixed Refrigerant, an adjust function was utilized to transfer the temperature from the mixing process to the cycle. In the CMR stage, the cycle temperature is exported from a spreadsheet. The exported temperature is the process temperature.

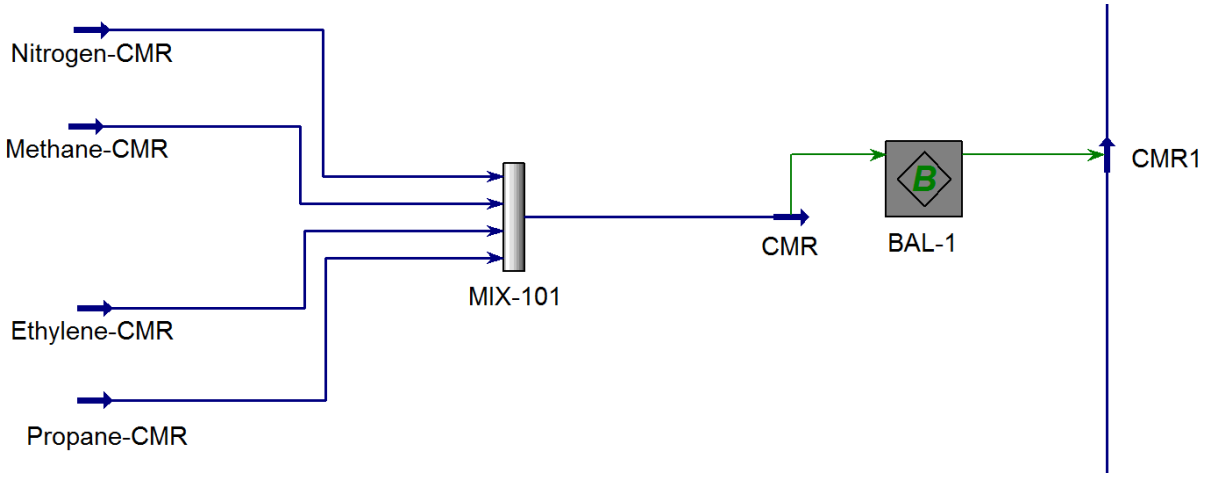

Figure 10: Mixing process of the different components that makes up for the composition in the CMR stream

5.2.3 Warm Mixed Refrigerant Circuit

The Warm Mixed Refrigerant circuit can be seen in Figure 11. The WMR circuit receives its composition and temperature from the WMR stream were its properties are duplicated and exported to the WMR1 stream. The WMR stream is cooled through SWHE-1 to -48.3°C, which is set to be the outlet temperature of SWHE-1 based on Kusmaya (2012). After SWHE-1, the stream enters VLV-100 where the pressure drops to an optimized value, which also will affect the temperature and liquid content of the stream. The obtained stream properties are utilized for an optimum cooling in the heat exchanger (SWHE-1) by evaporation. The streams that are cooled in SWHE-1 are WMR1, CMR1 and NGFeed. The pressure drop in SWHE-1 are 4 bar at the tube side and 0.4 bar at the shell side. After SWHE-1 the stream is controlled at WMR4 through a dew point controller, which makes sure that the compressor K-100 do not get two-phase inlet. The dew point controller is utilizing a balance (BAL-2) and a set (SET-2) controller. The DewpointControlWMR spreadsheet calculates the temperature difference between the two streams, which the optimizer utilizes in order to set a constraint in the WMR4 stream of maximum 6K approximation to the DP1 stream

Compressor K-100 and K101, separator (SEP1), pump P-100 and intercooler E-100 are components utilized in a two-stage compression. In the initial process, the spreadsheet PressureStepWMR are adjusting the pressures according to the formula, which can be seen in Eq. 1 from Chapter 2.4 and the set (SET-7) function is adjusting the pressure in WMRLiquid2 stream to be set according to the pressure in the WMRVapor2 stream. The separator (SEP1) is utilized to avoid two-phase inlet to compressor (K-101). After the two stage compression, both stream WMRLiquid2 and WMRVapor2 have a pressure of 46 bar in the non-optimized model, which is set in order to achieve the desired cooling temperature through P-F HX after Valve1. After MIX-102, the stream WMR7 have a constraint that ensures that the refrigerant are in pure vapor phase to avoid two phase flow distribution issues. The stream continues to complete the cooling circuit. All the coolers have a pressure drop of 0.5 bar and are able to cool the stream to the selected process temperature.

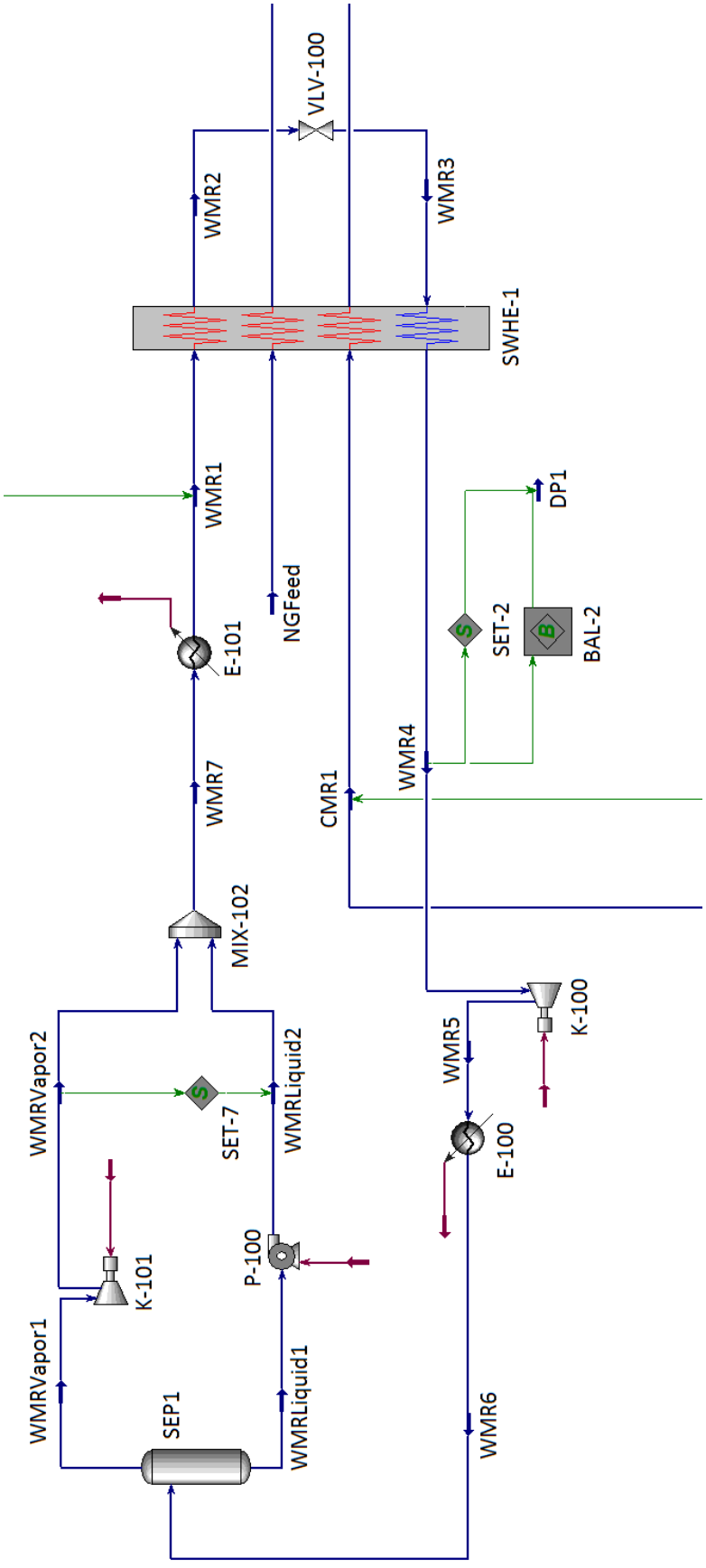

Figure 11: Warm mixed refrigerant circuit in the DMR process

5.2.4 Cold Mixed Refrigerant Circuit

The Cold Mixed Refrigerant circuit can be seen in Figure 12. The CMR circuit receives its composition from the CMR stream and temperature from the process temperature spreadsheet. The CMR1 stream is cooled in SWHE-1 heat exchanger to -48.30°C. This temperature will be optimized in one of the studies. After SWHE-1, separator (SEP2) is included in the MR circuit to separate the vapor phase from the liquid phase. The liquid phase will consist of heavier hydrocarbons and a small amount of Nitrogen, while the vapor phase will consist of lighter hydrocarbons and a significant part of Nitrogen. The SWHE-2 heat exchanger is separated into two parts in the flowsheet, this is done in order to illustrate the two stage cooling that occur in the heat exchanger. The CMR2Vapor stream is cooled through both SWHE2-1 and SWHE2-2 before it enters the JT-valve VLV-102 where it obtain its desired properties to cool both CMR2Vapor2 and NG-SWHE2-2 streams.

The liquid phase that exits SEP2, (CMR2Liquid) is cooled through SWHE2-1 before it enters the JT-valve VLV-103 to obtain the desired properties before it enters the mixer MIXER4 together with the CMR2V-Liquid3 stream.

The two streams form the CMR3 stream, which is utilized to cool CMR2Liquid and precool the CMR2Vapor and NG-SWHE2 streams. The pressure is optimized at CMR4. The pressure obtained through optimization is affecting the entire cooling process through SWHE2-1 and SWHE2-2, because the pressure drops in both heat exchangers are set to be 2 bar tube side and 0.2 bar shell side, in which combining the two heat exchangers is the same pressure drop as in the warm mixed refrigerant circuit. Since the pressure drop is fixed in the heat exchangers, the entire cooling process in the CMR cycle is dependent on the pressure value at CMR4. Considering that the temperature of the outlet streams after SWHE1 are set to be -48.3°C, a constraint is added in order to have a 3K temperature difference between the CMR4 and the inlet streams to SWHE2-1.

In addition, the stream is controlled at CMR4 by utilization of a set (SET-6) and a balance (BAL-5) function, which duplicate the pressure and molar flow from CMR4 and export the values to the DP2 stream. The DP2 stream has the temperature automatically set according to the dew point temperature. A spreadsheet, DewpointControlCMR calculates the temperature difference between the two streams and export the value to the optimizer so it can be utilized as a constraint in order to avoid two-phase inlet stream to the compressor K-102.

The compressors, K-102, K-103 and K-104 and intercoolers, E-102 and E-103 are utilized in a three stage compression. The initial pressure ratios are calculated in the spreadsheet, PressureStepsCMR by utilization of Eq. 1 from Chapter 2.4. As in the cold mixed refrigerant cycle, all the coolers has a fixed pressure drop at 0.5 bar.

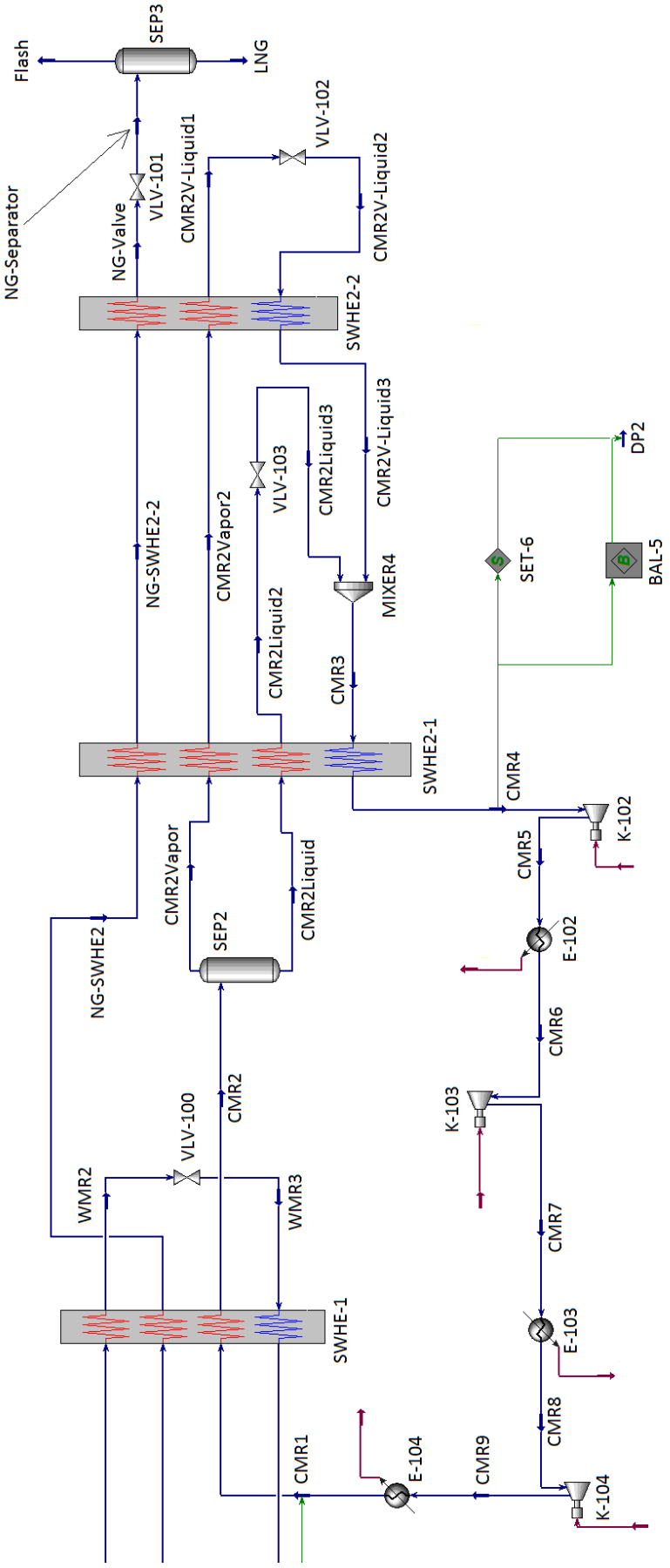

Figure 12: The Cold Mixed Refrigerant circuit in the DMR process

5.2.5 NGL Extraction (Applicable to the Kusmaya Process)

It can be seen from the model in Appendix B that the integrated DMR process is a far more complicated than the upstream DMR process; however, a thorough optimization of the integrated extraction process is not considered in this thesis. Therefore, the integrated extraction process have been greatly simplified by replacing the extraction process with one symbolic sub flowsheet. The simplifications made can be seen from Figure 13. Note that the SWHE2 heat exchanger is split in three parts and not two parts as it is in the original DMR model. However, the total pressure drop and the end temperature remains the same in both models.

The changes in the natural gas composition can be seen in Table 2 from Chapter 2.5. It can be seen that the gas is richer after the fractionation process than it was after the extraction process. This is because the LPG is mixed back with the natural gas to increase the calorific value of the natural gas. All C5+ components are removed in the fractionation process.

In terms of optimization, the integrated DMR process is simplified to a certain extent. The NGL extraction process itself will not be optimized, however, the process will include a reflux stream and a different natural gas composition in the three following places: before the extraction, after the extraction and after the LPG has been mixed back with the natural gas. The three places that involves different compositions can be seen in Figure 13 and the three different compositions can be seen in Table 2 in Chapter 2.5.

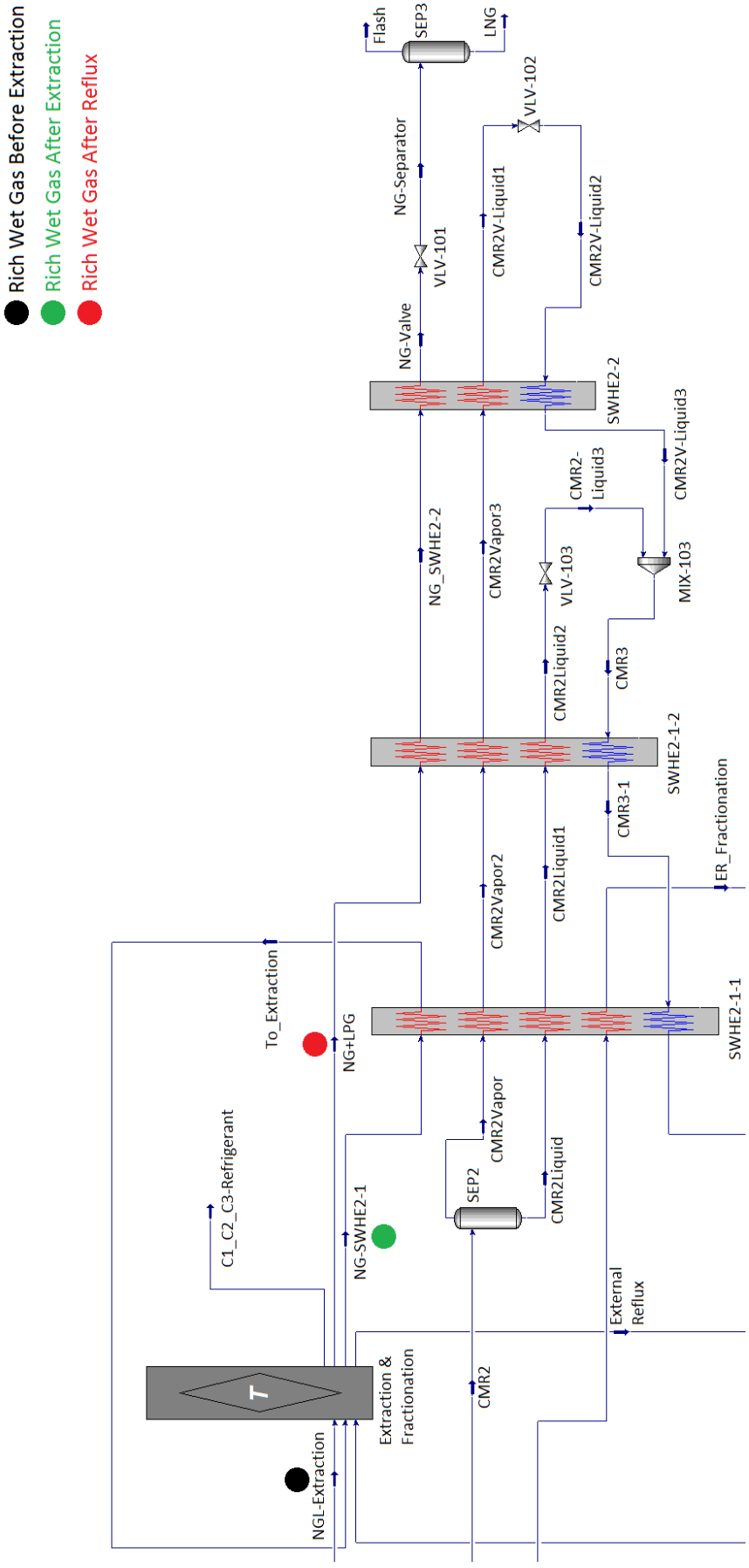

Figure 13: Simplified Integrated NGL Extraction

5.3 Process setup

To obtain the desired results from optimization, both the optimizer and the derivative utility needs to be configured according to the process. By configuring the optimizer and derivative in the right manner, a realistic process with optimum results may be achieved. This thesis focus on MR processes, which provide several challenges for the optimizer to find the optimum refrigeration according to the set constraints and conditions in the flow sheet.

5.3.1 Prico Process

The Prico process is the simplest process of the MR processes; however, by utilizing a two-stage compression, which in this case includes a separator and a pump, it becomes a bit more advanced than what it would be if only compressors were utilized. In regards to optimization, the selected Prico process is far simpler than the DMR process. By first optimizing the Prico process, the transition to optimizing the DMR process will be easier considering challenges that may arise. In the initial process, the pressure ratios are calculated according to Eq. 1 from Chapter 2.4.

The Prico process consists of several fixed and adjustable variables. The fixed equipment specifications and variables can be seen in Table 4 and Table 5 respectively. The adjustable variables can be seen in Table 6. Some of the adjustable variables may be included or excluded depending on what case study modification that is performed. The process temperature, which is user specified, affects the inlet natural gas stream and all streams attached to a cooler.

Table 4: Fixed Equipment specifications in the Prico process

Tag	Equipment	Property	Unit	Value
P-100	Pump	Adiabatic Efficiency	Percent (%)	75
K-100 – 101	Compressors	Polytropic Efficiency	Percent (%)	80
E-100 – 101	Coolers	Pressure Drop	[Bar]	0.5
P-F HX	Heat Exchanger	Pressure drop Tube side	[Bar]	2, 2 and 1.5 respectively

Table 5: Fixed Stream specifications in the Prico process

Tag	Property	Unit	Value
MR2	Temperature	[°C]	-153.4
NG1	Temperature	[°C]	-153.4
NG2	Pressure	[Bar]	1.2
NG_Feed	Pressure	[Bar]	55
NG_Feed	Molar Flow	[kgmole/h]	25650

Table 6: Adjustable variables included in the optimization of the Prico process

Tag	Connections	Property	Units
Nitrogen-WMR **Methane-WMR** **Ethylene-WMR** **Propane-WMR** **i-Butane-WMR** **n-Butane-WMR**	All the component streams makes up for the composition in the MR stream through the mixer (MIX-100). The composition in the MR stream is adjusted by manipulating the molar flow of the component streams accordingly to the desired amount of each component.	Molar Flow Molar Flow Molar Flow Molar Flow Molar Flow Molar Flow	[kgmole/h] [kgmole/h] [kgmole/h] [kgmole/h] [kgmole/h] [kgmole/h]
MR	Connects the stream properties to the MR-1 stream through "SET-1" and "BAL-1"	Pressure	[Bar]
MR4	Outlet stream of P-F HX connected directly to the compressor K-100.	Pressure	[Bar]
MR5	Outlet stream of compressor K-100, determines the inter stage pressure.	Pressure	[Bar]

The adjustable variable streams in Table 6 influence the process in different ways.

Component streams

The component streams makes up for the composition and mass flow in the refrigerant stream utilized in the cooling circuit (MR1). The composition and mass flow is affecting the cooling in the plate-fin heat exchanger (P-F HX) and also the compressor and pump work.

MR4

By adjusting the outlet pressure of MR4, the pressure ratio in the compressors will be affected. If the pressure is adjusted while keeping a constant mass flow, the compressor work, temperature profile in P-F HX and temperature in MR4 will be affected.

MR5

The pressure in this stream determines the compressor work in K-100 and also the compression ratio through the compressor stages.

MR

The pressure in this stream determines the pressure in **MR1**, which is affecting the compressor work.

5.3.2 DMR Process

The DMR process is a complex process model and choosing key variables for manipulation and constraints that will make the model realistic can be a challenging task. In regards to the case studies in Chapter 7, fixed equipment specifications and streams can be seen in Table 7 and Table 8 respectively. The adjustable variables can be seen in Table 9. Different variable combinations from Table 9 will be considered in the optimization process according to which modifications that are studied. Eq. 1 from Chapter 2.4 is utilized in order to calculate the pressure ratios in the compressors in the non-optimized process.

Table 7: Fixed Equipment specifications according to the DMR process in Chapter 7

Tag	Equipment	Property	Unit	Value
P-100	Pump	Adiabatic Efficiency	Percent (%)	75
K-100 – 104	Compressors	Polytropic Efficiency	Percent (%)	80
E-100 – 104	Coolers	Pressure Drop	[Bar]	0.5
SWHE-1	Heat Exchanger	Pressure drop Tube side	[Bar]	4, 4 and 4
SWHE-1	Heat Exchanger	Pressure drop Shell side	[Bar]	0.4
SWHE2-1	Heat Exchanger	Pressure drop Tube side	[Bar]	2 , 2 and 2
SWHE2-1	Heat Exchanger	Pressure drop Shell side	[Bar]	0.2
SWHE2-2	Heat Exchanger	Pressure drop Tube side	[Bar]	2 and 2
SWHE2-2	Heat Exchanger	Pressure drop Shell side	[Bar]	0.2

Table 8: Fixed Stream specifications according to the DMR process in Chapter 7

Tag	Property	Unit	Value
CMR2	Temperature	[°C]	-48.3
NG-SWHE2-1	Temperature	[°C]	-48.3
WMR2	Temperature	[°C]	-48.3
NG-SWHE2-2	Temperature	[°C]	-117
CMR2Vapor2	Temperature	[°C]	-117
CMRLiquid2	Temperature	[°C]	-117
NG-Valve	Temperature	[°C]	-153.4
CMR2V-Liquid1	Temperature	[°C]	-153.4
NG-Separator	Pressure	[Bar]	1.2
NGFeed	Molar Flow	[kgmole/h]	25650
NGFeed	Pressure	[Bar]	55

Table 9: Adjustable variables included in the optimization of the DMR process

Tag	Connections	Property	Units
Nitrogen-WMR	All the component streams in the WMR and CMR makes up for the composition in the WMR and CMR stream through the mixers MIXER1 and MIX-101 respectively. The composition in the streams are adjusted by manipulating the molar flow of the component streams accordingly to the desired amount of each component.	Molar Flow	[kgmole/h]
Methane-WMR		Molar Flow	[kgmole/h]
Ethylene-WMR		Molar Flow	[kgmole/h]
Propane-WMR		Molar Flow	[kgmole/h]
i-Butane-WMR		Molar Flow	[kgmole/h]
n-Butane-WMR		Molar Flow	[kgmole/h]
Nitrogen-CMR		Molar Flow	[kgmole/h]
Methane-CMR		Molar Flow	[kgmole/h]
Ethylene-CMR		Molar Flow	[kgmole/h]
Propane-CMR		Molar Flow	[kgmole/h]
WMR	Connects the stream properties to the MR-1 stream through “SET-3” and “BAL-3”	Pressure	[Bar]
WMR3	Determines the inlet pressure into SWHE-1 and K-100	Pressure	[Bar]
WMR5	Outlet stream of K-100 and is connected to the inlet of compressor K-100	Pressure	[Bar]
NG-SWHE2-1	Determines the inlet Temperature of SWHE2-1 and outlet of SWHE-1	Temperature	[°C]
CMR2Vapor2	Outlet stream of SWHE2-1 and inlet to SWHE2-2. The stream is in liquid phase	Temperature	[°C]
CMR2Liquid2	Liquid outlet stream of SEP2. The stream is entering SWHE2-1	Temperature	[°C]
CMR4	Determines the inlet pressure into SWHE2-1 and K-102	Pressure	[Bar]
CMR5	Outlet stream of compressor K-102 and inlet stream to cooler E-102	Pressure	[Bar]
CMR7	Outlet stream of compressor K-103 and inlet stream to cooler E-103	Pressure	[Bar]
CMR9	Outlet stream of compressor K-104 and inlet stream to cooler E-104	Pressure	[Bar]

The streams listed in Table 9 influence the process in different ways.

Component streams

The component streams decide the composition and mass flow in both the WMR and CMR circuits. The composition and mass flow in the two refrigeration circuits affect the cooling in the spiral wound heat exchangers, which is affecting the power consumption of the compressors and pumps as it can be seen from the theory in Chapter 2.6.

WMR

Determines the high pressure in the compression stages, which will affect the pressure ratio and energy consumption in the two-stage compression process. The pressure in this stream will also affect the vapor phase in the refrigerant.

WMR3

Determines the inlet temperature of SWHE-1, which at constant mass flow may determine the heat transfer in SWHE-1.

WMR5

Determines the intermediate pressure in the two-stage compression process. The intermediate pressure determines the energy use of compressor K-100 and K-101 and the pump P-100.

NG-SWHE2-1

Determines the inlet Temperature of SWHE2-1 and outlet of SWHE-1. Manipulation of this variable will affect the heat transfer in both spiral wound heat exchangers.

CMR2

Determines the inlet temperature into SEP2, which will determine the fraction of vapor and liquid in the stream, which again determines the capacities of both SWHE2-1 and SWHE2-2. The temperature in this stream will also affect the heat transfer in SWHE-1.

CMR2Vapor2

Determines the temperature between SWHE2-1 and SWHE2-2. By manipulating the temperature in CMR2Vapor2, the duty in SWHE2-2 will change, which will affect the pressure requirement of CMR2V-Liquid2, which is located after VLV-102.

CMR2Liquid2

Like CMR2Vapor2 this temperature affects the heat transfer in SWHE2-1. The temperature also determines how much the pressure needs to drop to achieve the needed temperature in order to mix with CMR2V-Liquid3 and cool the three streams in SWHE2-1.

CMR4, CMR5, CMR7 and CMR9

These streams determines the entire three stage compression process in order of pressure ratio at each of the compressors. CMR4 also determines the temperature of the CMR2V-Liquid2 stream, which is entering the shell side in both SWHE2-2 and SWHE2-1 in order to cool the hot streams that enter the tube side. Whether all of these streams are included in the optimization process or not is depending on the study.

5.4 Configuring the Derivative utility

In order to utilize the optimizer, the derivative utility needs to be configured. In order to optimize a realistic process, with a flow sheet that converges, the process needs certain constraints to uphold. The constraints are set according to each of the different cases and analyzed in order to validate the changes made in the parameters within the optimizer.

The objective value in the Prico process is set according to Eq. 8, which is similar to Eq. 7 from Chapter 4 with the exception of a small modification that includes pump work.

$$minf(x) = \frac{\dot{W}_{Comrpessors\ and\ Pump}}{\dot{m}_{LNG}} \qquad \text{Eq. 8}$$

It can be a challenging task to set the derivative utility to achieve an optimal realistic process. The ideal scenario would be to set high maximum and low minimum variable boundaries to provide the optimizer with a larger range of values to work with. It can be seen in the project Rødstøl (2014) that by having a huge gap in the variable boundaries may provide trouble within the flow sheet or the optimizer. However, tightening the variable boundaries and provide different variable starting values will assist the optimizer to work properly.

5.5 Configuring the optimizer

When the derivative utility is adjusted, the optimizer parameters needs to be configured in order to find an objective value that is both the presumed minimum and that is able to uphold the constraints. Considering that this project aims to test the Hyprotech SQP optimizer, time to converge is not as important as the objective value and its ability to uphold constraints. Therefore, two-sided gradient calculations will be performed instead of one-sided gradient calculations. The properties that are adjusted are listed with their default values in Table 10**,** and information in regards to each parameter can be seen in Chapter 3.5.2**.**

Table 10: Default values of the parameters in the Hyprotech SQP optimizer

Setup parameter	Default Value	Parameter ref.
Maximum Iterations	50	Chapter 3.5.2 A
Objective Scale Factor	0.01	Chapter 3.5.2 B
Accuracy Tolerance	1×10^{-4}	Chapter 3.5.2 C
Step Restriction	0.2	Chapter 3.5.2 D
Perturbation	0.001	Chapter 3.5.2 E
Maximum Feasible Point	5	Chapter 3.5.2 F

In order to obtain a good objective value that upholds the given constraints, adjustments of these parameters are necessary. Different sensitivity analyses are carried out in order to see how these values affect the objective value and its ability to uphold the constraints.

There are two termination reasons in the optimizer, which provides an objective value. Those termination reasons are the following:

- **Step Convergence**, which in general is pointing out that the optimizer is not able to uphold the set accuracy tolerance. Step Convergence as a termination reason, indicates that a step collapse below the step tolerance occurred during the optimization search.

- **OK**, which shows that the optimizer is able to converge to an objective value that is within the set accuracy tolerance.

After the studies in Chapter 6 were completed, a discovery was made in regards of the termination reasons. If the Step Restriction parameters is sufficient, the termination reason Step Convergence will provide the best result. However, if too low Step Restriction value causes the Step Convergence, the optimizer will provide a poor objective value.

In the graphs performed in these analyses, the two terminations reasons will be separated by colors.

- Step Convergence
- OK

It can be seen from Chapter 3.5.2 that after every optimization, the optimizer provides gradient evaluation, model evaluation, feasible point iterations and the total CPU time to converge to the objective value.

6 Case Study Prico process

To fulfill the case studies, the optimizer needs to be adjusted properly to each case in order to achieve a valid objective value that uphold the given constraints. First, an analysis of how to set up the Prico process in terms of the different optimizer parameters is fulfilled. After the first analysis, different process configurations and studies are carried out in order to investigate the process and to challenge the optimizer. The first study should be viewed as a systematic guide on how to set up the optimizer.

6.1 Prico Process with fixed intermediate and high-pressure

The Prico process in this study is as displayed in Chapter 5.1, with initial adjustable variable boundaries and variable values displayed in Table 11, and constraints displayed in Table 12. Improvements on the process are made as the studies continues in order to explore the capabilities of the optimizer.

6.1.1 Prico with fixed high and middle pressure and constant no set UA value

In the first study, a simple version of the Prico model with fixed intermediate and high pressure is considered. The process does not have a fixed UA value in the plate-fin heat exchanger, which makes it possible for the optimizer to keep a close temperature approach throughout the entire heat exchanger in accordance to the given constraints.

The variable boundaries should be set according to the assumed combination of variable values, which have been obtained by knowledge in regards to liquefaction processes. After a series of trial and error, the variable values and variable boundaries achieved are listed in Table 11**.**

Table 11: Manipulative variables with their variable boundaries utilized in the Prico process from Chapter 6.1

Tag	Property	Unit	Minimum	Initial Value	Maximum
Nitrogen	Molar Flow	[kgmole/h]	5000	12000	20000
Methane	Molar Flow	[kgmole/h]	5000	16000	25000
Ethylene	Molar Flow	[kgmole/h]	5000	25000	33000
Propane	Molar Flow	[kgmole/h]	2000	8000	15000
i-Butane	Molar Flow	[kgmole/h]	200	5000	10000
n-Butane	Molar Flow	[kgmole/h]	200	5000	10000
MR4	Pressure	[Bar]	1.2	5.25	8

The initial value of the constraints are determined by the variable values from Table 11. The constraints and their initial values can be seen in Table 12.

Table 12: Constraints utilized in the Prico process from Chapter 6.1

Tag name	Restriction	Minimum	Initial value	Maximum
P-F HX	Temperature approach	3	3.6232	Empty
MR4-MR4R	Temperature approach	6	17.6360	Empty

The constraint in P-F HX is set in order to avoid temperature cross in the heat exchanger, and to make the process more realistic, the MR4-MR4R temperature approach is set in order to avoid liquid inlet to the compressor K-100.

A. Iterations and Feasible Points

The Iterations and Feasible Points parameters are assisting the optimizer in finding the minimum value by allowing the optimizer to search and iterate more. By considering that the optimizer may need more iterations and feasible points as the study progresses, only values higher than the default values will be considered. It can be seen from Chapter 3.5.2 that a maximum iteration is the number of major iterations that the optimizer can utilize. A major iteration consists of a sequence of minor iterations. When adjusting the maximum iterations, it can be seen from Figure 14 that by increasing the maximum number of iterations, the optimizer provides the same objective value, which indicates that 50 major iterations is enough at this point.

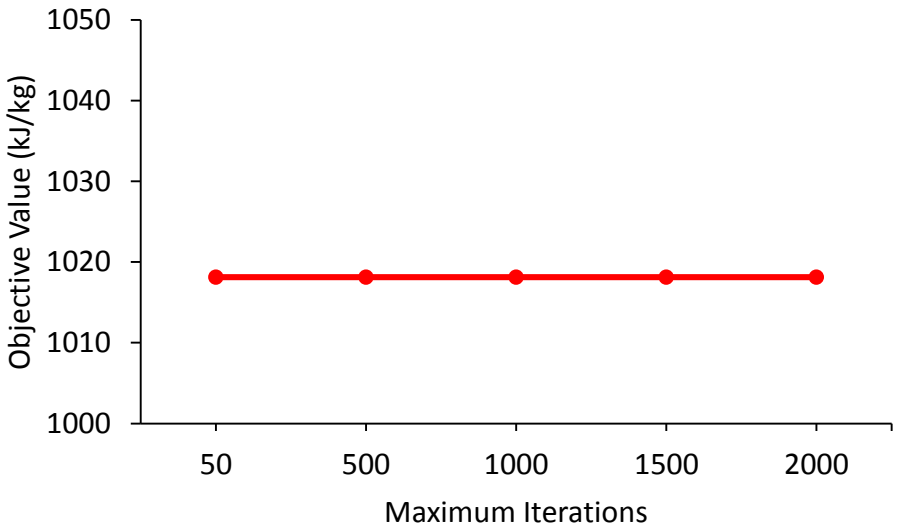

Figure 14: Adjustments in the maximum number of iterations according to the objective value in the Prico process

It can be seen from Chapter 3.5.2, that the maximum feasible point parameter is deciding the maximum number of iterations that can be utilized in the line search procedure. To

avoid the possibility that the optimizer terminates the search at a wrong minimum, this parameter needs adjustment. It can be seen from Figure 15 that the default value at 5 feasible points is too low for the optimizer to provide the optimum value. By adjusting the Maximum Iterations parameter, it can be seen that the optimizer is able to obtain another objective value. The new objective value stay stable when increasing the parameter, which indicates that the value needs to be adjusted from its default value.

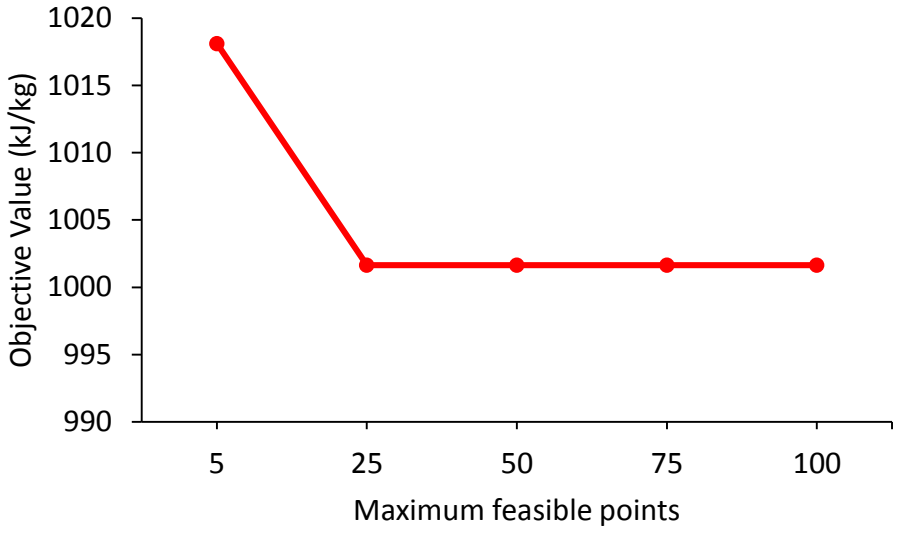

Figure 15: Adjustments of the maximum feasible points according to the objective value in the Prico process

Considering that this project aims to test the Hyprotech SQP optimizer in terms of capacity, the maximum iterations and feasible points will be adjusted very high. Time taken to convergence in Chapter 6.1 can be seen in Appendix G**.**

To be 100% sure that the number of maximum iterations and feasible points are not restricting the optimizer when modifications are made, the new values are set high. The new values are set as: Maximum iterations = 2000, Maximum feasible points = 500.

B. Objective Scale Factor

The Objective Scale Factor will influence the search of a minimum objective value and the optimizer constraints, as it can be seen from Chapter 3.5.2. The objective scale factor was tested as a logarithmic decrease in values from 1 to 1×10^{-9} and a final value at 0 at the end. By looking at Figure 16 and considering the constraint violations from Figure 17, the values in focus will be 1×10^{-1}, 1×10^{-6} and 0. The objective scale factor at 0 were able to obtain "OK" in the termination reason, and were also able to provide the best objective value with respect to constraint violations. It is important to note that when the Objective Scale Factor is set to 0, the optimizer is selecting a value for the Objective Scale Factor parameter.

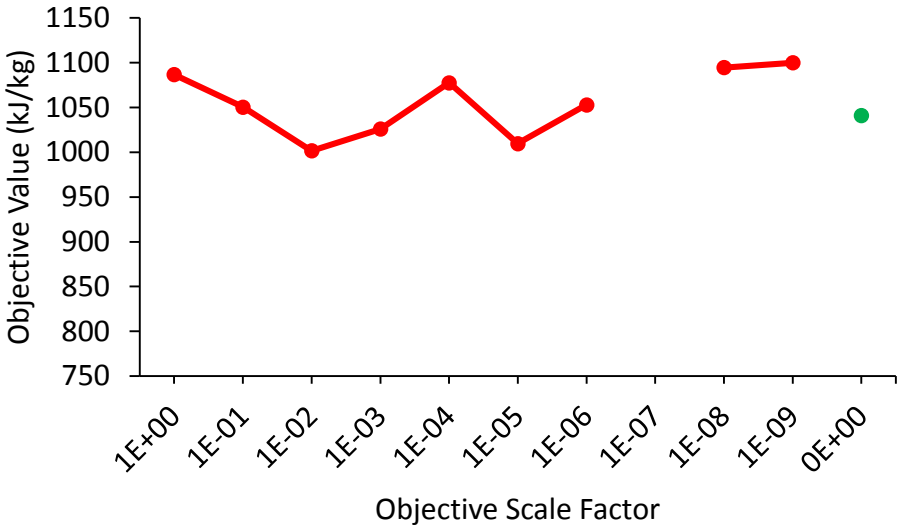

Figure 16: Adjustments of the Objective Scale Factor according to the Objective Value in the Prico process

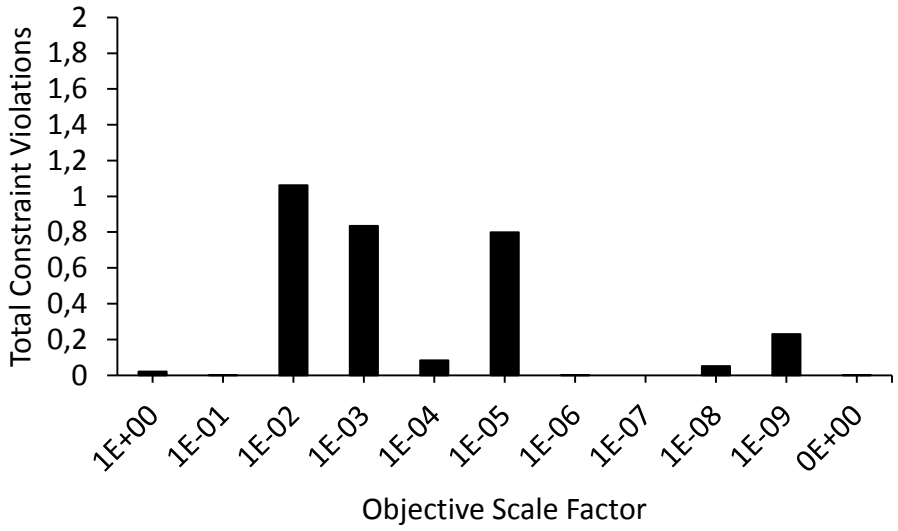

Figure 17: Total Constraint Violations according to the adjustment of the Objective Scale Factor in the Prico Process

C. Accuracy Tolerance

It can be seen from Chapter 3.5.2 that the accuracy tolerance determines how accurate the objective value is calculated. By setting a high accuracy tolerance value, the optimizer may provide a poor objective value compared to what it could have been if the accuracy tolerance value had been lower. If the accuracy tolerance is set too low, the optimizer may display step convergence as the termination reason. The step convergence indicates that the

optimizer is not able to provide an objective value that uphold the given accuracy. To find the maximum accuracy that the optimizer is able to provide at the given conditions and parameter values, iterations may be fulfilled until the border between “Step Convergence” and “OK” are found. However, the answer that contain the termination reason of “Step Convergence” will be more accurate than an answer that display the termination reason “OK” as long as the Step Restriction parameter value is sufficiently high.

Objective scale factor set to 0.1

While analyzing the objective scale factor, it could be seen that there were three points that needed to be further addressed in order to explore which objective scale factor that will provide the optimum objective value. The scale factors will be studied separately in descending order. Analyses of the objective scale factor with 0.1 in value can be seen in Figure 18 and Figure 19.

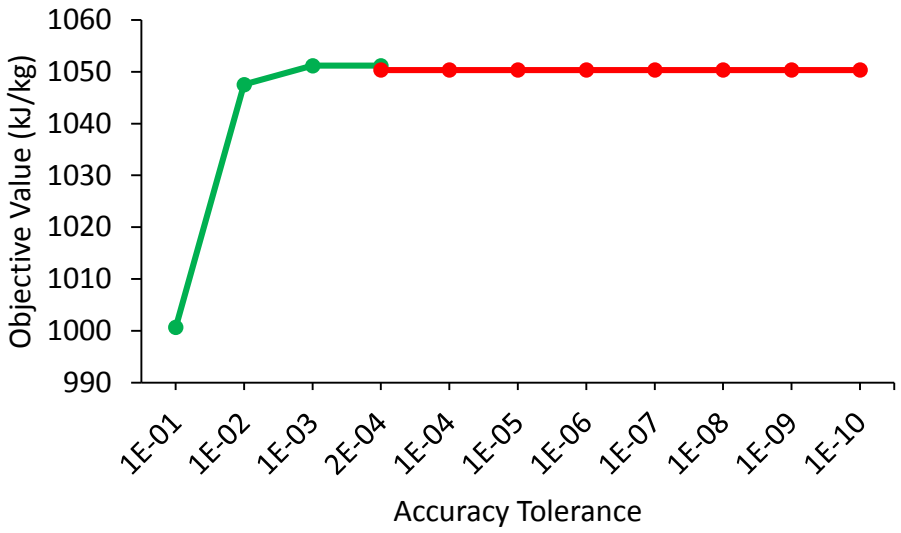

Figure 18: Adjustments of the Accuracy Tolerance according to the objective value in the Prico process when the Objective Scale Factor is set to 0.1

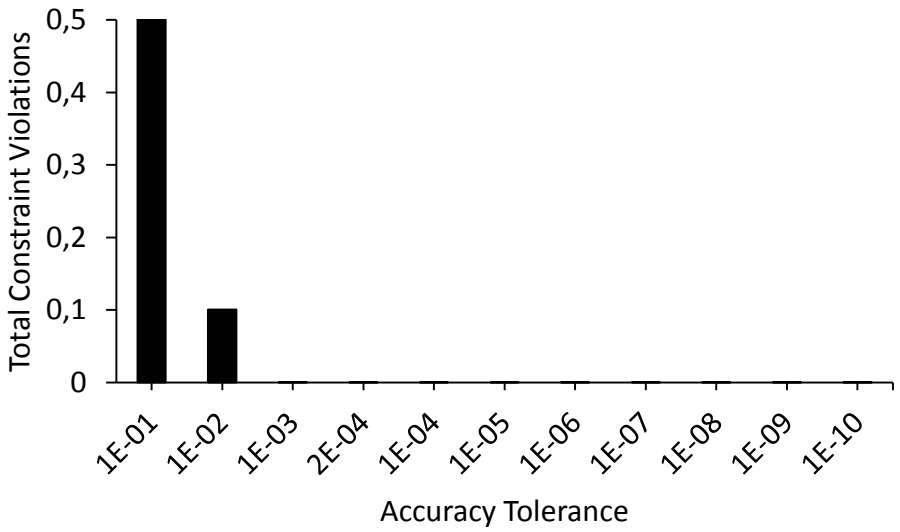

Figure 19: Total Constraint Violations according to adjustments of the Accuracy Tolerance in the Prico process when the Objective Scale Factor is set to 0.1

Studying the constraint violations provided in Figure 19**,** the violations stayed constant when the accuracy tolerance value reached 1×10^{-3} and descended. The results from Figure 18 and Figure 19 indicates that as expected, the objective values that had the termination reasons that displayed "step convergence" were able to provide the best objective value.

Objective scale factor set to 1×10^{-6}

Considering the case where the objective scale factor were set to 1×10^{-6} , it can be seen from Figure 20 that by having an accuracy tolerance at 3×10^{-4} and lower, the optimizer displayed the termination reason as "step convergence".

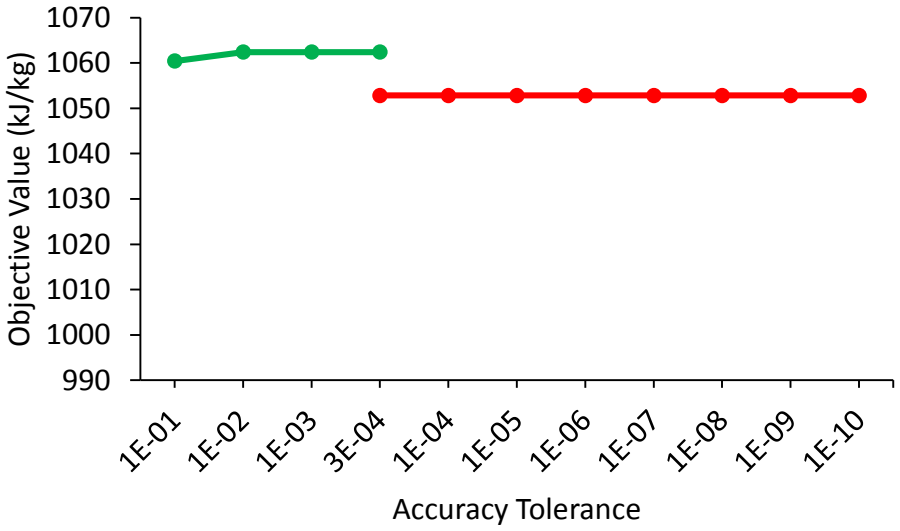

Figure 20: Adjustments of the Accuracy Tolerance according to the objective value in the Prico process when the Objective Scale Factor is set to 1×10^{-6}

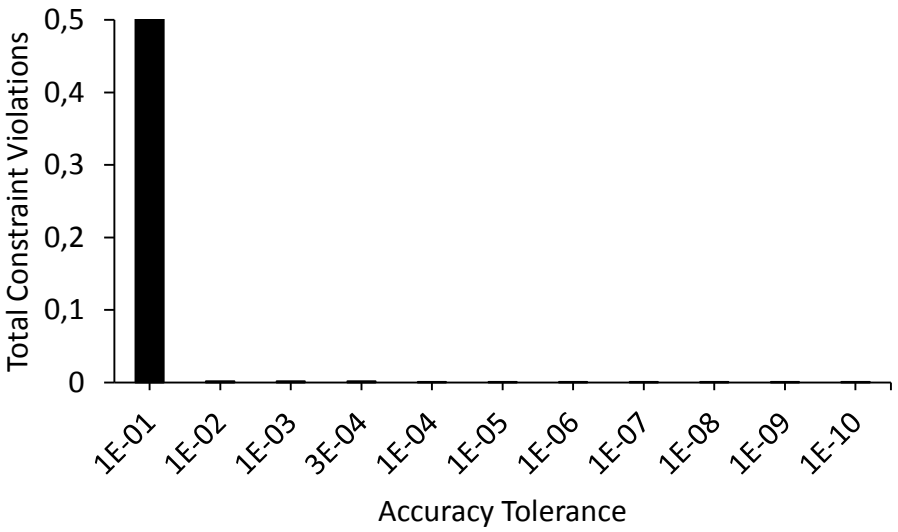

Figure 21: Total Constraint Violations according to adjustments of the Accuracy Tolerance in the Prico process when the Objective Scale Factor is set to 1×10^{-6}

Considering the constraint violations in Figure 21, the total constraint violations stayed at the same value when reaching the accuracy tolerance of 1×10^{-2} and below. Combining the objective value from Figure 20 with the constraint violations from Figure 21, the best results were achieved at "Step Convergence".

Objective scale factor set to 0

Considering the case where the objective scale value factor were set to 0 (which forces Hysys to choose the scale value), it can be seen by Figure 22 that the optimizer was able to display the termination reason as "OK" until the accuracy tolerance were set below 7×10^{-5}. Values beneath 7×10^{-5} had termination reason that displayed "Step Convergence".

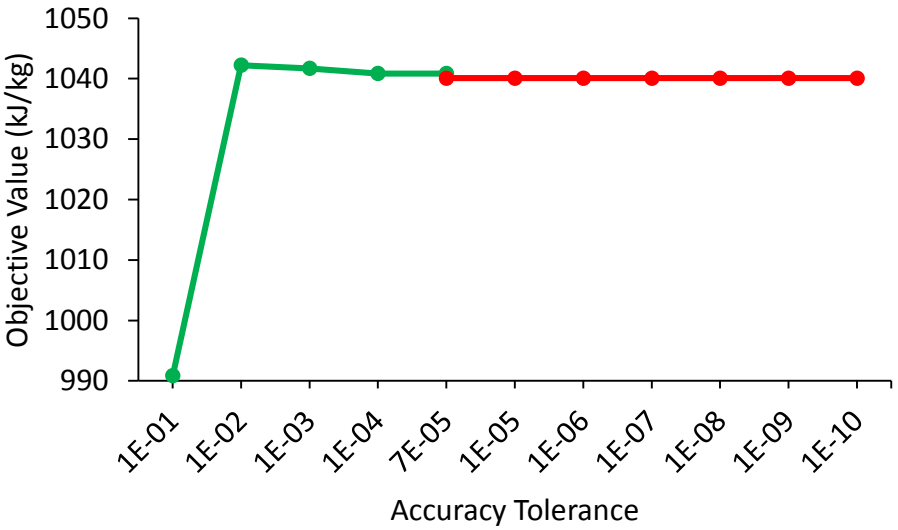

Figure 22: Adjustments of the Accuracy Tolerance according to the objective value in the Prico process when the Objective Scale Factor is set to 0

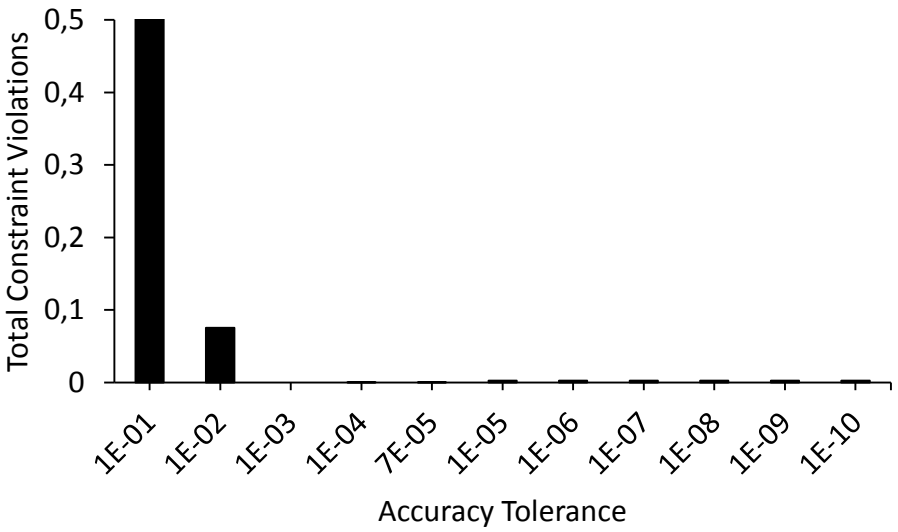

Figure 23: Total Constraint Violations according to adjustments of the Accuracy Tolerance in the Prico process when the Objective Scale Factor is set to 0

Considering the total constraint violations displayed in Figure 23, the constraint violations were lowest at the accuracy tolerance value 1×10^{-3}. However, considering that the total constraint violations were as low as 0.0027 at the objective values that displayed "step convergence" as termination reason, the optimum value is hard to choose in this case. The fact that the lowest constraint violations were achieved at 1×10^{-3} should be viewed as a coincidence.

Considering the three different Objective Scale Factors according to Constraint Violations and Objective value

Studying the three objective scale factors, the case where the objective scale factor was set to 0 provided the best accuracy and also the best objective value. Therefore, in continuing setting up the optimizer, the objective scale factor at 0 will be considered.

D. Step Restriction

Information in regards to the Step Restriction parameter can be seen in Chapter 3.5.2. The step restriction has a decent default value in the optimizer, however, when time is not an important factor compared to the objective value, the steps should not be restricted. Setting the step restriction to 1 or higher results in no step restriction. Therefore, the objective scale factor and accuracy tolerance tests were crosschecked with higher values as maximum step restriction to make sure that the maximum number of step restriction did not prevent the optimizer of reaching a lower minimum objective value.

The case that provided the lowest objective value with respect to constraint and in regards to objective scale function and accuracy tolerance had the following values:

Table 13: Parameter settings that provided the best Objective value with respect to constraint violations

Best values		Parameter Ref
Max. Iterations	2000	Chapter 3.5.2 A
Objective Sale Factor	0	Chapter 3.5.2 B
Accuracy Tolerance	0.00007	Chapter 3.5.2 C
Step Restriction	In scope	Chapter 3.5.2 D
Perturbation	0.001	Chapter 3.5.2 E
Max. Feasible Point	500	Chapter 3.5.2 F

An analysis in regards to Step Restriction carried out based on the values from Table 13 can be seen in Figure 24 and Figure 25 with respect to objective value and constraint violations respectively.

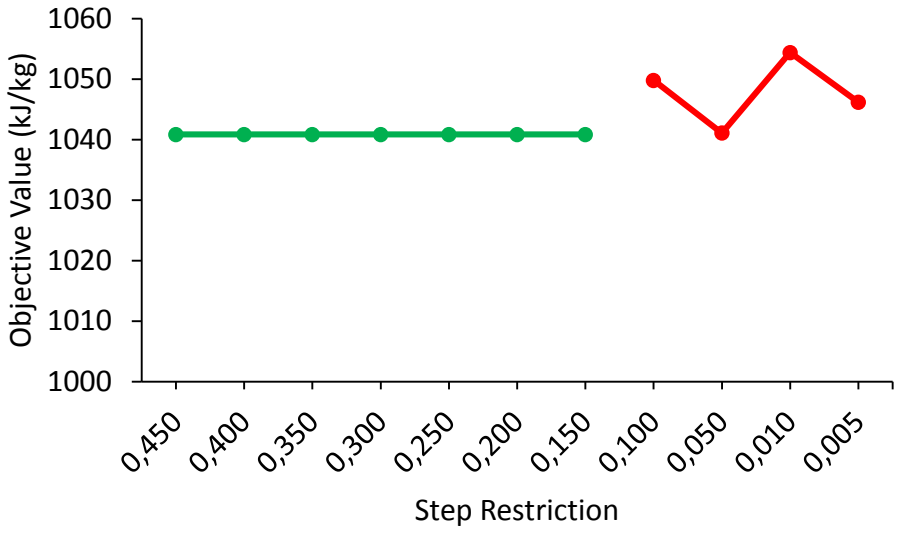

Figure 24: Adjustments of the Step Restriction according to the objective value in the Prico process when utilizing the parameter values from Table 9

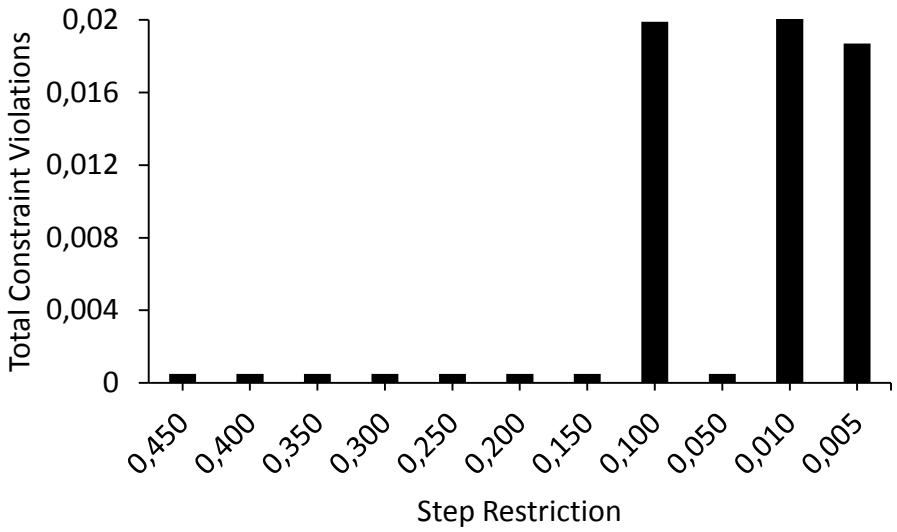

Figure 25: Total Constraint Violations according to adjustments of the Step Restriction in the Prico process when the utilizing the parameter values from Table 9

It can be seen that 0,150 is the lowest step restriction that the optimizer was able to manage in order to fulfill the given accuracy tolerance of 7×10^{-5} with a termination reason that display "OK". Studying Figure 24 in regards to the constraint violations from Figure 25, can it be seen that as soon as the termination reason displays "Step Convergence", the optimizer is unstable in terms of objective value.

It should be mentioned that the worst constraint violations in this case are very small in general, however, they do not uphold the given accuracy tolerance.

It is important to distinguish between the "Step Convergence" in this case compared to the case where the accuracy tolerance were analyzed. If the reason for "Step Convergence" is caused by an accuracy tolerance that is too low for the optimizer, while the other parameters are set at sufficient values, the optimizer will converge to a value that obtain the best accuracy tolerance possible. If the "Step Convergence" is caused by a step restriction that is too low, the optimizer may experience Maratos Effect, which is explained in detail in Chapter 3.4.

E. Perturbation

Information on the Perturbation parameter is found in Chapter 3.5.2. The Perturbation parameter is quite sensitive, so when analyzing the perturbation size the x-axis will not be logarithmic. This analysis will utilize the properties from Table 13 with an exception in the accuracy tolerance, which in this case is adjusted down to 1×10^{-4} in order to see if other Perturbation values can achieve similar accuracy. The results can be seen from Figure 26 and Figure 27 in regards to objective value and constraint violations respectively.

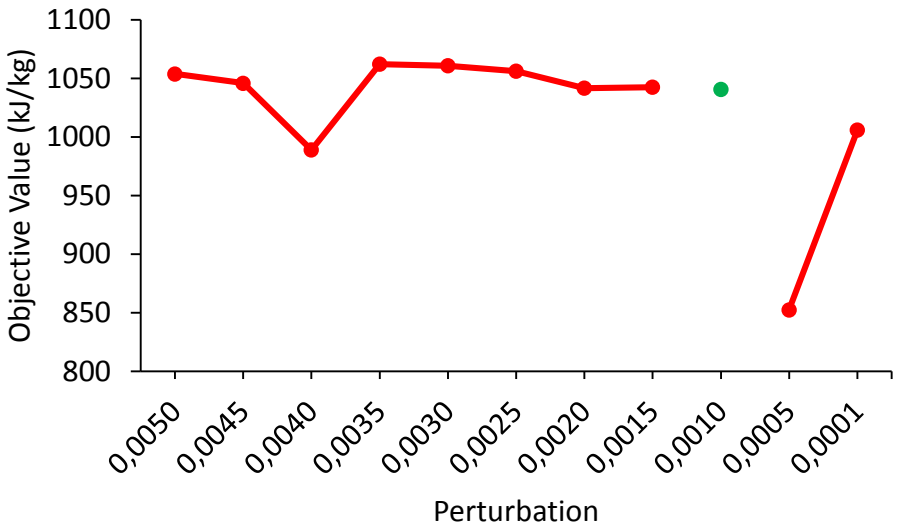

Figure 26: Adjustments of the Perturbation value according to the objective value in the Prico process

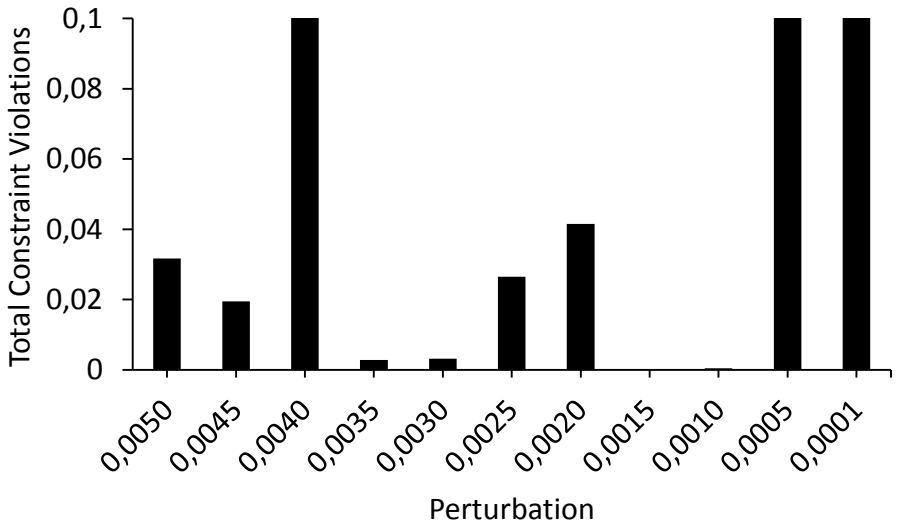

Figure 27: Total Constraint Violations according to adjustments of the Perturbation value in the Prico process

The only perturbation value that managed to obtain a good objective value was the default value at 0.001, which also had a termination reason that displayed "OK". This is to be expected considering the objective scale factor was adjusted according to that value.

At the obtained parameter values, the optimizer was able to provide the following objective value subjected to total constraint violations and a UA value in the heat exchanger (P-F HX):

$$Objective\ value = 1040.08\ kJ/kg$$

$$UA\ value = 101.9 MW/K$$

$$Total\ Constraint\ Violations = 0.0027$$

By utilizing Eq. 1 to set the pressure levels, the best-case scenario achieved the variable values displayed in Table 14.

Table 14: Variable values for the best parameters in the Prio process from Chapter 6.1.1

Tag	Property	Unit	Minimum	Final Value	Maximum
Nitrogen	Molar Flow	[kgmole/h]	5000	13341	20000
Methane	Molar Flow	[kgmole/h]	5000	15732	25000
Ethylene	Molar Flow	[kgmole/h]	5000	26138	33000
Propane	Molar Flow	[kgmole/h]	2000	6919	15000
i-Butane	Molar Flow	[kgmole/h]	200	289	10000
n-Butane	Molar Flow	[kgmole/h]	200	10000	10000
MR4	Pressure	[Bar]	1.2	6.75	8

6.1.2 Analysis of molar flow in the n-Butane stream

It can be seen from Table 14 that the molar flow of n-butane in the best case scenario has its value at the maximum of its boundaries. When a value is at the maximum of its boundaries, it should be safe to assume that the optimizer may provide a lower objective value if the maximum boundary is increased. The analysis in regards to both objective value and constraint violations can be seen in Figure 28 and Figure 29 respectively.

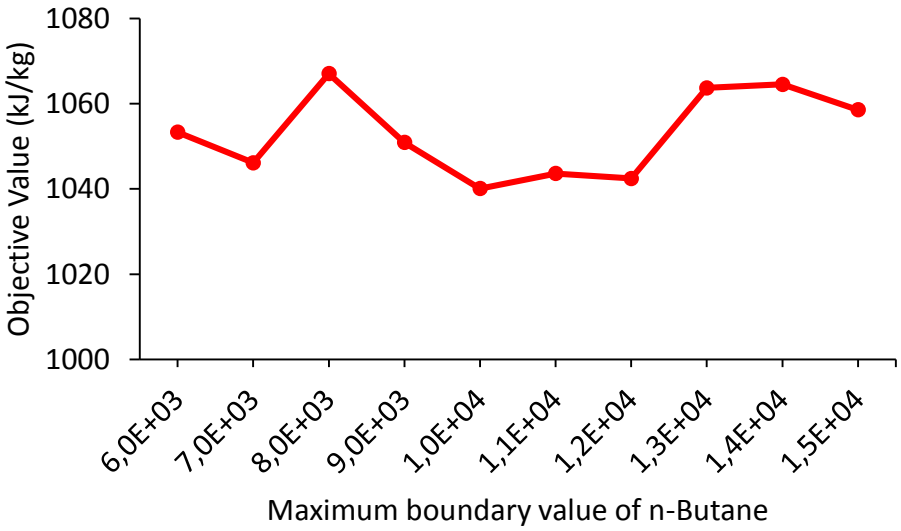

Figure 28: adjustment of the maximum boundary value of n-Butane according to the parameters from Table 9 with respect to the Objective value

It can be seen from Figure 28 that while utilizing a boundary value at 10 000, the optimizer was able to provide the optimum objective value in accordance with the constraints in Figure 29.

It is clear that the optimizer is not providing the global minimum with the given optimizer parameters, variable boundaries, variable values and constraints. By adjusting the boundary value of n-Butane, the optimizer parameter also needs to be adjusted for each step.

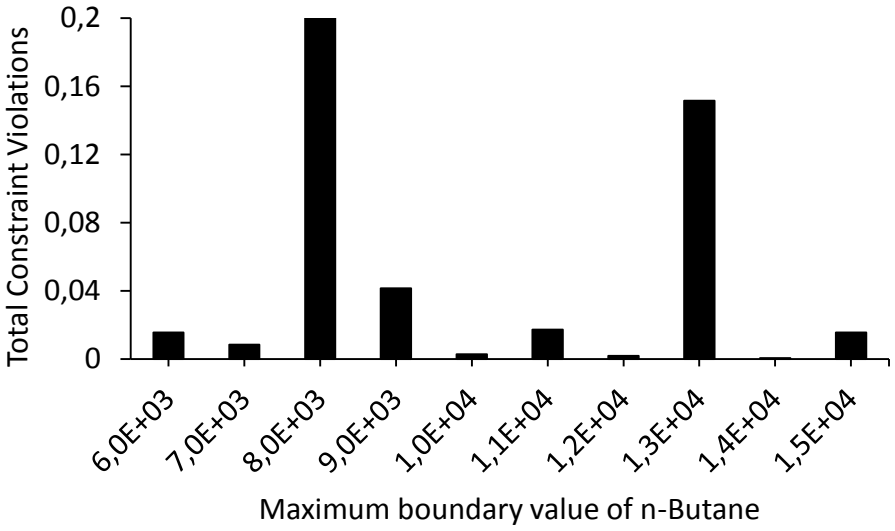

Figure 29: Total Constraint Violations according to adjustment of the maximum boundary value of n-Butane

In regards to this analysis, looking more into the Prico process, the n-butane boundary value at 10 000 will stay constant.

6.1.3 The importance of the initial variable value in the Prico process

To explore the capabilities of the optimizer to start from different initial values, ten random start values of the optimizer was created by utilizing the function in Microsoft excel that creates random numbers.

Considering the molar flow of the different component streams which makes up for the MR composition, no decimals were considered since these numbers have high value. For the component streams, the following function was utilized:

$$= RANDBETWEEN(Lower\ boundary\ ; Upper\ boundary)$$

For the MR4 pressure variable, decimals were needed in order to have a higher number selection. The following function was utilized:

$$= RANDBETWEEN(Lower\ boundary\ ; (Upper\ boundary - 1)) + RAND()$$

Where RANDBETWEEN is providing whole digits, while the $RAND()$ function creates a high number of decimal between the values 0 and 1.

The result from this study can be viewed in Appendix F. It is clear that the initial variable

values have an influence on the objective value and its ability to uphold constraints. Both the objective value and total constraint violations have large aviation from the best case value. This signifies the importance of sticking to the same initial values each time an optimization is performed when adjusting the optimizer parameters.

6.1.4 Different Process Temperatures

At an FLNG unit, the environment determines the process temperature, but the equipment within the process may also play an important role. At the previous studies, the process temperatures has been set to be 15°C. While these temperatures are achievable in cold climates, there will be cases where the process temperature will be higher.

In this study, consider three different process temperatures at 5°C, 15°C, 25°C and 35°C. The objective value, UA value in the heat exchanger and total constraint violations can be seen in Table 15, and an analysis in regards to the manipulative variables can be seen in Table 16**.**

Table 15: Results from Optimization according to different process temperatures

Process Temperature	UA value (P-F HX)	Constraint Violations	Objective Value
5°C	88280 kW/C	0.0013	946.61 kJ/kg
15°C	101900 kW/C	0.0027	1040.08 kJ/kg
25°C	103700 kW/C	0.0106	1162.77 kJ/kg
35°C	109700 kW/C	0.0051	1297.39 kJ/kg

Table 16: Refrigerant composition and variable values after process optimization according to different process temperatures

TAG	Unit	5°C	15°C	25°C	35°C
Nitrogen	%	17,13	18,42	17,66	17,60
Methane	%	24,81	21,72	21,36	20,18
Ethylene	%	34,34	36,09	36,71	35,29
Propane	%	12,68	9,55	2,86	2,55
i-Butane	%	0,31	0,40	11,22	11,81
n-Butane	%	10,73	13,81	10,19	12,58
MR1	[kgmole/h]	63795	72420	74987	79445
MR4	[Bar]	5.97	6.75	6.36	6.22

In order to obtain the objective values in Table 15, sensitivity analyses were carried out to obtain the suitable Objective Scale Factors, which resulted in the final objective values.

It can be seen that the objective values from Table 15 increase as the process temperature increase. By considering the process temperature at 5°C as a base case, the changes in the objective and UA values by adjusting the process temperature can be seen in Table 17**.**

Table 17: Changes in the objective and UA values as the process temperature increases. Base case is set to be 5°C (100%), both the intermediate and high pressure is fixed.

Process Temperature	Changes in the objective value	Changes in the UA value
5°C	100.00 %	100.00 %
15°C	109.87 %	115.43 %
25°C	122.84 %	117.47 %
35°C	137.06 %	124.26 %

It can be seen from Table 15 and Table 17 that both the objective and UA values increase as the process temperature increase. However, the UA value does not increase in the same manner as the objective value.

The reason for the smaller increase in the UA value, especially from 15 to 25 is that the low-pressure value is decreasing, which makes it possible for the process to maintain a low flow through the heat exchanger. However, with a lower pressure in the low-pressure stream, the pressure ratios in the compressors will increase in order to reach the defined intermediate and high pressure. A higher pressure ratio may result in a lower increase in the UA value, but the objective value will be affected, as the objective function includes compressor work as it can be seen from Eq. 8.

The increasing molar flow in the refrigerant stream and varying low pressure can be seen from Table 16. It can also be seen from Table 16 that the amount of heavier hydrocarbons in the refrigeration circuit increases drastically compared to the amount of lighter hydrocarbons as the process temperature increases. This is because the need for refrigerant components that vaporize at higher temperatures are needed to cool the high temperature streams that enter the Plate-Fin Heat Exchanger.

6.2 Prico with adjustable compression stages

To improve the objective value in the Prico model, the intermediate and high pressures was included in the optimization variables. By including the intermediate and high pressures among the optimization variables will allow the optimizer to adjust the pressure ratio according to the inlet temperatures, which may improve the result, as it can be seen in the theory in Chapter 2.4. The list of the optimization variables can be seen in Table 18.

6.2.1 Prico with adjustable intermediate and high pressures

Viewing the result from study the study in Chapter 6.1.1, has it been made clear that high step restriction, max.iteration and feasible point values have been providing the best results in combination with low accuracy values.

The manipulative variable boundaries, initial variable values and the constraint as a result from the initial values can be seen in Table 18 and Table 19 respectively.

Table 18: Manipulative variables with their variable boundaries utilized in the Prico process from Chapter 6.2

Tag	Property	Unit	Minimum	Initial Value	Maximum
Nitrogen	Molar Flow	[kgmole/h]	5000	12000	20000
Methane	Molar Flow	[kgmole/h]	5000	16000	25000
Ethylene	Molar Flow	[kgmole/h]	5000	25000	33000
Propane	Molar Flow	[kgmole/h]	2000	8000	15000
i-Butane	Molar Flow	[kgmole/h]	200	5000	10000
n-Butane	Molar Flow	[kgmole/h]	200	5000	10000
MR4	Pressure	[Bar]	1.2	5.25	8
MR5	Pressure	[Bar]	9	15.96	30
MR9	Pressure	[Bar]	31	45.50	60

The values in Table 18 have been selected according to uphold the constraint boundaries in Table 19.

Table 19: Constraints utilized in the Prico process from Chapter 6.2

Tag name	Restriction	Minimum	Initial value	Maximum
P-F HX	Temperature approach	3	3.6232	Empty
MR4-MR4R	Temperature approach	6	17.6360	Empty

From the study performed in Chapter 6.1.1 has it been made clear that the only parameters that needs adjustment in order to reach the minimum objective value are the Objective Scale Factor and the Perturbation, given that the other parameters are set to sufficient values, described in Chapter 6.1.1.

After several trials and errors, the parameter values from Table 20 were utilized in order to obtain the minimum value.

Table 20: Optimizer parameters chosen in order to achieve the best objective value with respect to constraints according to the Prico process in Chapter 6.2

New Optimizer parameters		Parameter Ref
Max. Iterations	2000	Chapter 3.5.2 A
Objective Sale Factor	1	Chapter 3.5.2 B
Accuracy Tolerance	1×10^{-8}	Chapter 3.5.2 C
Step Restriction	1	Chapter 3.5.2 D
Perturbation	0.0026	Chapter 3.5.2 E
Max. Feasible Point	500	Chapter 3.5.2 F

After the process had been optimized by utilizing the values from Table 20, the following UA value in the heat exchanger (P-F HX) and objective value were obtained:

$$UA = 100360\text{kW/K}$$

$$Objective\ value = 1038.49kJ/kg$$

$$Total\ Constraint\ Violations = 0.0036$$

The obtained variable values after the optimization can be seen in Table 21**.**

Table 21: Variable values according to the best case scenario from the Prico process in Chapter 6.2

Tag	Property	Unit	Minimum	Final Value	Maximum
Nitrogen	Molar Flow	[kgmole/h]	5000	11775	20000
Methane	Molar Flow	[kgmole/h]	5000	16573	25000
Ethylene	Molar Flow	[kgmole/h]	5000	27160	33000
Propane	Molar Flow	[kgmole/h]	2000	5612	15000
i-Butane	Molar Flow	[kgmole/h]	200	5714	10000
n-Butane	Molar Flow	[kgmole/h]	200	7331	10000
MR4	Pressure	[Bar]	1.2	5.64	8
MR5	Pressure	[Bar]	9	17.54	30
MR8	Pressure	[Bar]	31	35.93	60

Viewing the optimized values from Table 21 can it be seen that the high pressure has been significantly lowered compared to the values that were utilized before optimization, which can be seen from Table 18. It is also important to note that the pressure ratios in the compressors no longer obey the geometric mean from Eq. 1, which can be seen from the pressure difference between MR4, MR5 and MR8. The reason for this is that the inlet temperature to the first compressor at MR4 is lower than the MR5 temperature.

6.2.2 Varying process temperatures

While the different process temperatures in Chapter 6.1.4 resulted in higher flowrates of the refrigerant stream, which resulted in higher UA values in the heat exchanger, the varying process temperatures may have another impact when the intermediate and high pressures in the process can be manipulated.

Table 22: Results from Optimization according to different process temperatures from the Prico process in Chapter 6.2

Process Temperature	UA value (P-F HX)	Constraint Violations	Objective Value
5°C	101700 kW/C	0.0023	925.79 kJ/kg
15°C	103600 kW/C	0.0036	1038.49 kJ/kg
25°C	112500 kW/C	0.0057	1150.27 kJ/kg
35°C	93980 kW/C	0.0053	1331.85 kJ/kg

Table 23: Refrigeration components and variable values after process optimization according to different process temperatures from the Prico process in Chapter 6.2

Tag	Unit	5°C	15°C	25°C	35°C
Nitrogen	%	16,12	15,88	16,27	15,72
Methane	%	23,39	22,35	21,30	22,61
Ethylene	%	35,66	36,62	35,40	31,50
Propane	%	12,90	7,57	6,03	5,46
i-Butane	%	0,28	7,70	8,50	12,06
n-Butane	%	11,65	9,88	12,50	12,66
MR1	[kgmole/h]	71845	74165	78525	73462
MR4	[Bar]	5.82	5.64	5.79	4.97
MR5	[Bar]	16.72	17.54	18.73	21.53
MR8	[Bar]	34.82	35.93	37.67	45.63

Table 24: Changes in the objective and UA values as the process temperature increases. Base case is set to be 5°C (100%).

Process Temperature	Changes in the objective value	Changes in the UA value
5°C	100.00 %	100.00 %
15°C	121.17 %	101.87 %
25°C	124.25 %	110.62 %
35°C	143.86 %	92.41 %

It can be seen from Chapter 6.1.4 that when the intermediate and high pressures are fixed, the UA value in the heat exchanger increased as the process temperature increased, even though the degree of increase in the UA value was affected by the low-pressure variable.

When the intermediate and high pressures are included as optimization variables, the results differs, as it can be seen from Table 22 and Table 24. The most noteworthy change in terms of UA value is when the process temperature is set to be 35°C. As the process temperature changes from 25°C to 35°C, the UA value decreases as a result of lower flow in the refrigerant circuit, as it can be seen from Table 23. Lower flow in the refrigeration circuit leads to lower requirement of heat transfer in order to cool the refrigeration stream as it enters the P-F HX at the hot side. To compensate for the lower refrigerant mass flow, the process operates at higher pressure differences, which affects the vapor/liquid equilibrium in the refrigeration stream. An important notification is the higher amount of heavier hydrocarbons in the refrigerant composition as the process temperature increases. The reason that the refrigerant composition contains a higher amount of hydrocarbons is because the warm inlet streams is at higher temperatures, which increase the need for a larger amount of components that has a higher boiling point, as it can be seen from Table 1.

It is clear that while having fixed intermediate and high pressures, the process were able to utilize more energy in the heat exchanger as oppose to the process that had varying intermediate and high pressures, as it can be seen from Table 15 and Table 22 respectively. Considering these results and the objective function in Eq. 8, it may seem that the optimizer is prioritizing to adjust the pressure values instead of the composition.

6.3 UA values in plate-fin heat exchangers.

In order to validate the results achieved in Chapter 6, an analysis in regards of the UA values in the plate-fin heat exchanger is necessary.

A typical dimension of a Plate-fin heat exchanger core is $(1220 \times 1630 \times 7780)mm^3$, an LNG train that has a capacity between 1 to 1.25 MMTPA, eight of these cores are typical (Talib & Price 2011). Typical surface area density on an aluminum P-F heat exchanger is $1500m^2/m^3$ (Thulukkanam 2013) respectively. The U-value may differ in regards to the streams crossing in the heat exchangers. A reasonable U-value for a P-F heat exchanger is between $500 - 1000\frac{W}{(m^2 \times C)}$.

In regards to the Prico process in Chapter 6.1 and 6.2, the capacity is at 3.46 MTPA, which makes it reasonable to place 24 boxes in the cooling process considering that 1 to 1.25 MTPA train utilize 8 boxes. Using the information above, the following UA value is obtained.

$$UA = \frac{\left((1.220 \times 1.630 \times 7.780)m^3 \times 24 \times 1500\frac{m^2}{m^3} \times (500\ to\ 1000)\frac{W}{(m^2 \times K)}\right)}{1000W/kW}$$

$$UA = (278483\ to\ 556967)\frac{kW}{K}$$

This UA range is far larger than the calculated UA values obtained in Chapter 6.1 and Chapter 6.2, which signifies that the result obtained can be viewed as valid results in regard to the heat transfer in the plate-fin heat exchanger.

6.4 Summary of Chapter 6

In regards to the termination reason is it important to distinguish between the reasons that "Step Convergence" occur. By setting an accuracy value that the optimizer is not able to achieve, the optimizer will obtain the most accurate objective value that is possible for the optimizer to obtain within the given parameter specifications and derivative settings. If the accuracy tolerance cannot be achieved because the step restriction is set too low, thus providing "Step Convergence", the optimizer may experience Maratos Effect, which the optimizer is unable to exit from, as the relaxed steps are restricted to an insufficient value. The Maratos effect is explained in Chapter 3.4.3. Too low step restriction value will affect the optimization result in a negative manner, as the Merit function is unable to exit local minimums that may provide a high objective value or constraint violations. The Merit function is explained in Chapter 3.4.2.

Considering Chapter 6.1.2 and Chapter 6.1.3 can it be seen that changes in either the initial variable values or the variable boundaries has a great influence on the optimization process. Considering these findings is it easy to conclude that in order to tune the optimization parameters, the process needs to be reset to the initial condition after an optimization has been performed.

Chapter 6.1.4 studies the effect that different process temperatures have on the objective value, UA-value and variable values when the intermediate and high pressures variables are fixed. The objective value increased as the process temperature increased, however, even though the UA value increased with increasing process temperature, the increase were varying. The reason for the varying increase in the UA value is caused by the low-pressure variable, which affect the mass flow of the refrigeration, causing less or more increase in the mass flow in the refrigeration streams as it may increase or decrease the pressure ratio in the compressors. The amount of heavier hydrocarbon in the refrigeration stream increased as the process temperature increased, the reason for this is that the refrigerant demands components that vaporize at higher temperatures in order to cool the high temperature streams.

Chapter 6.2.2 studies the effect that different process temperatures have on the objective value, UA-value and variable values when the intermediate and high pressures variables are included as adjustable variables in the optimization process. Similar to the study in Chapter 6.1.4, the objective value increased as the process temperature increased, however, in this study, the UA value were at its lowest value at the highest process temperature. The reason is that in this model, the optimizer were able to control the pressure ratios to a larger degree, deciding to increase the pressure ratio rather than increasing the refrigerant mass flow. This is a poor decision of the optimizer considering that the objective value were higher than in Chapter 6.1.4, which had fixed middle and high-pressure variables. This issue should be noted when optimizing with the Hyprotech SQP optimizer.

The UA values obtained in Chapter 6 is within the maximum value that it should be for a plate-fin heat exchanger, making the results valid, which can be seen from Chapter 6.3.

Comparing results concerning the process temperatures in the process with fixed and adjustable pressure variables, which can be seen in Table 15 in Chapter 6.1.4 and Table 22 in Chapter 6.2.2 respectively, the objective values show minimal improvements from when the pressure variables were excluded and concluded in the process. Considering the temperatures at 35°C, the process with fixed pressure variables provided better objective value than the process with adjustable pressure variables. This result indicates that the Hyprotech SQP optimizer results are unstable and process simplifications should be made in order to assist the optimizer.

7 Case Study DMR process

The DMR process in this study is as shown in Chapter 5.2, with adjustable variables shown in Table 9 and explained under the table, which can be seen in Chapter 5.3.2. Considering the results for the Prico process, the DMR process is expected to provide challenges in regards of optimization. Improvements and adjustments in regards to the DMR process design will be made as the study progresses.

APCI states that in the WMR circuit in the DMR process, the warm mixed refrigerant consist of components from Table 2 in Chapter 2.3 (Bukowski et. al 2011). In the first part of this study, the WMR circuit will also contain a Nitrogen stream to observe the degree that the optimizer will include Nitrogen in the WMR circuit. In regards to the refrigerant conditions before it enters the first spiral wound heat exchanger (SWHE-1), it has been stated that if the refrigerant is fully liquefied, it gets evenly distributed in the tubes, while if it contains a two-phase flow with vapor fraction, the distribution might become uneven. Updated information in regards to the subject has stated that a two-phase flow with vapor fraction is acceptable (Roberts et al.). In regards to these statements, the DMR process will be optimized according to 3 different modifications in Chapter 7.1 and 7.3. These modifications will also show whether the optimizer is making the logical decisions or not. Considering the constraints from Table 27, the three modifications can be seen in Table 25.

Table 25: Modifications performed in the DMR process with overview over chapters according to each modification

Chapters	Constraints		Comments
	WMR7	WMR1	
7.1, 7.1.1 and 7.3.1	Activated	Deactivated	SWHE-1 may receive two-phase flow; E-101 will receive 100% vapor phase flow.
7.1.2 and 7.3.2	Deactivated	Deactivated	Both SWHE-1 and E-101 may contain two-phase flow.
7.1.3 and 7.3.3	Deactivated	Activated	SWHE-1 will receive 100% liquid flow; E-101 may receive two-phase flow.

The process that has both constraints deactivated is expected to achieve the lowest objective value. By optimizing the process in terms of the three different modifications, is it possible to observe if the optimizer is able to work as expected, and to see whether or not the optimizer will minimize the amount of Nitrogen in the WMR circuit. It is important to note that if the temperature between SWHE-1 and SWHE2-1 were not fixed, the WMR circuit would most likely lower the temperature between SWHE-1 and SWHE2-1 in order to utilize the Nitrogen component in the WMR circuit.

In this Chapter, the objective value that has included pump power does not have included pump power in the objective function; the pump power has been added in retrospect.

7.1 DMR with fixed intermediate and high pressures

A similar guide as in the Prico process has been performed for the DMR process according to the settings where the WMR7 constraint is activated and the WMR1 constraint is deactivated.

This study will consider the upstream DMR process with a fixed variable temperature between the WMR cycle and the CMR cycle. By having a fixed temperature between the two cycles will make it possible to study whether the optimizer will down prioritize the amount of Nitrogen in the WMR cycle, as it should. The fixed temperature in NG-SWHE2-1 and CMR2 is selected according to specifications utilized in a DMR process with integrated NGL extraction, provided by Kusmaya (2012), which has a temperature of -48.3°C.

The pressure ratios in the compressor arrangements are calculated in regards to Eq. 1 from Chapter 2.4**.** Since the inlet pressure to the compressor arrangements are varying, the pressure ratio are calculated and exported to the compressors by the use of a spreadsheet. In this study, the pressure ratios in the compressors are not included as adjustable variables in the optimizer derivative.

The objective function is the same as in Eq. 7, and can also be seen below. The manipulative variables and constraints in this model can be seen in Table 26 and Table 27 respectively.

$$minf(x) = \frac{\dot{W}_{Compressors}}{\dot{m}_{LNG\ stream}}$$

The DMR process is by far a more challenging process than the Prico process and therefore, the boundary values requires more adjustment.

In order to adjust the variable boundaries, the initial variable values needs to be approximated to a certain extent. To approximate the initial variable values, the constraints need to be adhered to, and keeping the temperature pinch in the heat exchanger relatively close to its constraints will give a proper estimation of decent initial values. Since the DMR process is a mixed refrigerant process each adjustment in the refrigerant composition will affect the equality constant in the mixture, as explained in Chapter 2.3 and thereby making it a difficult task to find decent compositions in both the WMR and CMR circuits.

After a series of trial and errors, the initial variable values that have been selected can be seen in Table 26, and the constraints obtained from these variable values can be seen in Table 27**.** The objective value calculated by Eq. 7 is:

$$Objective\ value = \ 1476.13$$

Note that the objective value provided by the initial variables from Table 26 will not be used as comparison to improved objective values, since the adjustable variables are user-defined and not relevant to a real process. However, the results from the optimized processes will have valid values considering that the fixed variables from Table 7 and Table 8 from Chapter 5.3.2 are realistic.

Table 26: Manipulative variables with their variable boundaries in the DMR process studied in Chapter 7.1

Tag	Property	Unit	Minimum	Initial Value	Maximum
Nitrogen-WMR	Molar Flow	[kgmole/h]	10	250	1000
Methane-WMR	Molar Flow	[kgmole/h]	750	1500	10000
Ethylene-WMR	Molar Flow	[kgmole/h]	20000	27227	35000
Propane-WMR	Molar Flow	[kgmole/h]	3500	9900	15000
i-Butane-WMR	Molar Flow	[kgmole/h]	50	800	5000
n-Butane-WMR	Molar Flow	[kgmole/h]	50	800	5000
Nitrogen-CMR	Molar Flow	[kgmole/h]	7500	11000	15000
Methane-CMR	Molar Flow	[kgmole/h]	10000	16000	20000
Ethylene-CMR	Molar Flow	[kgmole/h]	10000	24000	30000
Propane-CMR	Molar Flow	[kgmole/h]	500	1100	2000
WMR3	Pressure	[Bar]	1	6	20
CMR4	Pressure	[Bar]	1	6	15

Table 27: Constraints utilized in the DMR process in Chapter 7.1

Tag name	Restriction	Minimum	Initial value	Maximum
WMR7	Vapor Fraction	1	1	Empty
WMR1	Vapor Fraction	Empty	0	0
SWHE-1	Temperature approach	3	11.12	Empty
SWHE2-1	Temperature approach	3	5.23	Empty
SWHE2-2	Temperature approach	3	11.55	Empty
WMR4-DP1	Superheat	6	23.96	Empty
WMR4-CMR1	Temperature approach	3	11.12	Empty
CMR4-DP2	Superheat	6	17.48	Empty

As it can be seen in Table 25, the WMR7 and WMR1 constraints is activated or deactivated based on which process modification that is optimized. When going through the setup of the optimizer, the WMR1 constraint is deactivated while the WMR7 constraint is activated.

When pre work for this study was performed, challenges occurred when optimizing. In order to be able to optimize the process, adjustment of the Objective Scale parameter is necessary. In this process, adjustment of the Objective Scale parameter were very challenging. In order to simplify the process, several modifications were tested. Eventually, one of the simplifications made optimization of the process simpler. The part of the WMR cycle, which can be seen from Figure 30 were causing challenges**.** All the compressors in the

process utilize a constant polytropic efficiency, which makes the process more realistic in regards to the fact that polytropic efficiencies consider heat loss during the calculations, forcing a lower adiabatic efficiency as the pressure ratio increase. The pump (P-100) can only utilize adiabatic efficiency, which eventually will make a huge iteration process, which in combination with the other variables requires quite accurate adjustment of either the objective scale value or the perturbation value. WMR7 is constrained to have a vapor fraction of 1, which will make the energy use in the pump significantly smaller than in the compressor K-101.

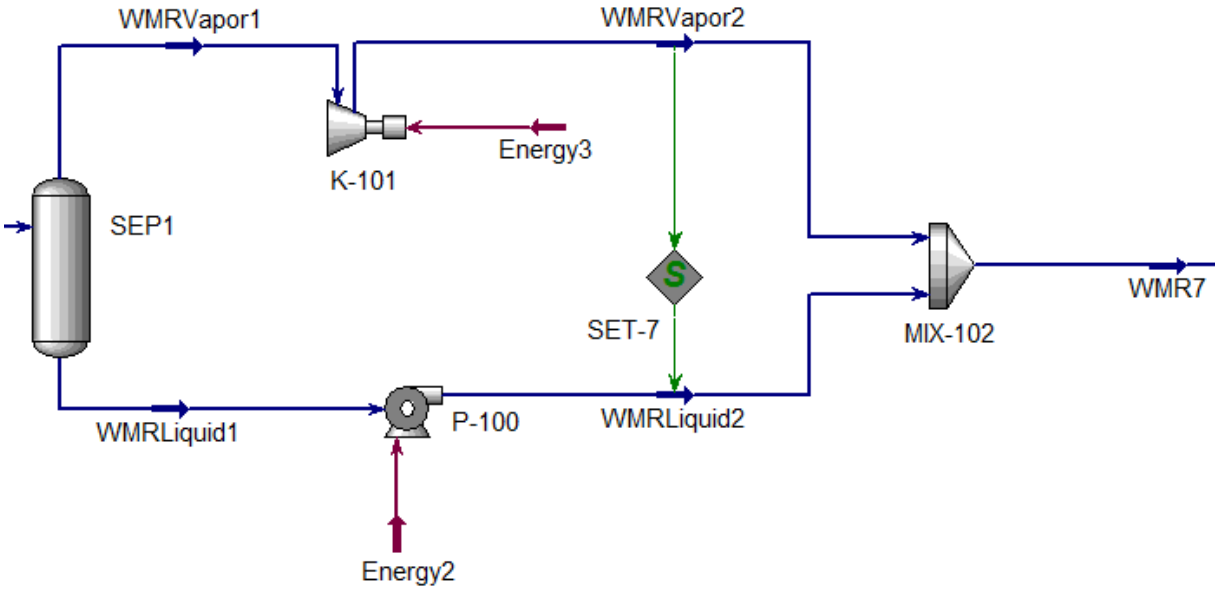

Figure 30: Separator and compressor in parallel in the DMR process. Both operates with differently defined efficiencies

In the Prico process, this part was not a problem for the optimizer. This indicates that the optimizer is easier to adjust when the process is simpler and the optimizer relates to fewer variables. This issue is the reason that Eq. 7 is utilized instead of Eq. 8 when calculating the objective value.

For the Prico process, an in depth study of the optimizer parameters were performed in order to configure the optimizer correctly. It was discovered that a high value maximum iterations and feasible points, a step restriction set to 0.2 or higher and a low value accuracy tolerance provided the best results.

In this study, the same analysis will be performed in order to analyze the results according to the DMR model to observe differences and similarities. The default start values can be seen in Table 28. These values are adjusted as each parameter have been studied. The best results from each of the parameters will make up for the parameter value that provides the best objective value.

Table 28: Default start values that are adjusted after every parameter study according to the best results

Default Optimizer parameters	
Max. Iterations	50
Objective Sale Factor	0.01
Accuracy Tolerance	0.0001
Step Restriction	0.2
Perturbation	0.001
Max. Feasible Point	5

A. Iterations and Feasible Points

In the Prico process the maximum number of iterations were not affecting the Objective value. It can be seen from Figure 31 that by adjusting the maximum number of iterations in the DMR process, the objective value and constraints are not improving.

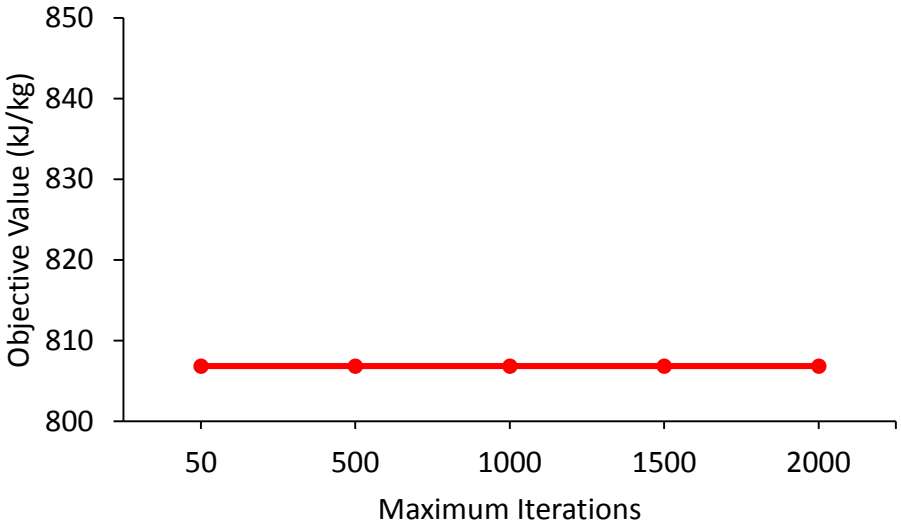

Figure 31: Adjustments in the maximum number of iterations according to the objective value in the DMR process from Chapter 7.1

From Figure 32, it can be seen that by increasing the maximum feasible points, the objective value is affected by the change, but as it seems, by increasing the maximum feasible points further than 25 does not affect the objective function or the constraints.

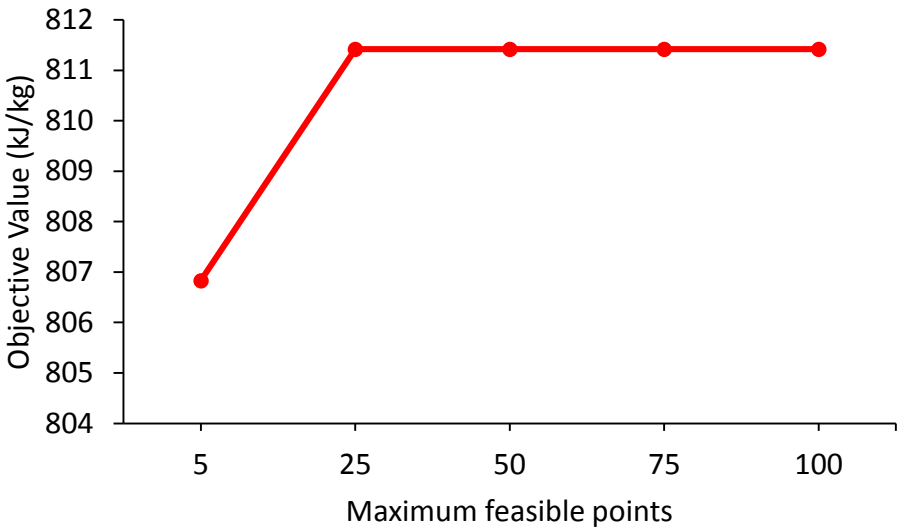

Figure 32: Adjustments in the maximum number of feasible points according to the objective value in the DMR process from Chapter 7.1

As in the Prico model, these values will be set high in order to avoid any potential trouble in regards to the number of feasible points and maximum iterations.

The new values will be set to maximum iterations = 2000, maximum feasible points = 500.

The time taken to converge can be seen in Appendix G**.** By considering the time spent to converge to an objective value will be important in order to see whether or not more feasible points or iterations is needed. Just to make sure, some of the analyses that use long time will also be tested with higher feasible points and iteration limits to see whether it has an impact on the objective value or the constraint violations.

The constraint violations obtained by utilizing the default values can be seen in Figure 33. Note that the y-axis contain high values.

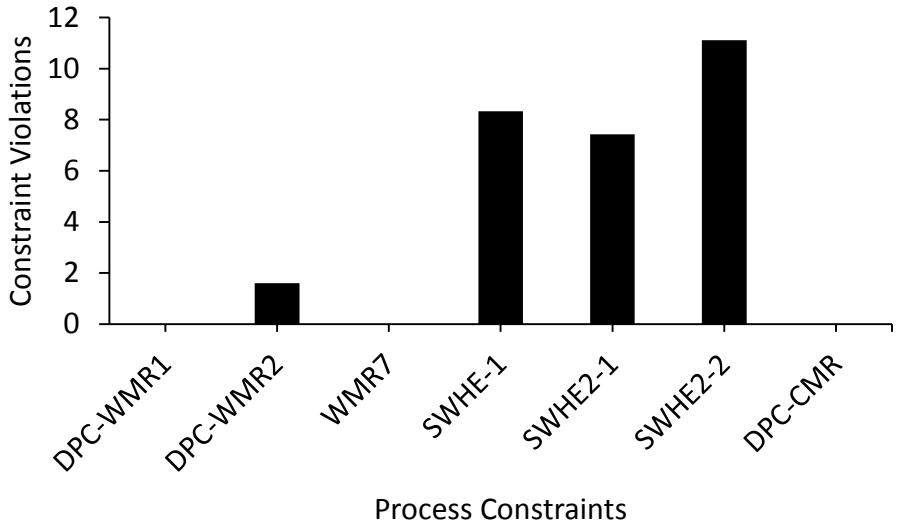

Figure 33: Constraint violations by optimizing with default values

B. *Objective Scale Factor*

From the Prico process is it clear that the Objective Scale Factor is an important parameter in regards of the final objective value and its constraint violations. The objective value were analyzed by utilizing a logarithmic decrease in the Objective Scale Factor value, which can be seen from Figure 34. An important note in regards of adjustments in the Objective Scale Factor value is that it is impossible to know properly whether a logarithmic or normal study should be performed. In Figure 34 and Figure 35, a logarithmic study is performed in order to see how unreliable the objective value and constraint violations are behaving when performing major changes.

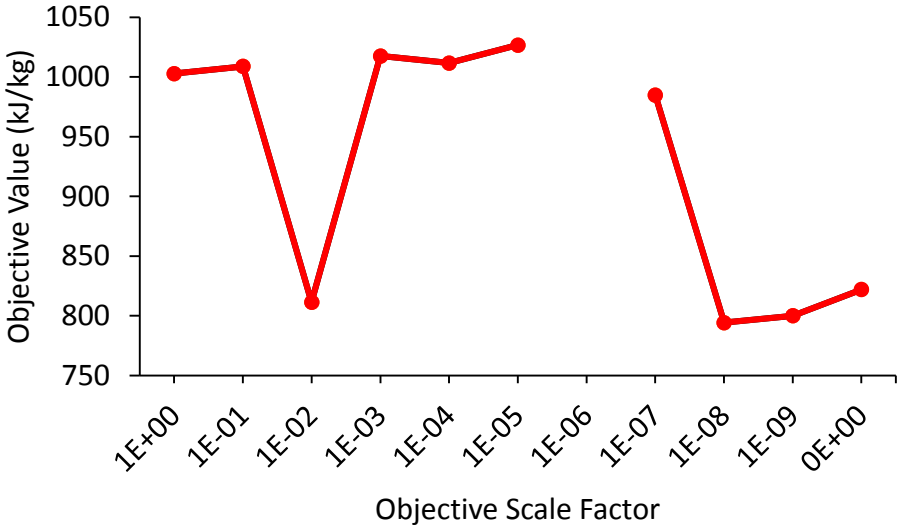

Figure 34: Adjustments of the Objective Scale Factor according to the Objective Value in the DMR process in Chapter 7.1

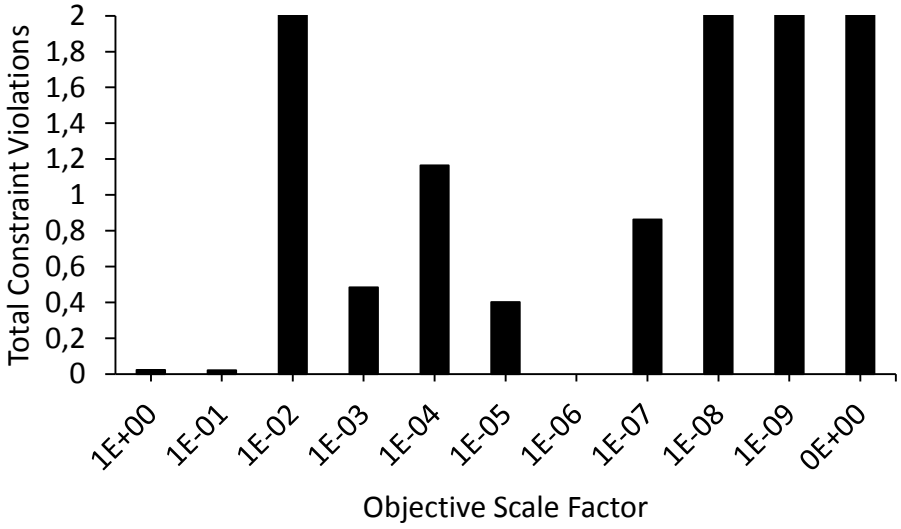

Figure 35: Total Constraint Violations according to the Objective Scale Factor from Figure 33

Viewing the results from the analysis, it can be seen that the lowest objective values are at the scale factors 10^{-2}, 10^{-8}, 10^{-9} and 0. However, to justify whether these objective values are valid or not, an analysis in regards to the constraints can be seen in Figure 35**.**

Figure 35 shows that the highest scale factors are more likely to uphold constraints than the lower ones, in this figure, the graphs that reach the value of 2, had up to 20 and over in total constraint violations. The time to converge were significantly higher when the Objective Scale Factor were set to a high value, which may indicate that the optimizer is able to find more minimum points at those values. Knowing from the Prico study that a Step Restriction value at 1 and a low Accuracy Tolerance value provides the best objective value, considering the results from the analysis in Figure 34 and Figure 35, the Hyprotech SQP configuration will have the objective scale factor set at 1.

In order to explore how accurate the objective value is, an accuracy tolerance and step restriction analysis are also carried out.

C. Accuracy Tolerance

Even though the optimizer result displayed the termination reason "Step Convergence" while utilizing an accuracy tolerance of 10^{-4} , higher Accuracy Tolerance values will be considered in order to see how accurate the optimizer can be at these settings. The result of the analysis can be seen in Figure 36, where the green bar represent achievable accuracies, which provides the termination reason "OK".

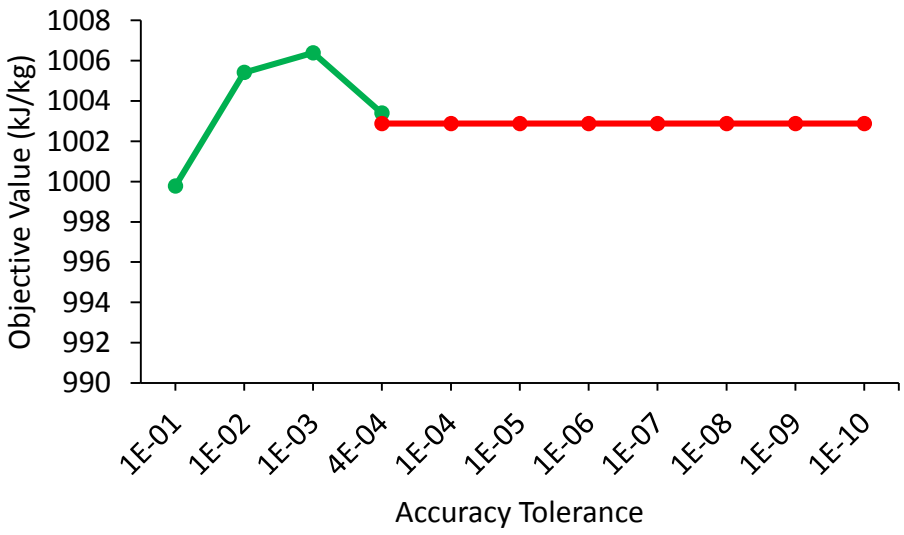

Figure 36: Adjustments of the Accuracy Tolerance according to the objective value in the DMR process in Chapter 7.1 when the Objective Scale Factor is set to 10^{-4}

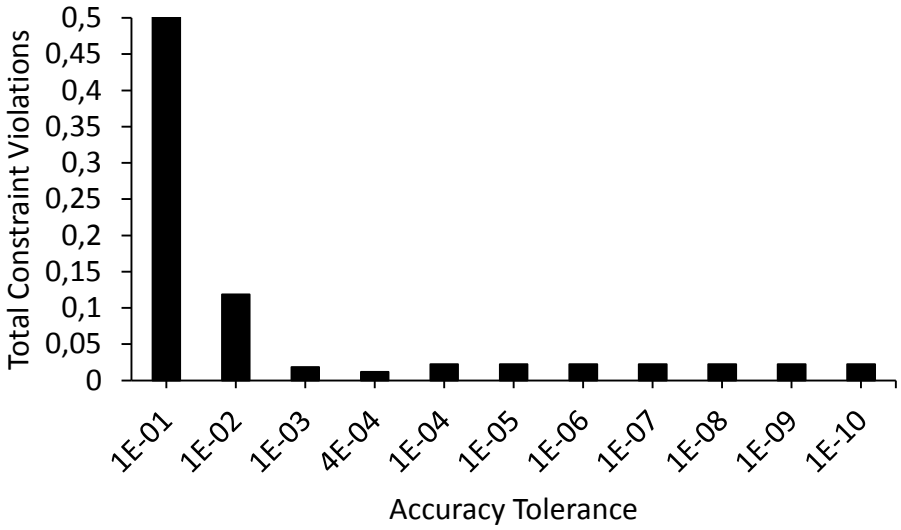

Figure 37: Total Constraint violations according to the accuracy tolerance displayed in Figure 35

In this analysis as the analysis of the Objective Scale Factor parameter, constraints needs to be adhered to in order to select an appropriate value. The constraint analysis can be seen in Figure 37.

The constraint analysis show that the constraint violations get lower and lower until the results start to converge through "Step convergence". The value with the smallest amount of constraint violations, and that also provides a good objective value is when the accuracy tolerance is set to 4×10^{-4}. This value is in the borderline where the result message change from "OK" to "Step Convergence". In order to choose which value to continue using, an evaluation concerning the total constraints violations in regards to the objective value needs to be made. In this case, considering that the results that provided the result screen "Step Convergence" had low constraint violations, the process should utilize the values that provided the termination reason "Step Convergence".

By considering the convergence time from Appendix G, the cases with higher Accuracy Tolerance value then 4×10^{-4} used significantly shorter time than the Accuracy Tolerance values below 4×10^{-4}. The reason may be that the optimizer is able to converge to an objective value with lesser amount of iterations when the objective value does not have to be that accurate. All results that had the Termination Reason "Step Convergence" used equally long time to converge.

D. Step Restriction

With experience from the Prico study, it was made sure that the Step Restriction were sufficient when analyzing the Objective Scale Factor and Accuracy Tolerance. With a Accuracy Tolerance of 4×10^{-4}, analysis in regards to both constraints and objective function have been carried out in Figure 38 and Figure 39 respectively.

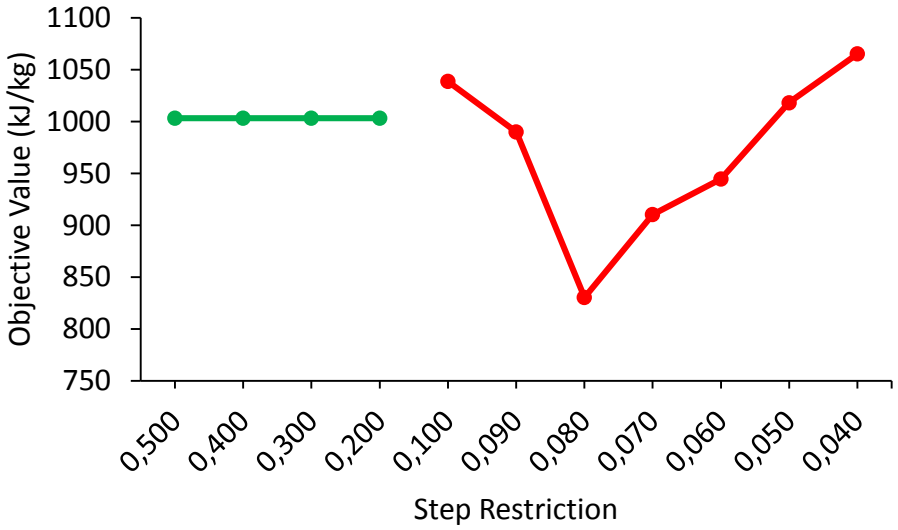

Figure 38: Adjustments of the Step Restriction in the DMR process in Chapter 7.1

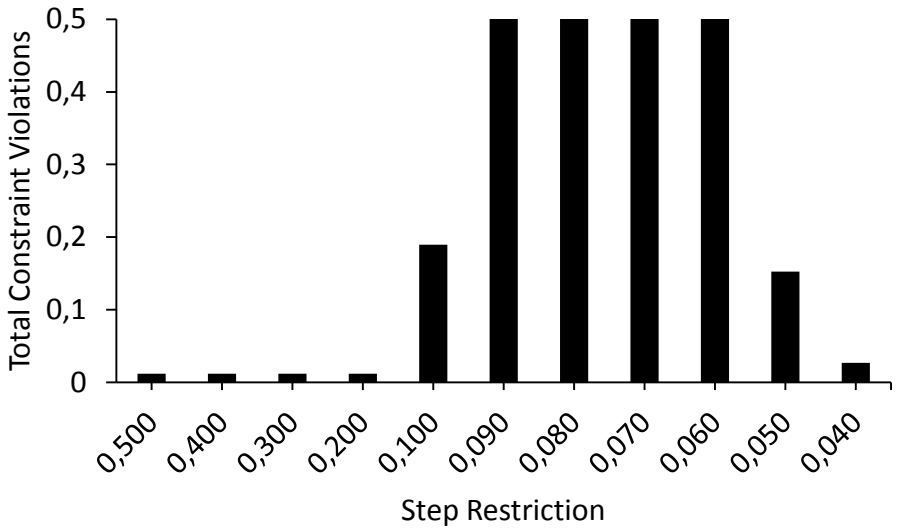

Figure 39: Total Constraint Violations according to the Step Restriction from Figure 37

As it can be seen, by restricting the steps further than 0.2, the results are unstable and results in "Step Convergence" in the optimizer.

The constraint violations show that the objective values with lower Step Restriction value than 0.200, are upholding the constraints poorly. Even the Step Restriction values at 0.1, 0.05 and 0.04 have higher constraint violations than the results with higher step restriction than 0.2, even though those values had higher objective values. It can be seen from Appendix G that all the step values below 0.2 use significantly shorter amount of time to converge than the Step Restriction values at 0.2 or higher. This may indicate that the optimizer is experiencing maratos effect, and after a time have to converge to the objective value shown in Figure 38.

It can be seen from Chapter 3.5.2 that by setting the Step Restriction to 1, the optimizer will operate with zero Step Restrictions. When the Step Restriction were set to 1, the optimizer provided the same objective value, constraint violations and convergence time as when the step restriction were 0.2, which indicates that a Step Restriction at 0.2 is sufficient in this case.

E. Perturbation

It can it be seen from Chapter 3.5.2 that the perturbation value is affecting the scaled variables in calculation. The theory states that by setting a lower value will result in faster gradient calculations, but it may limit the accuracy.

When adjusting the perturbation size in the analyses, the optimizer were not able to get more accurate values than at the default perturbation value 10^{-3}. Very small perturbation values resulted in "unbounded" as termination value, and high valued perturbation values resulted in either flow sheet errors, constraint violations or poor objective values. By being unable to obtain a better objective value when adjusting the Perturbation parameter signifies that the Objective Scale Factor, variable boundaries, variable values and constraints are set at an accurate level in regards to the Perturbation.

From these analyses, it is clear that it is highly necessary to adjust the Hyprotech SQP optimizer by variable values, variable boundaries, constraints and the main setup parameters. The initial variable values and variable boundaries are the same through entire Chapter 7.1 and its subchapters. In each of the tests, and through entire Chapter 7.1, the gradient calculations were performed by utilizing two-sided calculations, which is used in all case studies in this thesis.

7.1.1 WMR7 constraint activated, WMR1 constraint deactivated

By activating the WMR7 constraint and deactivating the WMR1 constraint, the SWHE-1 heat exchanger will receive a two-phase flow, while the cooler E-101 will receive an inlet stream with 100 percent vapor.

The optimizer parameters in order to obtain the lowest objective value, achieved in regards to low constraint violations can be seen in Table 29**.**

Table 29: Best case optimizer parameters according to the DMR modifications in Chapter 7.1.1

New Optimizer parameters	
Max. Iterations	2000
Objective Sale Factor	1
Accuracy Tolerance	1×10^{-8}
Step Restriction	1
Perturbation	0.001
Max. Feasible Point	500

By optimizing this process in regards to the parameter settings in Table 29, the following results were obtained:

Excluded Pump Power	**Included Pump Power**
$Objective\ value = \ 1002.88$	$Objective\ value = \ 1007.04$

Time taken to converge were around 12 minutes. Considering the constraint violations that can be seen in Figure 40, the objective values are valid.

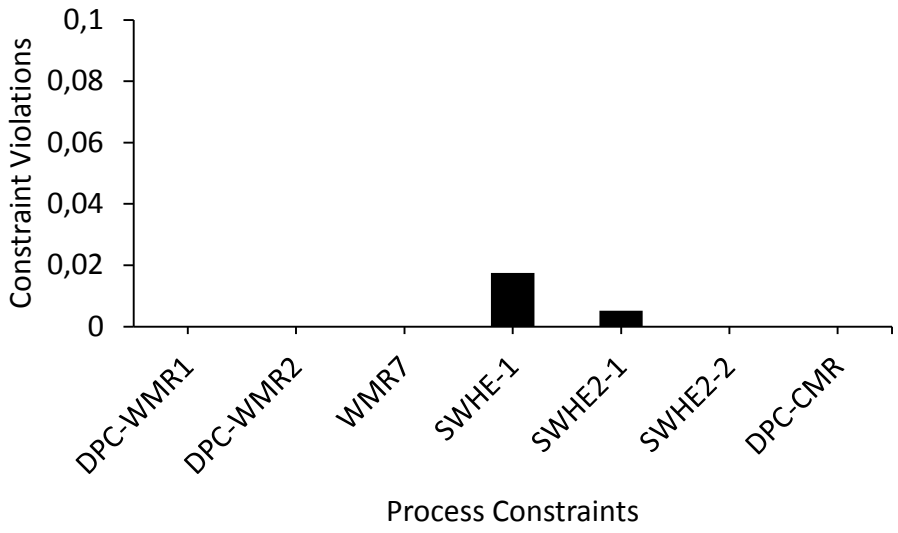

Figure 40: Constraint violations in the optimized process according to the DMR process with the modifications from Chapter 7.1.1

7.1.2 WMR7 constraint deactivated, WMR1 constraint deactivated

By deactivating both the WMR7 and WMR1 constraint, inlet flow to both the cooler E-101 and heat exchanger SWHE-1 may consist of two-phase flow.
The optimizer parameters in order to obtain the lowest objective value in respect to constraint violations can be seen in Table 30.

Table 30: Best case optimizer parameters according to the DMR modifications in Chapter 7.1.2

New Optimizer parameters	
Max. Iterations	2000
Objective Sale Factor	0.8
Accuracy Tolerance	1×10^{-8}
Step Restriction	1
Perturbation	0.001
Max. Feasible Point	500

By optimizing this process in regards to the parameters in Table 30, the following results were obtained:

Excluded Pump Power	**Included Pump Power**
$Objective\ value = 969.77$	$Objective\ value = 974.40$

Time taken to converge were around 7 minutes. Considering the constraint violations that can be seen in Figure 41, the objective values are valid.

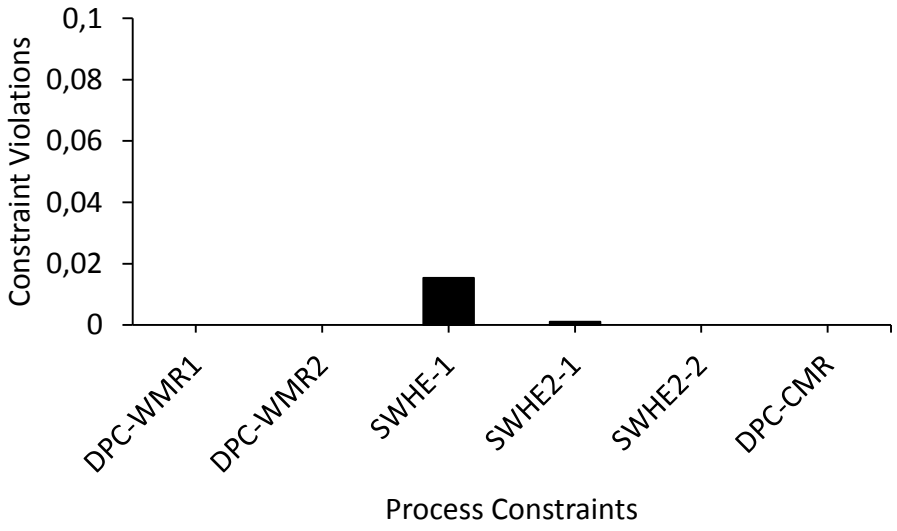

Figure 41: Constraint violations according to the modifications in Chapter 7.1.2

7.1.3 WMR7 constraint deactivated, WMR1 constraint activated

By deactivating the WMR7 constraint and having the WMR1 constraint activated, two-phase flow may enter the cooler E-101, while only liquid will enter the SWHE-1 heat exchanger. It can be seen from Chapter 7 that this will allow distribution that is equal in the SWHE-1 tubes if rocking of the FLNG unit occurs.
The optimizer parameters in order to obtain the lowest objective value in respect to constraint violations can be seen in Table 31.

Table 31: Best case optimizer parameters according to the DMR modifications in Chapter 7.1.3

New Optimizer parameters	
Max. Iterations	2000
Objective Sale Factor	1
Accuracy Tolerance	1×10^{-8}
Step Restriction	2
Perturbation	0.0041
Max. Feasible Point	500

By constraining the WMR1 stream to have a 100 percent liquid phase, the refrigerant composition in cooperation with the pressure level will be limited. However, by allowing two-phase flow into E-101, the refrigerant is not required to evaporate entirely through the second stage compression, which makes it possible for the optimizer to work within a higher variation of compositions. By optimizing this process in regards to the parameters in Table 31, the following results were obtained:

Excluded Pump Power
$Objective\ value = \ 982.28$

Included Pump Power
$Objective\ value = \ 986.78$

Time taken to converge were around 7 minutes. Considering the constraint violations that can be seen in Figure 42, the objective values are valid.

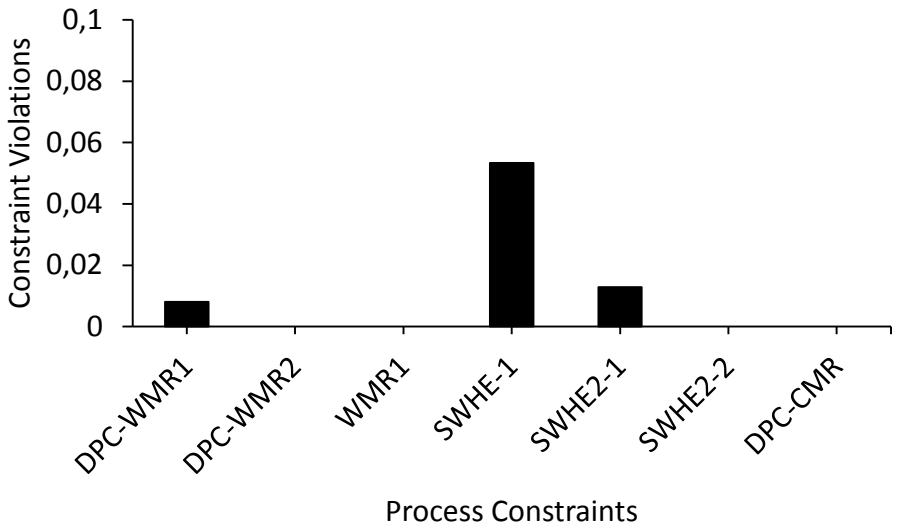

Figure 42: Constraint violations according to the DMR process modifications from Chapter 7.1.3

7.1.4 Result comparison between the three modifications

The three modifications provided different results in terms of both objective value and the amount of Nitrogen in the WMR circuit. The modification in Chapter 7.1.3 is the basis design for DMR processes, and the objective value from that modification is used as a base result (100%) when comparing the different modifications in regards to the objective value. The amount of Nitrogen is measured in comparison to the other components in the WMR circuit. Concerning the objective value, lower percentage equals a lower objective value compared to the result from the base case. The results can be seen in Table 32.

Table 32: Result Comparison between the three modifications in Chapter 7.1 in terms of the objective value and amount of Nitrogen in the WMR circuit. Concerning the objective value, the base case is the modification in Chapter 7.1.3 (100%). The Nitrogen percentage is based on mole fractions.

Chapter	Changes in the objective value	Percentage of Nitrogen in the WMR circuit	Vapor Inlet (E-101)	Vapor Inlet (SWHE-1)
7.1.3	100.00 %	0,03%	95.48 %	0.00 %
7.1.2	98.73 %	0.75%	95.28 %	2.84 %
7.1.1	102.10 %	1.94%	100.00 %	27.07%

Concerning the results in Table 32, the modification that provided the best objective value were the modification made in Chapter 7.1.2, which were 1.27% lower than the base case. This result is not surprising considering that the modification allows two-phase flow in both E-101 and SWHE-1.

The modification that provided the worst objective value were the case in Chapter 7.1.1, which is not surprising considering that the process model is forced to evaporate the

refrigeration stream at the second stage compression without being able to increase the high pressure. Because of that, the refrigerant stream will contain lighter hydrocarbons and a higher amount of Nitrogen, which will result in a high vapor phase after the refrigerant stream is cooled in E-101 before it enters SWHE-1 as it can be seen in Table 32.

In regards to the base case from Chapter 7.1.3, the amount of Nitrogen is at a low value considering that the refrigerant stream has to be at 100% liquid phase before entering SWHE-1. An important note is that the Nitrogen was at its minimum boundary value in this modification.

The WMR composition in all three modifications can be seen in Appendix I.

Concerning whether or not the Nitrogen component should be in the composition, it is safe to say that with the exception of the modification in Chapter 7.1.1, the Nitrogen should be viewed as a superfluous component.

7.2 DMR with included pump power in the objective function

Results from the previous studies indicates that there is little to gain by including the pump power in the objective function.
When optimizing without the pump power included in the objective function, it would be logical for the process model having a higher mass flow of liquid entering the pump than it would in the study where the pump efficiency is included. In order to figure this out, a process with equal adiabatic efficiencies in the compressor and pump is made. The adiabatic efficiencies will be set to 80%, which is higher than in the previous case. The refrigerant mixture may differ, so the mass flow of the refrigerant through the pump will be calculated as a fraction of the total mass flow.

Objective function with excluded pump power:

$$liquid\ mass\ flow\ =\ 74.86Kg/s$$

Considering the mass flow of the refrigerant, the pump received the following share:

$$x = \frac{74.86}{444.2} = 0.169$$

Objective function with included pump power:

$$liquid\ mass\ flow\ =\ 65.52Kg/s$$

Considering the mass flow of the refrigerant, the pump received the following share:

$$x = \frac{65.52}{364.20} = 0{,}180$$

Considering the total mass flow, can it be seen that by including the pump in the objective function while optimizing, the pump actually received more liquid than when it was excluded. This indicates that whether the pump is included in the objective function or not

does not affect whether or not the optimizer is trying to liquefy more of the composition before it enters the separator SEP-1.

The reason that the process is more complex when the compressor efficiency is set to polytropic is because the pump can only be set at adiabatic efficiency. If however, the compressor in parallel with the pump is set to have the same adiabatic efficiency as the pump, the two units would work as "one". In other words, the optimization process do not need to iterate between the refrigeration components in order to send a higher mass flow to the component with the highest efficiency and at the same time achieve a good MR composition.

7.3 DMR with adjustable intermediate and high pressures

Adding more variables in the optimization, adjustment of the Objective Scale Factor or the Perturbation parameters is necessary in order to obtain a valid objective value. Considering the improvements on the Prico process, which were small when including the middle and high pressure signifies that the optimizer were not adjusted properly even with various attempts. By allowing the optimizer to vary the intermediate and high pressures levels, the optimizer can mix the composition in regards to the pressure levels.

After a series of optimization processes and variable adjustments, the initial variable values in Appendix H will be utilized in cooperation with the constraints from Table 27, which can be seen in Chapter 7.1.

7.3.1 WMR7 constraint activated, WMR1 constraint deactivated

By activating the WMR7 constraint and deactivating the WMR1 constraint, the SWHE-1 heat exchanger will receive a two-phase flow, while the cooler E-101 will receive an inlet stream with 100 percent vapor.

The optimizer parameters in order to obtain the lowest objective value, achieved in regards to low constraint violations can be seen in Table 33.

Table 33: Best case optimizer parameters according to the DMR modifications in Chapter 7.3.1

New Optimizer parameters	
Max. Iterations	2000
Objective Sale Factor	25
Accuracy Tolerance	10^(-8)
Step Restriction	1
Perturbation	0.001
Max. Feasible Point	500

By optimizing this process in regards to the parameters in Table 33, the following results were obtained:

Excluded Pump Power

$$Objective\ value = 937.80$$

Included Pump Power

$$Objective\ value = 941.17$$

Time taken to converge were around 11 minutes. Considering the small constraint violations that can be seen in Figure 43, the objective values are valid.

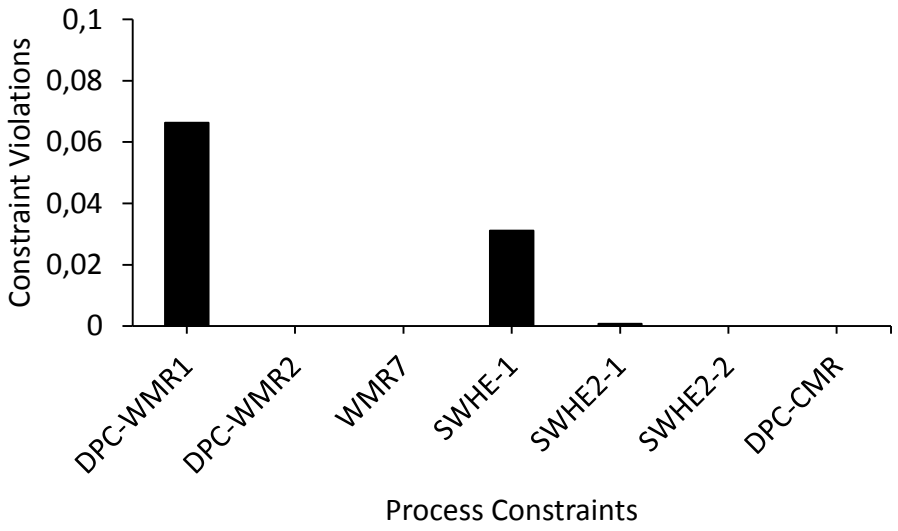

Figure 43: Constraint violations according to the parameter values from Table 25

7.3.2 WMR7 constraint deactivated, WMR1 constraint deactivated

By removing both the WMR7 and WMR1 constraints, the stream entering the cooler E-101 and the heat exchanger SWHE-1 may contain both vapor and liquid phase.

The optimizer parameters in order to obtain the lowest objective value, achieved in regards to low constraint violations can be seen in Table 34.

Table 34: Best case optimizer parameters according to the DMR modifications in Chapter 7.3.2

New Optimizer parameters	
Max. Iterations	2000
Objective Sale Factor	25
Accuracy Tolerance	10^(-8)
Step Restriction	1
Perturbation	0.002
Max. Feasible Point	500

By optimizing this process in regards to the parameters in Table 34, the following results were obtained:

Excluded Pump Power

$$Objective\ value = 922.26$$

Included Pump Power

$$Objective\ value = 927.74$$

Time taken to converge were around 7 minutes. Considering the small constraint violations that can be seen in Figure 44, the objective values are valid.

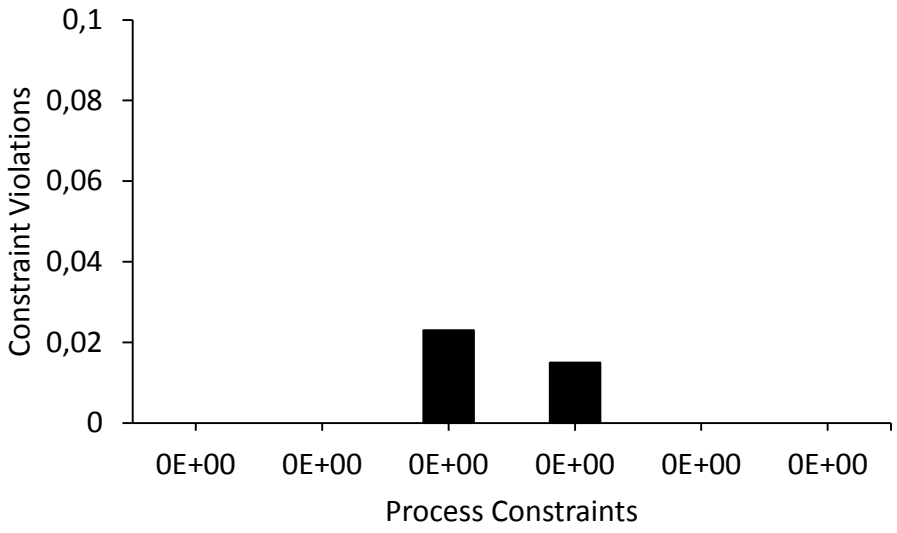

Figure 44: Constraint violations according to the parameter values from Table 26

7.3.3 WMR7 constraint deactivated, WMR1 constraint activated

By deactivating the WMR7 constraint and activating the WMR1 constraint, the stream into SWHE-1 will consist of 100% liquid, while the stream into E-101 will most likely contain two-phase flow. The optimizer parameters in order to obtain the lowest objective value, achieved in regards to low constraint violations can be seen in Table 35.

Table 35: Best-case optimizer parameters according to the DMR modifications in Chapter 7.3.3

New Optimizer parameters	
Max. Iterations	2000
Objective Sale Factor	25
Accuracy Tolerance	10^(-8)
Step Restriction	1
Perturbation	0.00205
Max. Feasible Point	500

By optimizing this process in regards to the parameters in Table 35, the following results were obtained:

Excluded Pump Power	**Included Pump Power**
$Objective\ value = 928.39$	$Objective\ value = 933.85$

Time taken to converge were around 12 minutes. Considering the small constraint violations that can be seen in Figure 45, the objective values are valid.

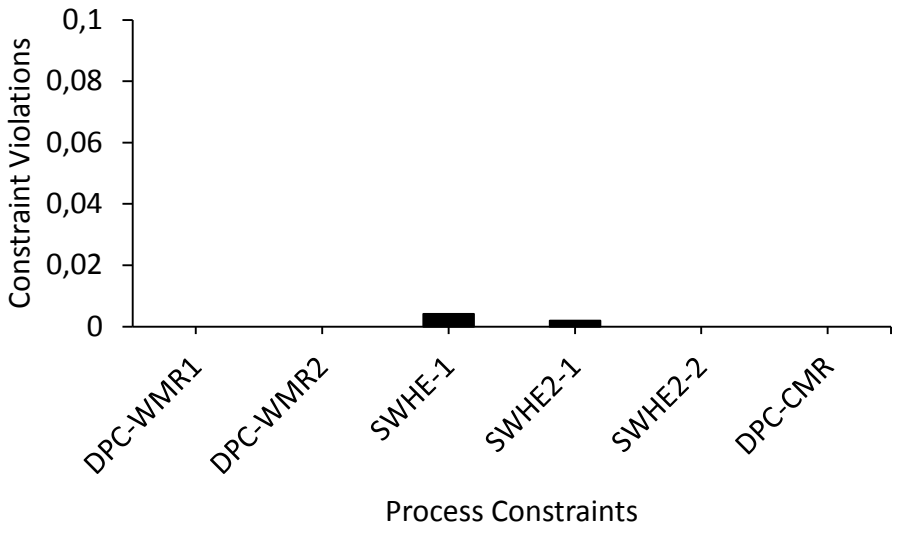

Figure 45: Constraint violations according to the parameter values from Table 27

7.3.4 Result comparison between the three modifications

As in Chapter 7.1, the three modifications provided different results in terms of both objective value and amount of Nitrogen in the WMR circuit. The modification in Chapter 7.3.3 is the basis design for DMR processes, and the result from this modification is therefore used as a base result (100%) when comparing the different modifications. The amount of Nitrogen is measured in comparison to the other components in the WMR circuit. Concerning the objective value, lower percentage equals a lower objective value compared to the results from the base case.

Table 36: Result Comparison between the three modifications in Chapter 7.3 in terms of the objective value and amount of Nitrogen in the WMR circuit. The amount of Nitrogen percentage is based on mole.

Chapter	Changes in the Objective value	Percentage of Nitrogen in the WMR circuit	Vapor inlet (E-101)	Vapor inlet (SWHE-1)
7.3.3	100.00 %	0.27%	69.73 %	0.00 %
7.3.2	99.34 %	0.03%	67.86 %	9.53 %
7.3.1	101.01 %	0.22%	100.00%	2.49 %

Concerning the study where the intermediate and high pressures were fixed, which can be seen in Table 32, the results in Table 36 differs. The case that had the highest percentage of Nitrogen in the WMR circuit were the base case from Chapter 7.3.3, which is surprising. However, considering the composition from Appendix J, the base case had lower amount of Methane, which is the reason that the process is able to have 0% vapor inlet to SWHE-1. All of the modifications in Table 36 had closer objective values than the modifications from Chapter 7.1, which can be seen in Table 32. The reason for that may be that in Chapter 7.3, the process could adjust the pressure levels in regards to the composition in order to obtain a lower objective value.

Considering whether the Nitrogen component should be in the composition, considering the optimization results is it safe to say that the Nitrogen should be viewed as a superfluous component.

From the Prico process, the case that included the middle and high pressures in the optimization were not able to significantly improve the objective value. However, in the DMR process, the optimizer provided significantly better results in the process that had adjustable intermediate and high pressures, which can be seen in Table 37.

Table 37: Comparison between the results between the DMR process with fixed intermediate and high pressures, and the DMR model with adjustable intermediate and high pressures

Chapter	Objective Value (kJ/kg)	Chapter	Objective Value (kJ/kg)
7.1.1	1007.04	**7.3.1**	941.17
7.1.2	974.40	**7.3.2**	927.74
7.1.3	986.78	**7.3.3**	933.85

7.4 DMR with adjustable intermediate and high pressures with fixed compositions

By utilizing the different compositions obtained in the studies from Chapter 7.1 and Chapter 7.3, is it possible to analyze whether the optimizer is able to obtain the best compositions in regards to pressure level. These studies will be carried out in regards to constant composition in both refrigeration streams, with the only manipulative variables shown in Table 38. The Constraints are the same as used in Chapter 7.1.1 and Chapter 7.3.1, which considers the DMR modification with pure vapor stream into cooler E-101.

Table 38: Manipulative variables according to fixed compositions from Chapter 7.1 and Chapter 7.3

Tag	Property	Unit	Minimum	Initial Value	Maximum
WMR3	Pressure	[Bar]	1	6	20
CMR4	Pressure	[Bar]	1	6	15
WMR5	Pressure	[Bar]	8	16	25
WMRVapor2	Pressure	[Bar]	30	46	55
CMR5	Pressure	[Bar]	10	12.56	32
CMR7	Pressure	[Bar]	21	25.23	45
CMR1	Pressure	[Bar]	41	54.50	70

Pressure optimization based on the composition from Chapter 7.1.1 in regards to WMR7 activated

By optimizing the pressure levels when utilizing the composition that was obtained when just the low pressure and refrigeration were optimized, the following objective value was obtained:

Excluded Pump Power
$Objective\ value = 958.17$

Included Pump Power
$Objective\ value = 962.38$

$$Total\ Constraint\ Violations = 0.0006$$

Pressure optimization based on the composition from Chapter 7.3.1 where WMR7 was activated and WMR1 Deactivated

By optimizing the pressure levels when utilizing the composition that was obtained from the case where the composition was optimized simultaneously as the pressure stages were optimized, the following objective value was obtained:

Excluded Pump Power
$Objective\ value = 937.15$

Included Pump Power
$Objective\ value = 940.51$

$$Total\ Constraint\ Violations = 0{,}0329$$

This indicates that the objective value can be further improved either in regards of lowering its value, upholding the constraints or in both aspects. The reason that the optimizer is able to obtain a better objective value and less constraint violations in this chapter compared to the studies in the previous chapters is because when the compositions are set, the optimizer is able to handle a much lower accuracy.

7.5 DMR with adjustable intermediate and high pressures with varying process temperature

In a DMR process applicable to FLNG, the process modification from Chapter 7.3.3 will be considered. Considering the UA values in the heat exchangers, the different results according to the process temperature can be seen in Table 39, Table 40, Table 41 and Table 42.

Table 39: Results in the DMR process from Chapter 7.3.3 according to a process temperature of 5°C

Process Temperature = 5°C		
Unit	UA	LMTD
SWHE-1	36170 kW/K	4.064°C
SWHE2-1	34960 kW/K	4.148°C
SWHE2-2	6006 kW/K	5.151°C
Excluded Pump Power $\boldsymbol{minf(x) = 840.22}$	**Included Pump Power** $minf(x) = 844.73$	
Total Constraint Violations = 0.0085		

Table 40: Results in the DMR process from Chapter 7.3.3 according to a process temperature of 15°C

Process Temperature = 15°C		
Unit	UA	LMTD
SWHE-1	39860 kW/K	4.386°C
SWHE2-1	35690 kW/K	4.155°C
SWHE2-2	6413 kW/K	4.918°C
Excluded Pump Power $\boldsymbol{minf(x) = 928.39}$	**Included Pump Power** $minf(x) = 933.85$	
Total Constraint Violations = 0.0061		

Table 41: Results in the DMR process from Chapter 7.3.3 according to a process temperature of 25°C

Process Temperature = 25°C		
Unit	UA	LMTD
SWHE-1	39590 kW/K	4.939°C
SWHE2-1	34290 kW/K	4.073°C
SWHE2-2	5470 kW/K	5.391°C
Excluded Pump Power $\boldsymbol{minf(x) = 1022.29}$	**Included Pump Power** $minf(x) = 1028.43$	
Total Constraint Violations = 0.0089		

Table 42: Results in the DMR process from Chapter 7.3.3 according to a process temperature of 35°C

Process Temperature = 35°C		
Unit	UA	LMTD
SWHE-1 **SWHE2-1** **SWHE2-2**	44300 kW/K 30680 kW/K 4915 kW/K	5.096°C 4.208°C 5.439°C
Excluded Pump Power $\boldsymbol{minf(x) = 1113.93}$		**Included Pump Power** $minf(x) = 1122.82$
Total Constraint Violations = 0.0363		

As a guiding value, 40 000 – 60 000 kW/K should be considered as a maximum value in SWHE-1 and 40 000 kW/K should be considered as an absolute maximum in both SWHE2-1 and SWHE2-2 (Pettersen, Personal communication 04.05.2015).

In regards to the UA values from Table 39, Table 40, Table 41 and Table 42, the results seem to be within the allowed UA limits. It should also be mentioned that the optimizer were able to maintain a close Logarithmic Mean Temperature Difference, considering that the temperature approach in the Spiral Wound heat exchangers are 3°C.

7.6 Summary of Chapter 7

It can be seen in Chapter 7.1 that by simplifying the spreadsheet is it possible to assist the optimizer by avoiding a number of iterations that would have made it more challenging for the user to set the parameter values.

By optimizing the DMR process in terms of three different constraint modifications in the WMR circuit, different aspects can be considered. It is clear from the optimizations that with the only exception of the modifications in Chapter 7.1.1, the Nitrogen within the WMR circuit should be considered as superfluous and should not be included in the process. By deactivating both WMR1 and WMR7 constraint in the WMR circuit, allowing both vapor and liquid before E-101 and SWHE1 as were done in Chapter 7.1.2 and 7.3.2 provided the best objective value.

The modification that provided the second best objective value were the modification made in Chapter 7.1.3 and 7.3.3. This modification is the process design used in real DMR processes, and is therefore used as a base case when comparing the three different modifications in terms of objective value. The results from all three modifications concerning fixed intermediate and high pressures and adjustable intermediate and high pressures can be seen in Table 32 and Table 36 respectively. Chapter 7.1 and Chapter 7.3 shows that the optimizer made logical decisions and that the optimizer is easily adjustable to new challenges by adjustment of the optimizer parameters. A comparison concerning the objective values obtained in the DMR process with fixed and adjustable intermediate and high pressures shown in Table 37 in Chapter 7.3.4 show that the Hyprotech SQP optimizer significantly improves the objective values in all three modifications when the intermediate

and high pressures are included as adjustable variables. Comparing the results from Table 37 with the minor improvement in the Prico process indicates that the simplification from Chapter 7.1, which involved utilizing Eq. 7 instead of Eq. 8 as the objective function may have provided better objective values.

Concerning Chapter 7.2, which studies the effect of not including the pump power in the objective function, the refrigeration stream did not have a higher liquid phase when entering the separator, which signifies that the pump power is so low that the optimizer is more effective by adjusting the refrigerant composition in regards to the compressor power alone.

Chapter 7.4 shows that the optimizer is able to optimize well with respect to the combination of pressure levels and refrigeration components. It can also be seen that by first optimizing the process in regards to both pressure levels and composition and thereby removing the composition variables and optimize just the pressure levels, the optimizer is able to further improve the objective value.

Chapter 7.5 shows that the optimizer is able to optimize the DMR process in regards of different process temperatures and still provide good LMTD and objective values with UA values that does not exceed the maximum limit of what the value should be in a realistic DMR liquefaction process.

8 Improvement of existing Liquefaction Models by Optimization

It can be seen from Chapter 7 that the Hyprotech SQP optimizer is able to optimize a self-made process in several aspects. However, to further challenge the optimizer, an optimized process by Kusmaya (2012) is studied. In Chapter 8.1, 8.2, 8.3, 8.4 and 8.5, the upstream DMR process is studied, while in Chapter 8.6, a simplified optimization of an integrated DMR process optimized by Kusmaya (2012) is studied.

Similar to the DMR process in Chapter 7, the objective function in this Chapter does not have included pump power in the objective function, the pump power has been added in retrospect.

8.1 DMR process, optimized by Kusmaya, provided in regards to APCI design.

Kusmaya (2012) has optimized the following model in regards to an upstream DMR process by APCI design. This process has an upstream NGL extraction, and the conditions of the natural gas stream that enters the liquefaction process is a lean dry gas that can be seen in Table 3. Other than process specifications, the difference between the DMR process from Chapter 7.1, which is described in Chapter 5.2 is that this process does not contain Nitrogen in the WMR circuit and it also contain one more compression step in the CMR circuit, which can be seen in Figure 46.

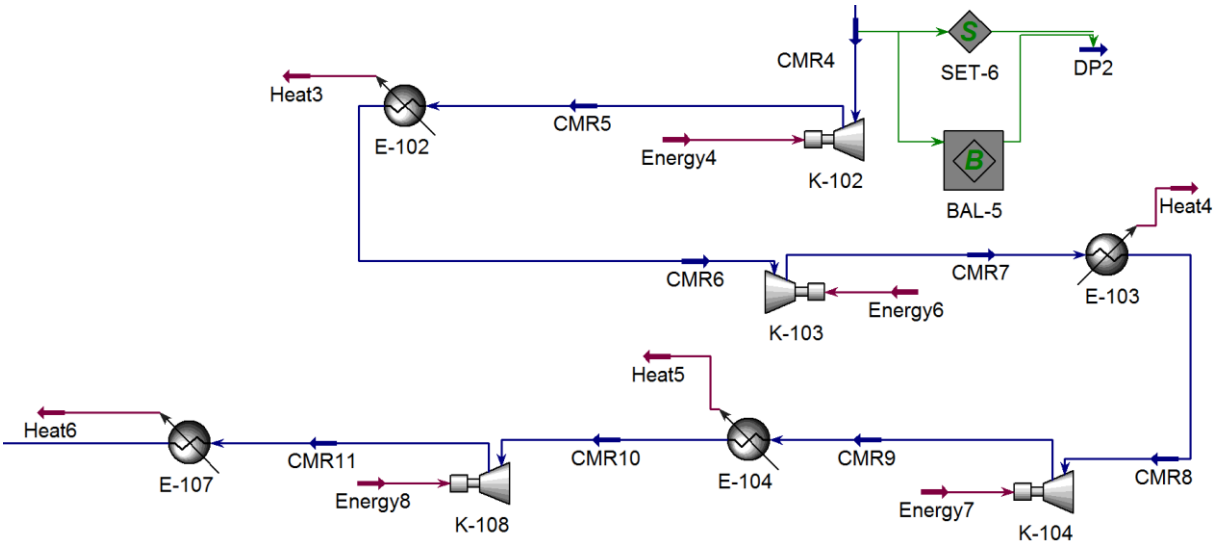

Figure 46: Illustration of the extra pressure step modification in the Kusmaya process

Even though the process is very similar to the process in Chapter 7.1 and Chapter 7.3, the process specifications differs. In addition to the process temperature, which is set to be at 22°C, a list of the component specifications and non-manipulative variable values can be seen in Appendix K. The natural gas stream has the same composition as the model in Chapter 7.1 and Chapter 7.3, which the composition can be seen in Table 3 from Chapter 2.5 in the lean gas column.

In regards to optimization, the adjustable initial variable values with their boundaries and the process constraints can be seen in Appendix L. Note that the temperature approach in the heat exchangers is set to be 2 instead of 3 as it is in the DMR process from Chapter 7.1 and Chapter 7.3.

An important note is when optimizing this process, the adjustable variables that are optimized has a different initial value than the optimized model by Kusmaya (2012). The initial variable values and their boundaries on the adjustable variables have been set according to the variables in Chapter 7 with few modifications, by doing that, the optimizer parameters may not need as much adjusting as if the starting values on the adjustable variables were different. However, since the fixed variables, compressor efficiencies, pressure drop, process temperature etc. are the same as in the Kusmaya process, the optimization results are 100% valid.

The Original DMR model by Kusmaya (2012), managed to provide the following objective value before the adjustable variables were manipulated:

Excluded Pump Power (1)	**Included Pump Power (2)**
$Objective\ value = \ 1138.90\ kJ/kg$	$Objective\ value = \ 1140.67\ kJ/kg$

$$Total\ power\ consumption = 128MW$$

In order to achieve the lowest minimum objective value with respect to constraint violations, the optimizer parameter values displayed in Table 43 were utilized:

Table 43: Best case optimizer parameters according to the DMR modifications in Chapter 8.1

New Optimizer parameters	
Max. Iterations	2000
Objective Sale Factor	25
Accuracy Tolerance	10^(-8)
Step Restriction	1
Perturbation	0.0066
Max. Feasible Point	500

After the process had been optimized first in terms of both refrigeration components and pressure, the following results were obtained:

Excluded Pump Power (1)	**Included Pump Power (2)**
$minf(x) = 937.69\ kJ/kg$	$minf(x) = 943.61\ kJ/kg$

$$Total\ power\ consumption = 105.2MW$$

$$Total\ Constraint\ violations = 0.0131$$

A comparison between the process optimized by Kusmaya (2012), and the process optimized by Hyprotech SQP can be seen in Table 44.

Table 44: Comparison between the objective value from the model optimized by Kusmaya (2012) and the model optimized by Hyprotech SQP. Ref. number 1 is for excluded pump power, ref. number 2 is for included pump power

Ref.	Objective value (kJ/kg) Kusmaya (2012)	Objective value (kJ/kg) Hyprotech SQP	Reduced Power Consumption
1	1138.90	937.69	17.67%
2	1140.67	943.61	17.28%

Considering the pressure levels and refrigerant streams, a comparison between the model optimized by Kusmaya (2012) and the Hyprotech SQP optimizer can be seen in Appendix N. Note that the mass flow in both the refrigerant streams were almost similar, which means that the main difference were the pressure levels that are lower in the Hyprotech SQP model. The Hyprotech SQP model transferred more heat in the Spiral Wound Heat Exchangers, which signifies that the Hyprotech SQP model were able to provide more suitable refrigerants. The heat transfer in regards to the Kusmaya (2012) model and the Hyprotech SQP optimized model can be seen in Table 45 and Table 46 respectively.

Table 45: UA values in the process optimized by Kusmaya (2012)

Unit	UA	LMTD
WMR CWHE	21210 kW/K	8.492°C
CMR CWHE Lower	17110 kW/K	6.878°C
CMR CWHE Upper	4585 kW/K	6.588°C

Table 46: UA values in the process optimized according to Chapter 8.1

Unit	UA	LMTD
SWHE-1	52820 kW/K	3.300°C
SWHE2-1	38150 kW/K	3.135°C
SWHE2-2	9485 kW/K	3.199°C

Note that even though the UA values in the Hyprotech SQP optimized model are higher, they are still within the limits provided in Chapter 7.5. The model optimized by the Hyprotech SQP optimizer were able to maintain a close temperature pinch in the Spiral Wound Heat Exchangers. A comparison between the temperature pinch in the model optimized by Kusmaya (2012) and the model optimized by the Hyprotech SQP optimizer can be seen in Appendix O and Appendix P respectively.

8.2 DMR process optimized by Kusmaya, provided in regards to APCI design, optimized in regards to equal UA values

It can be seen in Chapter 8.1 that by improving the objective value, the DMR process also got higher UA value in the heat exchangers. The new UA values that Hysys calculated had realistic values, but in order to optimize the process at equal terms considering CAPEX, the UA values in the new process will be set equally to the UA value in the original Kusmaya model.

A challenge while utilizing the same UA values is that the values of both streams that exits the SWHE-1 heat exchanger and continues to SWHE2-1 cannot be given fixed temperatures. Only one of the streams can have a constant temperature, while the other stream has to get its value calculated by the heat exchanger. In order to achieve the desired temperature of the natural gas, the natural gas stream has set temperatures throughout the entire process, while the CMR stream has varying temperature out of SWHE-1.

In the heat exchangers SWHE2-1 and SWHE2-2, is it impossible to set fixed UA values because the temperature of CMR2 decides the mass flow of the vapor and gas out of separator SEP2. The cooling combination of these heat exchangers needs to be set as one UA value. In order to achieve this, a constraint is set in the optimizer were the combined UA value of the two heat exchangers SWHE2-1 and SWHE2-2 (upper and lower bundle) is specified.

Constraining the two heat exchangers in the CMR circuit to a specific value provided several challenges while optimizing. In order to simplify the optimization, the optimizer were provided with a wiggle room in the constraint, given by an inequality constraint with upper and lower limits. The heat exchanger specifications can be seen in Table 47. By including the constraints in Table 47 with the constraints utilized in the previous case studies, which can be seen in Appendix L, the Hyprotech SQP optimizer were able to optimize the process.

Table 47: Heat exchanger constraints in order to achieve similar UA values as the Kusmaya (2012) model

Unit	UA	Action
SWHE1	21210 kW/K	Specified
SWHE2-1 & 2-2	(21600 – 22000) kW/K	Constraint

The optimizer parameters that provided the best result can be seen from Table 48.

Table 48: Best case optimizer parameters according to the DMR modifications in Chapter 8.2

New Optimizer parameters	
Max. Iterations	2000
Objective Sale Factor	25
Accuracy Tolerance	10^(-8)
Step Restriction	1
Perturbation	0.0029
Max. Feasible Point	500

By utilizing the optimizer parameters in Table 48, the following objective values were achieved:

Excluded Pump Power (1)
$minf(x) = 1039.27\ kJ/kg$

Included Pump Power (2)
$minf(x) = 1043.53\ kJ/kg$

$$Total\ constraint\ violations = 0.0021$$

$$Total\ UA\ value = 43203\ kW/K$$

The optimizer used around 15 minutes to optimize the model. A comparison in regards of the objective values between the model optimized by Kusmaya (2012) and the Hyprotech SQP optimized model can be seen in Table 49.

Table 49: Comparison between the objective value from the model optimized by Kusmaya (2012) and the model optimized by Hyprotech SQP concerning similar UA values. Ref. number 1 is for excluded pump power, ref. number 2 is for included pump power

Ref.	Objective value (kJ/kg) Kusmaya (2012)	Objective value (kJ/kg) Hyprotech SQP	Reduced Power Consumption
1	1138.90	1039.27	8.75%
2	1140.67	1043.53	8.52%

The model optimized with Hyprotech SQP had 298 kW/K higher UA value than the model optimized by Kusmaya. However, closing in the UA value difference would not affect the objective value in a noticeable manner.

Considering the pressure levels and refrigerant streams, a comparison between the model optimized by Kusmaya (2012) and the Hyprotech SQP optimizer can be seen in Appendix Q. The model optimized by the Hyprotech SQP optimizer were able to have less mass flow and lower pressure steps in both refrigeration circuits.

8.3 DMR process optimized by Kusmaya, provided in regards to APCI design, optimized in regards to equal compressor drivers

The upstream DMR process by Kusmaya (2012), is based upon the use of 4 x LM6000 gas turbines as drivers. At a process temperature of 22°C, these gas drivers deliver about 32MW shaft power each, which is a total of 128MW (GE Energy 2008), (Kusmaya 2012).

Table 50: Turbine drivers in the DMR model optimized by Kusmaya (2012)

Compressor Tag	Power requirement (MW)	Turbine Ref.
LP Warm / K-100	27.07	**1**
HP Warm / K-101	22.71	**2**
LP Cold / K-102	32.14	**3**
MP Cold / K-103	16.86	**4**
HP Cold / K-104	15.32	**4**
HHP Cold / K-108	13.71	**2**

Considering the optimized model by Kusmaya (2012), the compressor power utilized can be seen in Table 50. It can be seen that the total compressor work is 127.81MW, and that one of the turbine drivers, which is referred to as Turbine ref. 2 has a compressor work of 36,42MW, which is above the allowed limit.

Considering the optimizer ability to operate with the exact same process in regards of compressor power and natural gas feed, the natural gas feed stream will be included as an optimization variable in terms of its molar flow, and the compressor power will be constrained to similar power output as the Kusmaya model.

By optimizing in regards of compressor power, the compressor driver settings will more or less be the same. By including the compressor power in the optimization, the objective in scope will be the amount of LNG the Hyprotech SQP optimized process is able to produce compared to the Kusmaya (2012) process. The objective function will remain the same as in Eq. 7, because by producing more LNG will lower the objective value. The initial variables and constraints can be seen in Appendix R. Considering the given constraints, each of the compressor were given a wiggle room of 1MW. In order to achieve the best-case scenario, the optimizer parameters provided in Table 51 were utilized:

Table 51: Best case optimizer parameters according to the DMR modifications in Chapter 8.3

New Optimizer parameters	
Max. Iterations	2000
Objective Sale Factor	25
Accuracy Tolerance	10^(-8)
Step Restriction	1
Perturbation	0.0069
Max. Feasible Point	500

By utilizing the optimizer parameters in Table 51, the improvement in the LNG production can be seen in Table 52.

Table 52: Improvement in the LNG production by utilizing the same compressor drivers as in the Kusmaya (2012) model

LNG Production rate Original model	LNG Production rate Optimized model	Improvement
$\dot{m}_{LNG} = 112.2 kg/s$	$\dot{m}_{LNG} = 131.5$	17.20%

In addition to significantly higher production, the optimized model utilized 0.8 MW less compressor power. The compressor power utilized in the optimized process can be seen in Table 54.
A comparison in regards to the objective value between the Kusmaya (2012) optimized model and the Hyprotech SQP optimized model can be seen in Table 53, where the objective value is measured both with excluded and included pump power in Ref. 1 and Ref. 2 respectively.

Table 53: Comparison between the objective value from the model optimized by Kusmaya (2012) and the model optimized by Hyprotech SQP concerning similar Compressor drivers. Ref. number 1 is for excluded pump power, ref. number 2 is for included pump power

Ref.	Objective value (kJ/kg) Kusmaya (2012)	Objective value (kJ/kg) Hyprotech SQP	Reduced Power Consumption
1	1138.90	967.58	15.04%
2	1140.67	971.69	14.81%

Table 54: Compressor drivers according to the DMR model optimized by Hyprotech SQP

Compressor Tag	Power requirement (MW)	Turbine Ref.
LP Warm / K-100	26.50	**1**
HP Warm / K-101	22.00	**2**
LP Cold / K-102	32.50	**3**
MP Cold / K-103	17.00	**4**
HP Cold / K-104	16.00	**4**
HHP Cold / K-108	13.00	**2**

The compressors in Table 54 provided a total power consumption of 127MW, which is 0.81MW less than the model provided by Kusmaya (2012). The compressor drivers are also more realistic with the highest violation being the Turbine ref.2 at 35MW compared to 36.42MW in the Kusmaya (2012) model.

The UA values from the Kusmaya (2012) model can be seen in Table 45 from Chapter 8.1, while the UA values from the optimized model can be seen in Table 55. Considering the UA values, the UA values in the optimized model is far higher than the UA values in the original model, which is logical considering that by increasing the mass flow of the natural gas feed

stream, the refrigerant also needs higher mass flow because of the constrained compressor power.

Table 55: UA values in the heat exchangers according to the modifications in Chapter 8.3

Unit	UA	LMTD
SWHE-1	65100 kW/K	3.164°C
SWHE2-1	44600 kW/K	3.158°C
SWHE2-2	11510 kW/K	3.111°C

A note concerning the UA value in Table 55 is that both the SWHE-1 and SWHE2-1 surpassed the maximum limit of realistic spiral wound heat exchangers. This may indicate that the SWHE-1 and SWHE2-1 should both be separated into two Spiral Wound Heat Exchangers.

8.4 Upstream DMR process made by Kusmaya, with similar compressor drivers and fixed UA values

To further challenge the optimizer, a model that has constrained compressor drivers as in Chapter 8.3 and constrained UA values as in Chapter 8.2 will be optimized. Considering that the process will utilize similar compressor drivers and have constrained UA values in the Spiral Wound Heat Exchangers, the optimizer will only be able to improve the process by mixing a greater composition and adjust the pressure values to its mass flow.

The UA constraints will be the same as in Chapter 8.2, with specified SWHE1 UA value and a constraint that control the SWHE2-1 and SWHE2-2 UA values, which can be seen in Table 56. The compressor drivers will be constrained as in Chapter 8.3, the constraints can be seen in Appendix R.

Table 56: Heat exchanger constraints in order to achieve similar UA values as the pre optimized Kusmaya model

Unit	UA	Action
SWHE1	21210 kW/K	Specified
SWHE2-1 & 2-2	(21600 – 22000) kW/K	Constraint

In order to obtain the best value, the optimizer parameters in Table 57 were utilized:

Table 57: Best case optimizer parameters according to the DMR modifications in Chapter 8.4

New Optimizer parameters	
Max. Iterations	2000
Objective Sale Factor	25
Accuracy Tolerance	10^(-8)
Step Restriction	1
Perturbation	0.0074
Max. Feasible Point	500

By utilizing the optimizer parameters from Table 57, the improvement in the LNG production can be seen in Table 58.

Table 58: Improvement in the LNG production by utilizing the same compressor drivers and UA values as in the Kusmaya (2012) model

LNG Production rate Original model	LNG Production rate Optimized model	Improvement
$\dot{m}_{LNG} = 112.2 kg/s$	$\dot{m}_{LNG} = 114.1\ kg/s$	1.7%

In addition to higher LNG production rate, the optimized model utilized 2.7 MW less compressor power than the original model, which provided the objective values shown in Table 59.

Table 59: Comparison between the objective value from the model optimized by Kusmaya (2012) and the model optimized by Hyprotech SQP concerning similar UA values and compressor drivers. Ref. number 1 is for excluded pump power, ref. number 2 is for included pump power

Ref.	Objective value (kJ/kg) Kusmaya (2012)	Objective value (kJ/kg) Hyprotech SQP	Reduced Power Consumption
1	1138.90	1095.71	3.79%
2	1140.67	1098.53	3.69%

When setting the objective function to maximizing the production of LNG, which can be seen in Eq. 9, the process had difficulties to achieve a good objective value and improving the mass flow of LNG. 80 different optimization were carried out in regards of different objective scale factor and perturbations. Almost all of the optimizations provided the same results, which can be seen in Table 60.

$$max f(x) = \dot{m}_{LNG} \qquad \text{Eq. 9}$$

Table 60: Achieved objective value when Eq. 9 is utilized as objective function

Objective value	Total Compressor power
111.40 kg/s	127.81 MW

Table 60 show that when the objective value were shifted, the optimizer provided a poorer mass flow of LNG than the DMR process optimized by Kusmaya (2012). This signifies the importance of the objective value.

8.5 Further improvement on the optimized DMR Process by (Kusmaya 2012)

In order to further improve the process, the importance of the outlet temperatures of SWHE-1 needs to be optimized as well as the parameters from Chapter 8.1. Considering that the outlet streams should have the same temperatures, a process modification, which can be seen in Figure 47, had to be made. The two set functions, SET-4 and SET-5 connected to WMR2 and CMR2 respectively are exporting the outlet temperature of stream NG-SWHE2-1, making sure that the outlet streams of SWHE-1 have equal temperatures.

By optimizing the outlet temperatures of SWHE-1, the CMR composition will have to adjust to the temperature changes, the cooling load through the heat exchangers will vary, which will lead to different compressor usage compared to the previous studies.

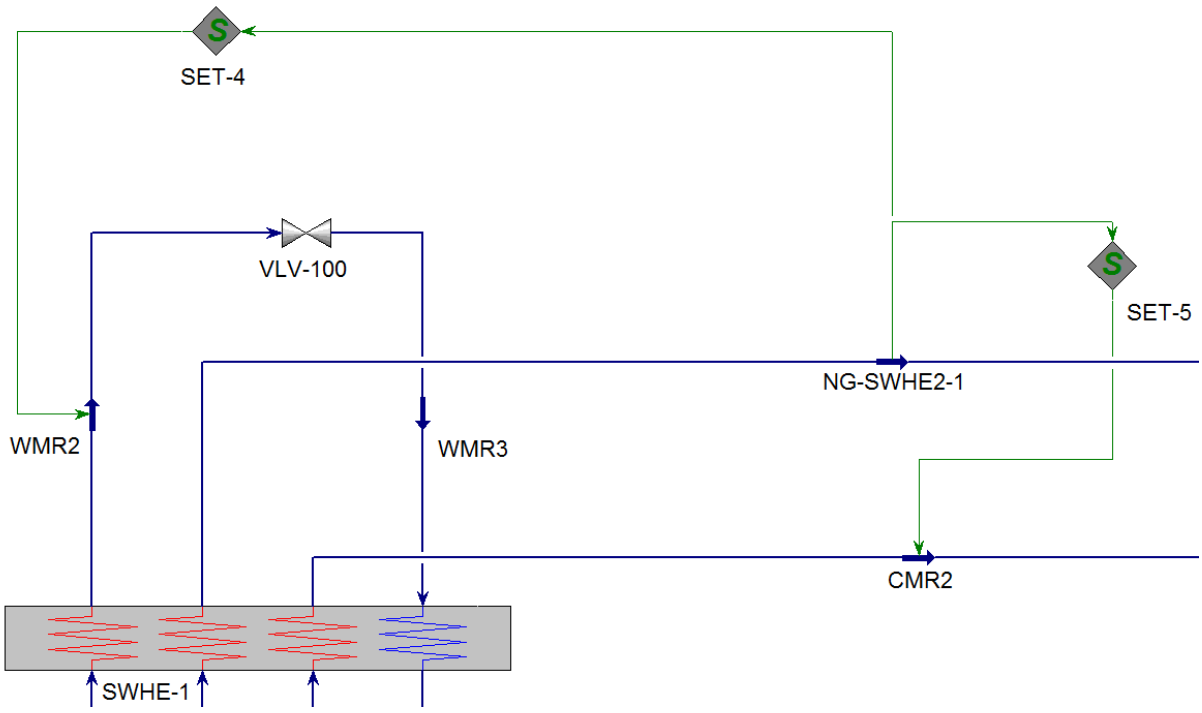

Figure 47: Applied process modifications in order to fulfill the study in Chapter

The optimizer parameters utilized in order to achieve the best objective value can be seen in Table 61.

Table 61: Best-case optimizer parameters according to the DMR modifications in Chapter 8.5

New Optimizer parameters	
Max. Iterations	2000
Objective Sale Factor	25
Accuracy Tolerance	10^(-8)
Step Restriction	1
Perturbation	0.0063
Max. Feasible Point	500

By utilizing the parameters in Table 61, the following objective value were achieved:

Excluded Pump Power (1)
$minf(x) = 934.97\ kJ/kg$

Included Pump Power (2)
$minf(x) = 940.51\ kJ/kg$

$$Total\ Compressor\ power = 104.9MW$$

$$Total\ Constraint\ violations = 0.0217$$

$$Outlet\ temperature\ of\ SWHE1 = -45.91°C$$

A comparison between the Kusmaya (2012) model and the model from Chapter 8.5 can be seen in Table 62.

Table 62: Comparison between the objective value from the model optimized by Kusmaya (2012) and the model optimized in Chapter 8.5. Ref. number 1 is for excluded pump power, ref. number 2 is for included pump power

Ref.	Objective value (kJ/kg) Kusmaya (2012)	Objective value (kJ/kg) Hyprotech SQP	Reduced Power Consumption
1	1138.90	934.97	17.91%
2	1140.67	940.51	17.56%

UA values from the optimized process can be seen in Table 63.

Table 63: UA values in the optimized process from Chapter 8.5

Unit	UA	LMTD
SWHE-1	52920 kW/K	3.213°C
SWHE2-1	38520 kW/K	3.208°C
SWHE2-2	9444 kW/K	3.231°C

The optimizer provided slightly better objective value when the temperature after SWHE-1 was fixed, however, the constraint violations were also higher, which may question whether the result in Chapter 8.1 should be considered equally good.

8.6 DMR process with integrated NGL extraction optimized by Kusmaya in regards to APCI design

Considering the DMR process with integrated NGL extraction, which can be seen in Appendix B, the complexity of the process is simplified, in which the simplifications can be seen in Chapter 5.2. The simplified model can be viewed as a DMR process with upstream NGL extraction with modifications in the natural gas stream at three points places, which can be seen in Figure 13 in Chapter 5.2.5, and a reflux stream with constant flow that goes through SWHE-1 and SWHE2-1-1. The simplified model can be seen in Appendix C.

The three different compositions that the natural gas stream will contain during the liquefaction process can be seen in Table 3 from Chapter 2.5. The inlet gas pressure is at 60 bara and the process temperature is at 22°C. The reflux stream has a mass flow of $1.61 \times 10^{-5}\ kg/s$.

Since the temperatures after all Spiral Wound Heat Exchangers have been set, the optimization variables will be the same as in Chapter 8.1. The objective value before optimizing are the following:

Excluded Pump Power (1)	**Included Pump Power (2)**
$minf(x) = 1063.01\ kg/s$	$minf(x) = 1064.26\ kg/s$

The optimizer parameters that were used to optimize the model can be seen in Table 64.

Table 64: Best-case optimizer parameters according to the DMR modifications in Chapter 8.6

New Optimizer parameters	
Max. Iterations	2000
Objective Sale Factor	25
Accuracy Tolerance	10^(-8)
Step Restriction	1
Perturbation	0.0060
Max. Feasible Point	500

By utilizing the optimizer parameters in Table 64, the following objective value were obtained:

Excluded Pump Power (1)	**Included Pump Power (2)**
$minf(x) = 960.38$	$minf(x) = 966.29$

A comparison between the objective value from the Kusmaya (2012) model and the Hyprotech SQP optimized model can be seen in Table 65.

Table 65: Comparison between the objective value from the DMR model with integrated NGL extraction optimized by Kusmaya (2012) and the model optimized by Hyprotech SQP in Chapter 8.6 concerning similar UA values and compressor drivers. Ref. number 1 is for excluded pump power, ref. number 2 is for included pump

Ref.	Objective value (kJ/kg) Kusmaya (2012)	Objective value (kJ/kg) Hyprotech SQP	Reduced Power Consumption
1	1063.01	960.38	9.65%
2	1064.26	966.29	9.21%

An important note concerning the results is that either the Kusmaya (2012) or the model optimized by Hyprotech SQP considered the energy use in the NGL extraction process. Considering the results from Table 65, the optimizer were able to improve the DMR process with integrated NGL extraction significantly even though the process were simplified. This result indicates that the process could be further improved when the entire NGL extraction is included in the optimization.

8.7 Comparison between pressure ratios

According to the theory from Chapter 2.4, the geometric mean pressure ratio should be the optimum ratio if the inlet temperature to each compressor is the same at each step. According to the studies by Austbø (2015), the optimum solution concerning the 2nd, 3rd and 4th pressure step in the CMR circuit, proved to be very close to the geometric mean pressure ratio, which can be seen in Eq. 1.

By considering the study from Chapter 8.1 with a modification that involves zero pressure drop in the coolers in the CMR circuit, is it possible to study whether or not the optimizer is providing a result according to the geometric mean pressure levels. In Table 66 can it be seen a comparison between the objective values in three modifications in regards to pressure ratio in the CMR circuit. The CMR4 and CMR11 variables represents the low and high pressure respectively, the other variables are the pressure ratios in the four-stage compression.

Table 66: Objective value comparison among three different modifications in regards to pressure ratio in the CMR circuit. The objective value is calculated with zero drop in the coolers

Variable	Unit	Best-Case	Geometric (4 compressors)	Geometric (3 compressors)
CMR4	Bar	5.711	5.711	5.711
CMR11	Bar	48.530	48.530	48.530
K-102	Pressure Ratio	3.970	1.708	3.970
K-103	Pressure Ratio	1.297	1.708	1.289
K-104	Pressure Ratio	1.298	1.708	1.289
K-108	Pressure Ratio	1.272	1.708	1.289
Objective value	kJ/kg	924.42	964.54	924.43

It can be seen from Table 66 that the Best-Case scenario provided by the Hyprotech SQP optimizer, resulted in the lowest objective value. In the Best-Case results can it be seen that with an exception in the first compressor stage, the pressure ratios were quite similar.

In the Geometric (3 compressors) scenario, three of the pressure ratios from the Best-Case scenario that had a pressure ratio close to geometric were manipulated to exact geometric differences to observe whether the objective value would improve. The objective value were slightly poorer than the Best-Case scenario.

The case that had all four compressor ratios calculated by the geometric mean had the highest objective value. The reason for that is that the inlet temperature of the first compressor differs drastically from the inlet temperatures in the two intermediate and high-pressure compressors, which are determined by the process temperature.

These results show both that the Hyprotech SQP optimizer is able to optimize pressure ratios in a good manner, and that the geometric mean approximation is a good approximation when calculating pressure ratios, as long as the required conditions are fulfilled.

8.8 Summary of Chapter 8

It can be seen in Table 67 and Table 68 that the Hyprotech SQP optimizer were able to improve the DMR model optimized by Kusmaya (2012) in several process modifications carried out in Chapter 8.1, 8.2, 8.3 and 8.4. It is important to notice that the small increase in LNG production in Chapter 8.4 is affected by the decrease in the total compressor power, which is 2.7MW less power consumption than in the Kusmaya (2012) model. When changing the objective function in Chapter 8.4, the optimizer provided a worse objective value, which should be noted considering that the objective function were set to increase the mass flow of produced LNG.

Considering Chapter 8.5 can it be seen that by including the outlet temperatures that exits SHWE-1 in the objective function does not contribute to a noticeable difference in the objective value in regards to process constraints. It can therefore be concluded that an outlet temperature of -48.3°C that was selected by Kusmaya (2012) is a decent temperature when optimizing a DMR model that has the same process conditions.

Considering the DMR process that can be seen in Appendix C, which is a simplified model described in Chapter 8.6. The optimizer managed to improve the process by 9.21% when the NGL extraction were not included in the calculation. From these results is it clear to see that there is much to gain by optimizing the entire DMR process that contain integrated NGL extraction.

Chapter 8.7 illustrates the importance of optimizing the pressure ratios in the compressors, even though the low and high pressures are set. The optimized pressure ratios provided significantly better objective value than the pressure ratio that relied on the geometric mean ratio. The Hyprotech SQP optimizer were also able to provide a better objective value than the case with three of the compressors with same inlet temperature adjusted accordingly to the pressure ratio provided by the geometric mean. The results can be seen in Table 66.

Table 67: Results from Chapter 8.1, 8.2, 8.3 and 8.4 according to objective value in regards to the objective function that includes pump power

Modification by Chapter	Improvement in the objective value based on the DMR process optimized by Kusmaya (2012)
Chapter 8.1	17.28 %
Chapter 8.2	8.52 %
Chapter 8.3	14.81 %
Chapter 8.4	3.69 %

Table 68: Increase in LNG production according to Chapter 8.3 and 8.4

Modification by Chapter	Improvement in the LNG production based on the DMR process optimized by Kusmaya (2012)
Chapter 8.3	17.20 %
Chapter 8.4	1.70 %

9 Conclusion and Recommendations

As this project is a pioneer project in regards to the Hyprotech SQP optimizer, challenges were encountered, such as the unwillingness by Aspentech to cooperate with necessary information concerning the Hyprotech SQP optimizer, even though questions were sent to Aspentech through a license that included customer support. Considering the unwillingness of Aspentech to cooperate, some of the information regarding the theory in Chapter 3.5 may be outdated.

The Hyprotech SQP optimizer is sensitive to changes, and considering the variable values, variable boundaries and process constraints, modifications in either of these will affect the optimizer results, as well as Flowsheet modifications.

Concerning the variable values and variable boundaries, if the variable boundaries are too narrow, the optimizer may not be able to converge to a good objective value. However, if the variable boundaries are too wide, the optimizer may not be able to run at all. Therefore, knowledge in regards to the selected process that is optimized is necessary in order to select proper variable boundaries.

Concerning the Flowsheet and process constraints, the process constraints should be set in order to assist the Flowsheet to provide a realistic model. Modifications in either the Flowsheet or the process constraints will affect the optimizer results.

Considering that the optimizer is sensitive to modifications, adjusting the optimizer parameters is a key factor to obtain a good objective value. An important note to keep in mind when optimizing is that the Hyprotech SQP optimizer is not a global optimizer, which can be seen in Chapter 3.5.2, therefore, the results obtained from optimizing should be analyzed thoroughly to see if there is room for realistic improvements. By performing analysis concerning the optimizer parameters in Chapter 6.1.1 and Chapter 7.1 can it be seen that the Maximum Iterations, Feasible Points, Accuracy Value and Step Restriction parameters, as well as two sided gradient calculations should be set at fixed values to avoid limiting the optimizer.
The Maximum Iteration and Feasible Points parameters should be set to a high value to avoid search limitations. The Step Restriction should be set to 1 or higher, which means that there will be no Step Restriction. By setting the Accuracy Tolerance at a low value, the optimizer will provide an objective value with the best achievable accuracy value concerning the set parameter and derivative values, therefore, the Accuracy Tolerance should be set to such low value that the optimizer displays “Step Convergence” as termination reason. The optimization should be performed with two-sided gradient calculations, which performs twice as many calculations as one-sided gradient calculations. These parameter settings are provided in order to obtain a good objective value regardless of time consumption.

The parameter values that may need adjustments are the Objective Scale Factor and Perturbation parameters. An observation has been that small changes in the Perturbation parameter may solve small modifications in the processes, while modifications that are more extensive may require adjustments in the Objective Scale Factor parameter.

During this thesis, sensitivity analyses in regards of the optimizer parameters was carried out by performing 10 and 10 optimizations simultaneously, where each of the optimizations were carried out with equal Flowsheet and derivative specifications. If optimization is carried out on an old or slow computer, fewer optimizations should run simultaneously considering that 10 simultaneous optimizations is demanding. Considering the objective values obtained in this report, among 80 – 90 optimizations were performed and analyzed in order to obtain each of the objective values provided in the case studies, which means that several thousand optimizations were performed during this thesis. With exceptions in Chapter 6.1.1 and 7.1, the parameters that were adjusted were only the Objective Scale Factor or Perturbation parameters, as the others were set at fixed values.

In Chapter 6, the objective function had included pump power, which in Chapter 7 provided challenges when optimizing. The challenges arose from an iteration process that took place in a parallel circuit when utilizing different efficiencies in the compressor and pump, in which the efficiencies were polytropic and adiabatic, respectively. The challenges resulted in a new objective function with excluded pump power that was utilized in Chapter 7 and 8.

Concerning the results obtained while studying the Prico process in Chapter 6, with the pump power included in the objective function, can it be seen that the optimizer struggled in obtaining a good objective value, which can be seen when comparing the results with different temperatures at fixed and adjustable pressure levels. The optimizer provided in some cases better objective values when utilizing fixed pressure levels instead of adjustable pressure levels, which indicate that the optimizer is providing poor objective values in the Prico process with adjustable pressure levels.

When removing the pump power from the objective function, the case studies performed in Chapter 7 and 8 obtained good objective values, and it can be seen that the Hyprotech SQP optimizer is able to optimize advanced liquefaction processes. Even though the pump power was excluded from the objective function, the sub-chapters in Chapter 7 and Chapter 8 show objective values with both included and excluded pump power. This was achieved by adding the pump power to the objective value in retrospect.

Considering the DMR process in Chapter 7, the Hyprotech SQP optimizer were able to provide logical decisions throughout the Chapter concerning refrigerant composition and pressure variables. The optimizer results provided inputs to different process modifications and their effect on the process, in addition to keep the UA values of the Spiral Wound Heat Exchangers within the limits of what is normal in a DMR process. The optimizer also managed to optimize in regards to four different process temperatures and provide objective values that upheld the constraints. The reason that the optimizer were able to optimize the DMR process better than the Prico process may be that the objective function in the DMR process did not include the pump power with adiabatic efficiency, which made the optimizer avoid the extra iteration process with two units that has different efficiencies working in parallel.

When the Hyprotech SQP optimizer were challenged by improving an earlier optimized DMR process provided by Kusmaya (2012) designed according to APCI with an upstream NGL

extraction, two results stood out. When the process were optimized according to the conditions described in Chapter 8.1, the optimizer were able to improve the objective value by 17.28%. Considering that the DMR process provided by Kusmaya (2012) were based on compressor drivers, an optimization performed in Chapter 8.3, which utilized similar compressor drivers were able to improve the mass flow of produced LNG by 17.20%, thus improving the objective value by 14.81%.

Results from Chapter 7 and 8 shows the potential of utilizing the Hyprotech SQP optimizer concerning several modifications. When utilized correctly the optimizer is able to operate with a good accuracy and is able to provide great process improvements. The downside by the Hyprotech SQP optimizer is that it is not a global optimizer. This means that adjustments of the objective scale factor and perturbation value, as well as the initial variable values and variable boundaries are of great importance. Even after 90 optimizations in regards of different Perturbation or Objective Scale Factor values, the best objective value obtained is not necessarily the global minimum.

Considering the results from these studies and the fact that the Hyprotech SQP is not a global optimizer, the Hyprotech SQP optimizer should not be considered as a tool for providing the optimal solution, but rather an assisting tool utilized for process improvements.

10 Further Work

As this thesis were carried out in order to explore the Hyprotech SQP optimizer capabilities concerning optimization of liquefaction processes relevant to FLNG units, the Hyprotech SQP optimizer were studied in regards of its derivative utility and parameters. Flowsheet modifications were also carried out in order to achieve good objective values.

In order to further explore the Hyprotech SQP optimizers ability to optimize liquefaction processes, Flowsheet modifications in order to simplify the optimization task should be considered as important as adjusting the derivative utility and optimizer parameters.

By optimizing advanced liquefaction processes with integrated NGL extraction, the optimizer may experience several challenges according to the increasing number of adjustable variables and constraints. In addition to the process containing more variables and constraints, there will also be a separation column that has to perform its own iterations that may not cooperate well with the iterations that are being performed by the optimizer.

Optimization of other liquefaction processes may also be carried out. To further challenge the optimizer, including end flash in the optimization will also provide the optimizer with more variables and constraints.

Considering there are several optimizers utilized in process optimization, a study that compare results between other optimizers and the Hyprotech SQP optimizer in terms of simple and advanced liquefaction processes may assist the user whether or not the Hyprotech SQP optimizer is capable of providing a sufficient objective value concerning the process.

11 References

Aspelund, A., Gundersen, T., Myklebust, J., Nowak, M.P., Tomasgaard, A. (2009) "*An optimization-simulation model for a simple LNG process*" NTNU, Trondheim, Norway

Alkaya, D., Vasantharajan, S. & Biegler, L. T. (2001) "*Successive Quadratic Programming: Applications in the Process Industry".* Encyclopedia of Optimization, Kluwer Academic Publishers, Dordrecht, Netherland, p. 2574-2587

Aspentech Hysys software V8.3

Aspen HYSYS petroleum Refining (2011) "*Unit Operations Guide*" (For version 7.3)

Biegler, L.T (2010), "*Nonlinear Programming: Concepts, Algorithms, and applications to Chemical Processes".* Carnegie Mellon University Pittsburgh, Pennsylvania

Boyd, S. & Vandenberghe, L. (2004) "*Convex Optimization"* Cambridge University press, USA

Bukowski, J, Liu, Y. N., Boccella, S & Kowalski, L (2011) "*Innovations in Natural Gas Liquefaction technology for future LNG plants and floating LNG facilities"* Air Products and Chemicals, Inc, International Gas Union Research Conference (www.airproducts.com)

Cao, W., Lu, X., Lin, W. and Gu, A. (2005) "*Parameter comparison of two small-scale natural gas liquefaction processes in skid-mounted packages*" Shanghai jiao tong university, China. Applied Thermal Engineering, volume 26, issue 8-9

Chinneck, J. W. (2012) "*Practical Optimization: A gentle introduction"* Charleton University, Ottawa, Canada

GE Energy (2008), *LM6000-50/60 HZ Gas Turbine Generator Set Product Specification*, Houston Texas, USA

Gibbons, P. B., Abdelzaher, T., Aspnes, J. & Rao, R. (2006) "*Distributed Computing in Sensor Systems"* San Francisco, CA, USA) CH 4.2 (gradient-free stochastic algorithms).

Glandt, E. D., Klein, M. T. & Edgar, T.F. (1988) "*Optimization of chemical processes"* McGraw-Hill, USA

Hatcher, P., Khalipour, R., Abbas, A. (2012) "*Optimisation of LNG mixed-refrigerant processes considering operation and design objectives"* School of Chemical and Biomolecular Engineering University of Sydney, Australia. Computers & Chemical Engineering, volume 41, 2012, pg 123 – 133. Elsevier Ltd.

Koelet, P.C. & Gray,T.B. (1992) "*Industrial Refrigeration Principles, Design and Application"* Ohio state University, Columbus, Ohio

Kusmaya, M. (2012) *"LPG Extraction on FLNG"* Institute for Energy and Process Technology" NTNU, Trondheim, Norway

Luenberger, David G. & Yinyu Ye (2008) "*International series in operations research and management science, Linear and Nonlinear Programming third edition"* Stanford University, USA

Mahabadipour, H., Ghaebi, H. (2012) "*Development and comparison of two expander cycles used in refrigeration system of olefin plant based on exergy analysis"* Iran. Applied Therman Engineering volume 50, issue 1, 2013, pg 771 – 780, Elsevier Ltd.

Mokhatab, S. & Poe, W. A. (2012) "*Handbook of Natural Gas Transmission and Processing"* Elsevier Wyman Street, Waltham, USA

Nocedal, J & Wright, S. J. (1999) "*Numerical optimization"* Springer-Verlag New York, inc.

Pedersen, K. S., Christensen, P. L. & Azeem, J. S. (2006) "*Phase Behavior of Petroleum Reservoir Fluids"* CRC Press, Taylor & Francis Group

Pettersen, J. (2012) "*Compendium LNG Technology"* NTNU, Trondheim, Norway

Rangaiah, G.P. (2009) "Multi-Objective Optimization: Techniques and Applications in Chemical Engineering" Singapore

Roberts et al. "*United States Patents 6,269,655 B1*" 7 August 2001

Rødstøl, E. (2014) "*Optimization of liquefaction processes using built-in functions in Hysys* Institute for Energy and Process Technology" NTNU, Trondheim, Norway

Secanell, M. & Suleman, A. (2005) "*Numerical Evaluation of Optimization Algorithms for Low-Reynolds-Number Aerodynamic Shape Optimization"* University of Victoria, Canada

Shariq, M., Chaniago, Y. D., Getu, M & Lee, M. (2014) "*Energy saving opportunities in integrated NGL/LNG schemes exploiting: Thermal-coupling common-utilities and process knowledge"* Chemical Engineering and Processing: Process Intensification, Elsevier B.V. p. 54 – 64.

Talib, J. H. & Price, B. C. (2011) "*Development of Floating LNG Production Units with Modular/Scalable SMR Processes"* Offshore Technology Conference held in Houston USA 2–5 of May 2011.

Thulukkanam, K (2013) "*Heat Exchanger Design Handbook second edition"* CRC Press, Taylor & Francis Group.

Wang, M., Khalilpour, R., Abbas, A (2013) "*Operation optimization of propane precooled mixed refrigerant processes"* School of Chemical and Biomolecular Engineering, The University of Sydney, Australia. Journal of Natural Gas Science and Engineering, volume 15, 2013, pg 93 – 105, Elsevier Ltd.

Weise, T., Zapf, M., Chiong, R. & Nebro, A. J. (2009) "*Why Is Optimization Difficult?"* section 1 in: Chiong, R. (2009) "*Nature-Inspired Algorithms for Optimisation"* Springer-Verlag Berlin Heidelberg

Appendix A: Hysys DMR with upstream NGL extraction

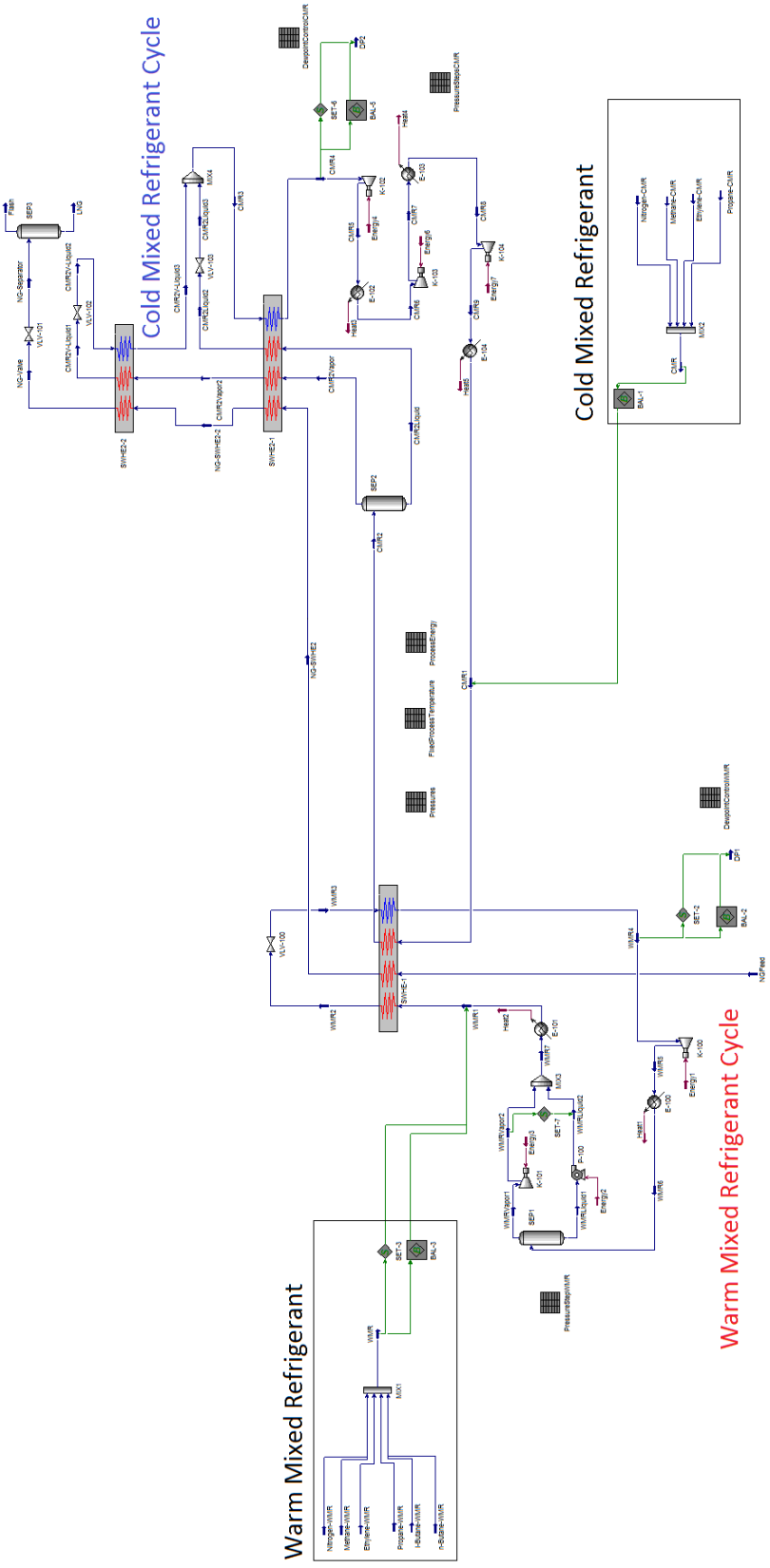

Appendix B: Hysys DMR with integrated NGL extraction

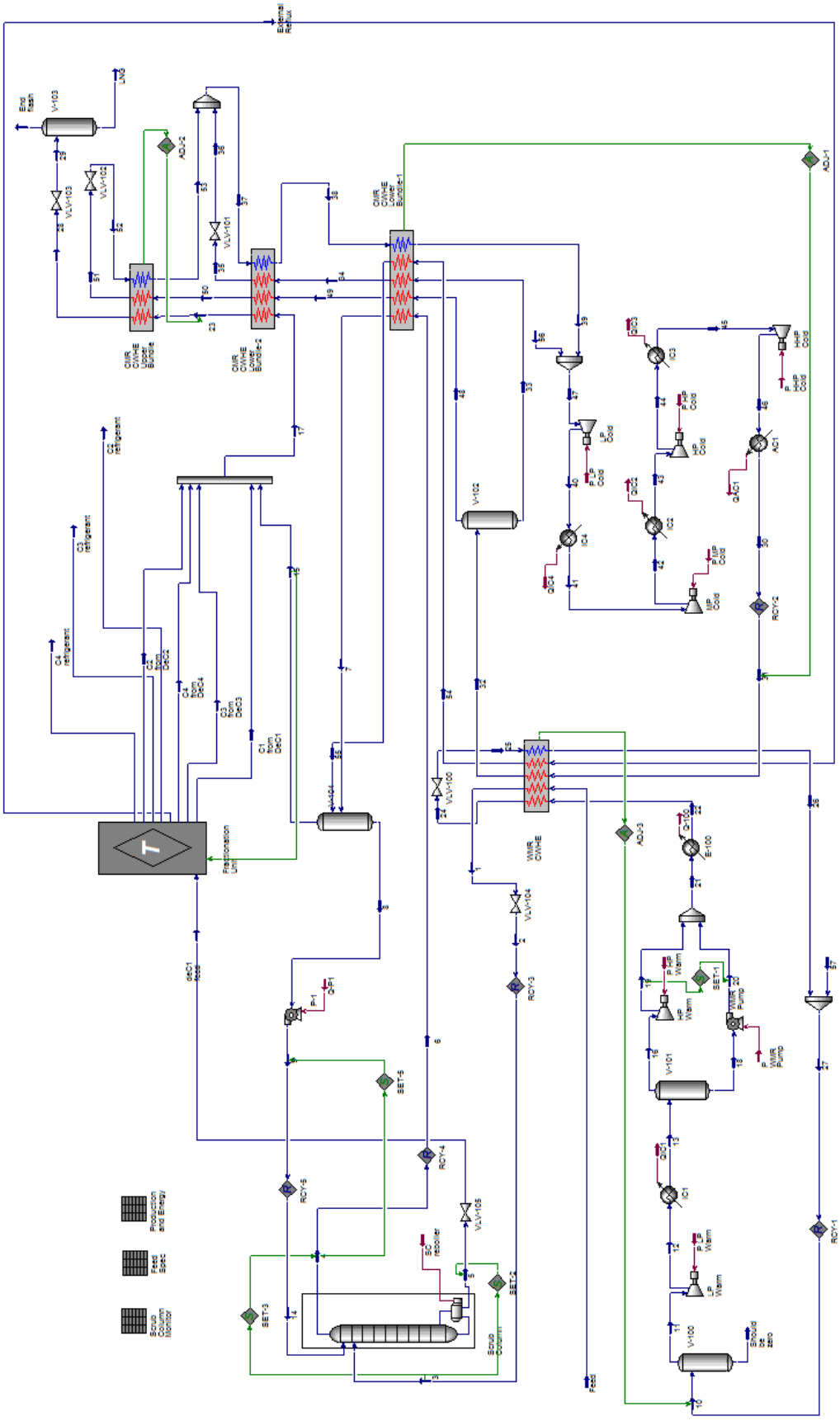

Appendix C: Hysys DMR with illustrated integrated NGL extraction

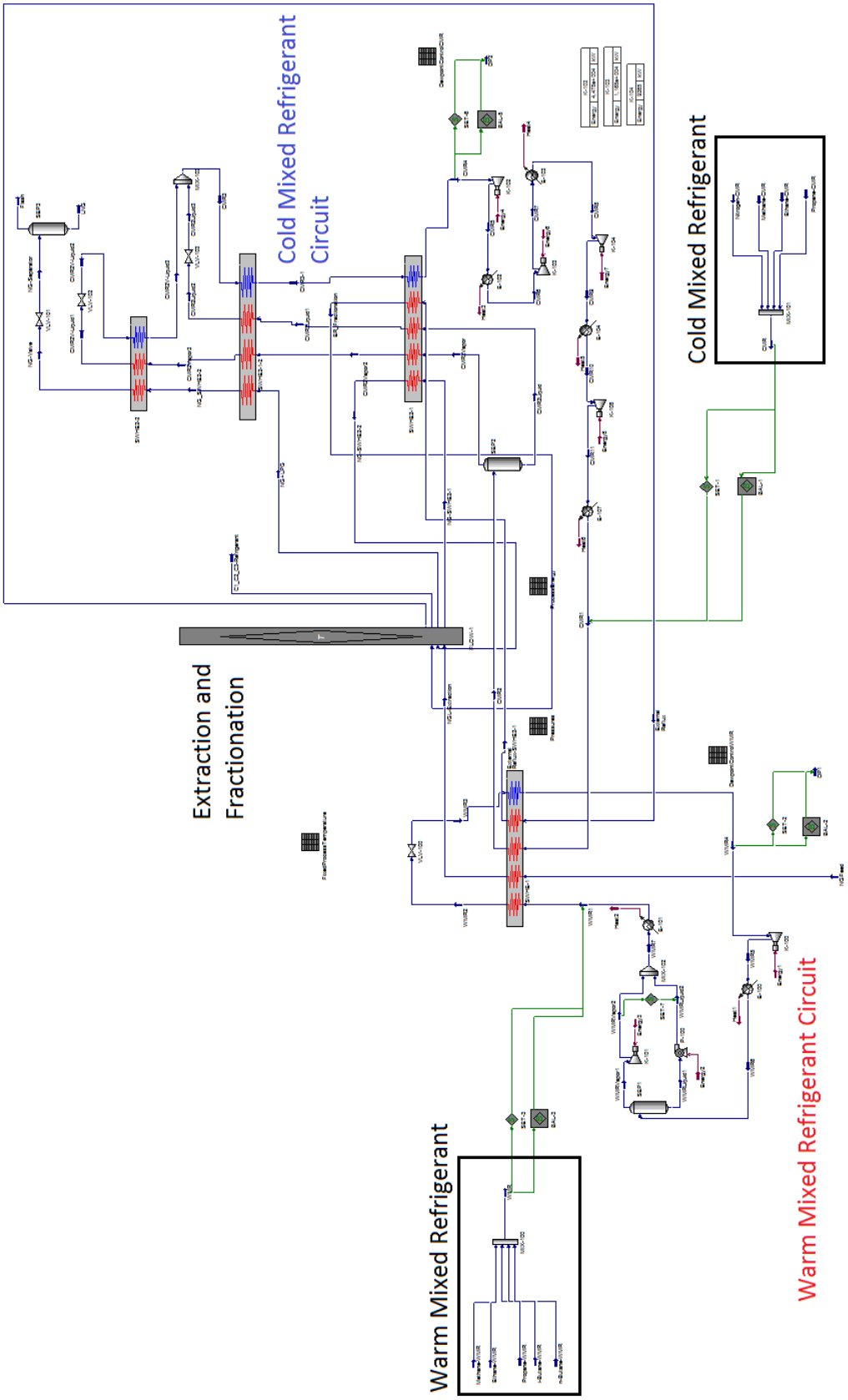

Appendix D: Hysys Prico Process

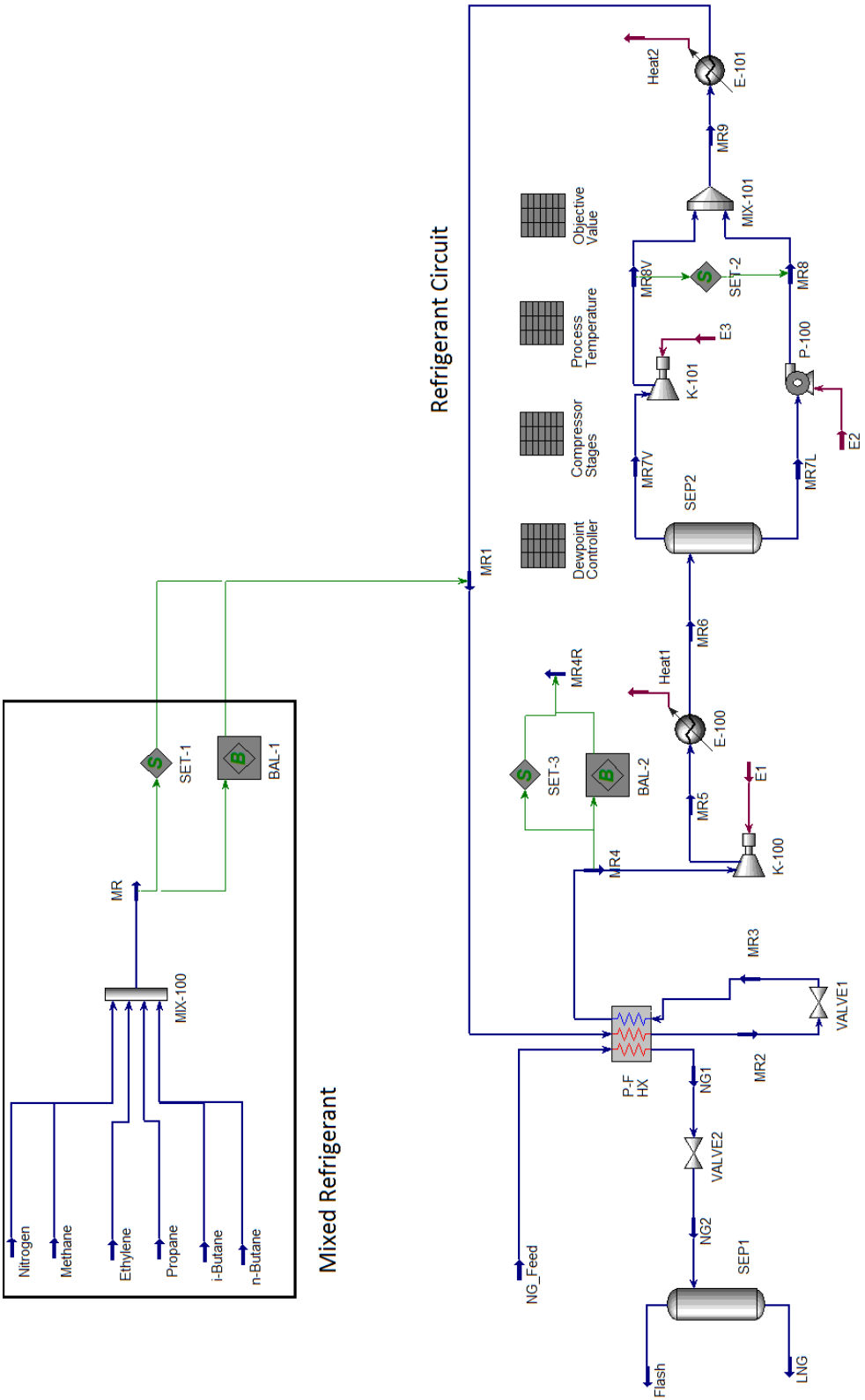

Appendix E: Convergence Time in the Prico process

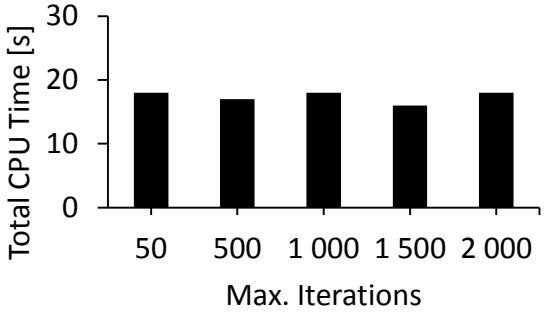

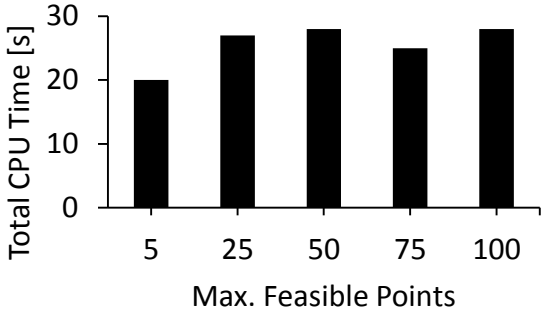

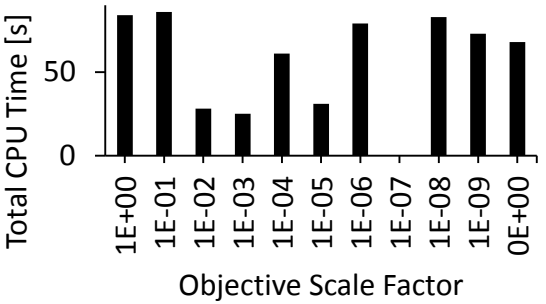

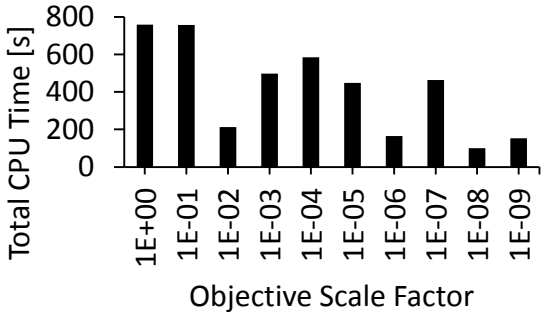

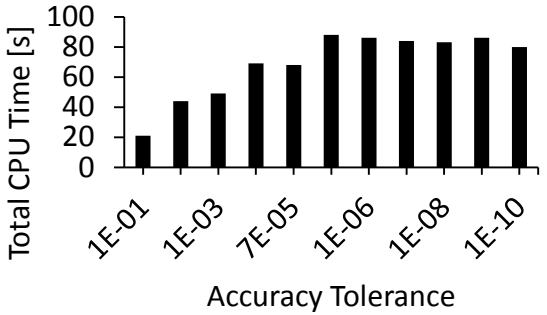

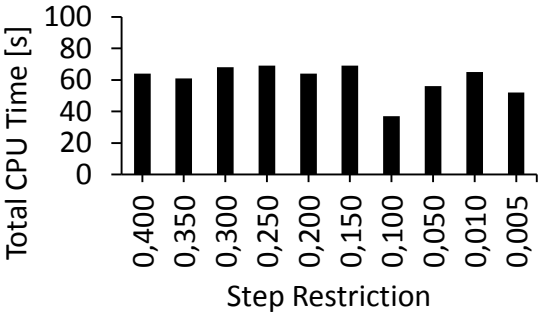

Appendix F: Randomly selected initial variable values in the Prico Process

Variable	1	2	3	4	5	6	7	8	9	10
	1	2	3	4	5	6	7	8	9	10
Nitrogen	13007	13354	11015	19281	11468	5925	6196	17381	6439	10615
Methane	16968	8977	17857	22749	18561	7391	14222	12155	22441	8460
Ethylene	28589	23824	21096	14592	23866	25248	19240	25374	31645	18326
Propane	8564	10077	6714	4164	4227	12775	3266	13064	8709	2968
i-Butane	536	6961	5605	7307	3243	7946	5392	8728	2278	8442
n-Butane	4659	8806	746	5846	9062	3696	584	1972	1965	9116
MR4	7,94	2,91	2,80	5,86	5,47	3,14	2,86	7,19	6,99	5,03

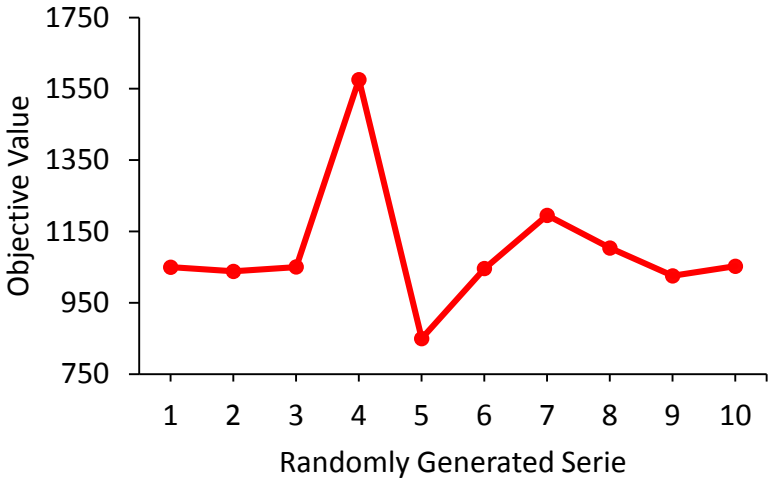

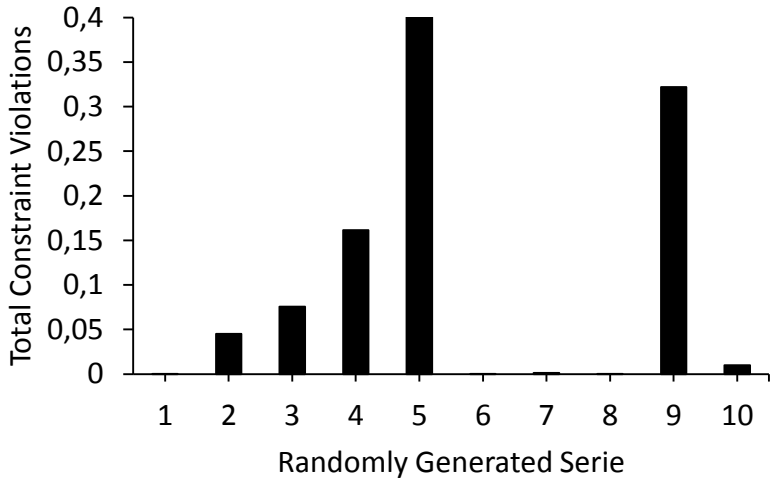

Appendix G: Convergence Time in the DMR process from Chapter 7.1

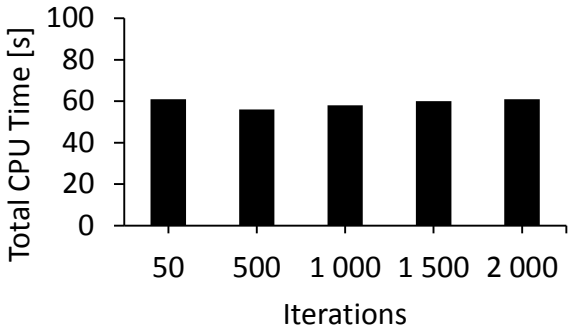

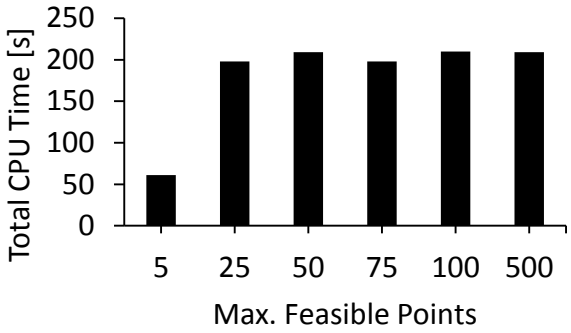

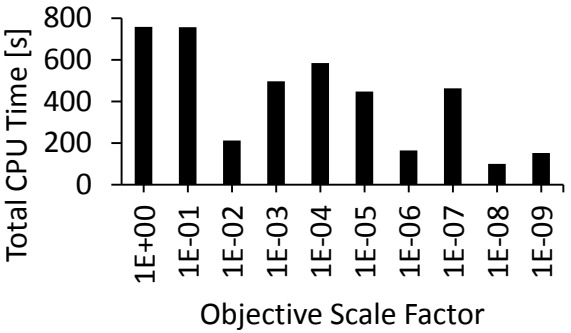

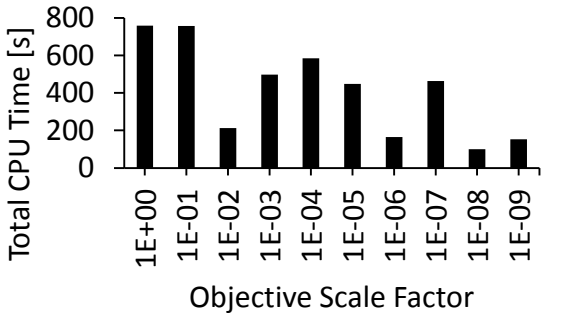

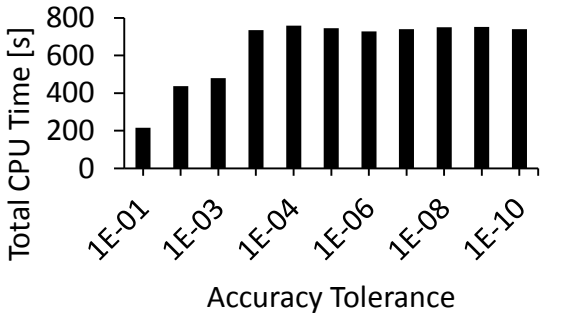

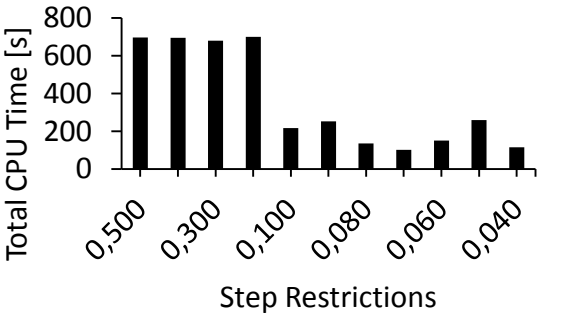

Appendix H: Optimization variables DMR with adjustable intermediate and high pressures

Optimization Variables in the DMR process with adjustable intermediate and high pressures

Tag	Property	Unit	Minimum	Initial Value	Maximum
Nitrogen-WMR	Molar Flow	[kgmole/h]	10	250	2000
Methane-WMR	Molar Flow	[kgmole/h]	750	1500	10000
Ethylene-WMR	Molar Flow	[kgmole/h]	20000	27227	35000
Propane-WMR	Molar Flow	[kgmole/h]	3500	9900	15000
i-Butane-WMR	Molar Flow	[kgmole/h]	50	800	5000
n-Butane-WMR	Molar Flow	[kgmole/h]	50	800	5000
Nitrogen-CMR	Molar Flow	[kgmole/h]	7500	11000	15000
Methane-CMR	Molar Flow	[kgmole/h]	10000	16000	20000
Ethylene-CMR	Molar Flow	[kgmole/h]	10000	24000	30000
Propane-CMR	Molar Flow	[kgmole/h]	500	1100	2000
WMR3	Pressure	[Bar]	1	6	20
WMR5	Pressure	[Bar]	8	16.05	25
WMRVapor2	Pressure	[Bar]	30	46	55
CMR4	Pressure	[Bar]	1	6	15
CMR5	Pressure	[Bar]	10	12.56	32
CMR7	Pressure	[Bar]	21	25.23	45
CMR1	Pressure	[Bar]	41	54.5	70

Appendix I: WMR Composition analysis in the DMR process from Chapter 7.1

WMR composition in Chapter 7.1.1

Component	Amount of each component (%)
Nitrogen	1.94
Methane	10.62
Ethylene	58.84
Propane	23.87
i-Butane	4.45
n-Butane	0.28

WMR composition in Chapter 7.1.2

Component	Amount of each component (%)
Nitrogen	0.75
Methane	7.15
Ethylene	61.65
Propane	23.37
i-Butane	3.69
n-Butane	3.38

WMR composition in Chapter 7.1.3

Component	Amount of each component (%)
Nitrogen	0.03
Methane	7.69
Ethylene	63.29
Propane	20.79
i-Butane	2.01
n-Butane	6.20

Appendix J: WMR Composition analysis in the DMR process from Chapter 7.3

WMR composition in regards to the modifcations from Chapter 7.3.1

Component	Amount of each component (%)
Nitrogen	0.22
Methane	4.50
Ethylene	63.61
Propane	21.52
i-Butane	2.25
n-Butane	7.90

WMR composition in regards to the modifcations from Chapter 7.3.2

Component	Amount of each component (%)
Nitrogen	0.03
Methane	7.15
Ethylene	57.73
Propane	30.25
i-Butane	0.34
n-Butane	4.51

WMR composition in regards to the modifcations from Chapter 7.3.3

Component	Amount of each component (%)
Nitrogen	0.27
Methane	3.61
Ethylene	61.77
Propane	26.43
i-Butane	0.13
n-Butane	7.78

Appendix K: Fixed specifications in the Kusmaya DMR process.

Component specifications in the DMR model provided by Kusmaya (2012)

Tag	Equipment	Property	Unit	Value
P-100	Pump	Adiabatic Efficiency	Percent (%)	75
K-100 – 104	Compressors	Polytropic Efficiency	Percent (%)	78
K-108	Compressor	Polytropic Efficiency	Percent (%)	78
E-100 – 104	Coolers	Pressure Drop	[Bar]	0.5
E-107	Cooler	Pressure Drop	[Bar]	0.5
SWHE-1	Heat Exchanger	Pressure drop Tube side	[Bar]	5, 5.5 and 4 respectively
SWHE-1	Heat Exchanger	Pressure drop Shell side	[Bar]	0.3
SWHE2-1	Heat Exchanger	Pressure drop Tube side	[Bar]	2.07, 2 and 1.9 respectively
SWHE2-1	Heat Exchanger	Pressure drop Shell side	[Bar]	0.22
SWHE2-2	Heat Exchanger	Pressure drop Tube side	[Bar]	4.95 and 2.7 respectively
SWHE2-2	Heat Exchanger	Pressure drop Shell side	[Bar]	0.11

Fixed stream specifications in the DMR model provided by Kusmaya (2012)

Tag	Property	Unit	Value
CMR2	Temperature	[°C]	-48.3
NG-SWHE2-1	Temperature	[°C]	-48.3
WMR2	Temperature	[°C]	-48.3
NG-SWHE2-2	Temperature	[°C]	-116.5
CMR2Vapor2	Temperature	[°C]	-116.5
CMRLiquid2	Temperature	[°C]	-116.5
NG-Valve	Temperature	[°C]	-162.0
CMR2V-Liquid1	Temperature	[°C]	-162.0
NG-Separator	Pressure	[Bar]	1.240
NGFeed	Molar Flow	[kgmole/h]	24670
NGFeed	Pressure	[Bar]	59.5

Appendix L: Pre Optimization specifications in the Kusmaya model

Adjustable variables utilized to improve the DMR process optimized by Kusmaya (2012)

Tag	Property	Unit	Minimum	Initial Value	Maximum
Methane-WMR	Molar Flow	[kgmole/h]	750	1500	10000
Ethane-WMR	Molar Flow	[kgmole/h]	20000	27227	35000
Propane-WMR	Molar Flow	[kgmole/h]	3500	9900	15000
i-Butane-WMR	Molar Flow	[kgmole/h]	50	800	5000
n-Butane-WMR	Molar Flow	[kgmole/h]	50	800	5000
Nitrogen-CMR	Molar Flow	[kgmole/h]	2000	11000	15000
Methane-CMR	Molar Flow	[kgmole/h]	10000	16000	20000
Ethane-CMR	Molar Flow	[kgmole/h]	10000	24000	30000
Propane-CMR	Molar Flow	[kgmole/h]	500	1100	2000
WMR3	Pressure	[Bar]	1	6	20
WMR5	Pressure	[Bar]	8	16	25
WMRVapor2	Pressure	[Bar]	30	46	55
CMR4	Pressure	[Bar]	1	6	15
CMR5	Pressure	[Bar]	10	12.56	32
CMR7	Pressure	[Bar]	21	25.23	35
CMR9	Pressure	[Bar]	35.2	39.45	45
CMR1	Pressure	[Bar]	41	54.5	70

Constraints utilized to improve the DMR process optimized by Kusmaya (2012)

Tag name	Restriction	Minimum	Initial value	Maximum
WMR1	Vapor Fraction	Empty	0	0
SWHE-1	Temperature approach	2	-11.10	Empty
SWHE2-1	Temperature approach	2	1.12	Empty
SWHE2-2	Temperature approach	2	-0.49	Empty
WMR4-DP1	Temperature approach	6	48.61	Empty
WMR4-CMR1	Temperature approach	3	-11.10	Empty
CMR4-DP2	Temperature approach	6	-4.98	Empty

Appendix M: Best case values in the Kusmaya process according to Chapter 8.1

Best Case variables in the improved Kusmaya (2012) DMR process according to Chapter 8.1

Tag	Property	Unit	Minimum	Initial Value	Maximum
Methane-WMR	Molar Flow	[kgmole/h]	750	2201	10000
Ethane-WMR	Molar Flow	[kgmole/h]	20000	20150	35000
Propane-WMR	Molar Flow	[kgmole/h]	3500	3500	15000
i-Butane-WMR	Molar Flow	[kgmole/h]	50	3129	5000
n-Butane-WMR	Molar Flow	[kgmole/h]	50	4347	5000
Nitrogen-CMR	Molar Flow	[kgmole/h]	7500	5115	15000
Methane-CMR	Molar Flow	[kgmole/h]	10000	16479	20000
Ethane-CMR	Molar Flow	[kgmole/h]	10000	17296	30000
Propane-CMR	Molar Flow	[kgmole/h]	500	701.64	2000
WMR3	Pressure	[Bar]	1	6.33	20
WMR5	Pressure	[Bar]	8	18.66	25
WMRVapor	Pressure	[Bar]	30	34.18	55
CMR4	Pressure	[Bar]	1	5.53	15
CMR5	Pressure	[Bar]	10	24.41	32
CMR7	Pressure	[Bar]	21	32.70	45
CMR9	Pressure	[Bar]	35.2	40.94	45
CMR1	Pressure	[Bar]	41	48.39	70

Appendix N: Comparison between the Original and Optimized Kusmaya model according to Chapter 8.1

Comparison between the pressure levels according to the optimization in Chapter 8.1 and the Kusmaya (2012) model

Tag Original/Optimized	Property	Unit	Kusmaya Model	Optimized Model
25/WMR3	Pressure	[Bar]	8.60	6.33
12/WMR5	Pressure	[Bar]	19.74	18.66
19/WMRVapor2	Pressure	[Bar]	46.95	34.18
35/CMR4	Pressure	[Bar]	4.68	5.53
40/CMR5	Pressure	[Bar]	14.50	24.41
42/CMR7	Pressure	[Bar]	23.00	32.70
44/CMR9	Pressure	[Bar]	36.00	40.94
30/CMR1	Pressure	[Bar]	55.00	48.39

Comparison between the WMR composition according to the optimization in Chapter 8.1 and the Kusmaya (2012) model

Property	Unit	WMR Stream Kusmaya Model	WMR Stream Optimized Model
Methane	Mole Fraction	0.1200	0.0661
Ethane	Mole Fraction	0.6850	0.6046
Propane	Mole Fraction	0.0789	0.1050
i-Butane	Mole Fraction	0.0614	0.0939
n-Butane	Mole Fraction	0.0547	0.1304
Molar Flow	[kgmole/h]	38030	33330
Mass Flow	[kg/s]	346	341

Comparison between the CMR composition according to the optimization in Chapter 8.1 and the Kusmaya (2012) model

Property	Unit	CMR Stream Kusmaya Model	CMR Stream Optimized Model
Nitrogen	Mole Fraction	0.1617	0.1292
Methane	Mole Fraction	0.3979	0.4162
Ethane	Mole Fraction	0.4304	0.4369
Propane	Mole Fraction	0.0100	0.0177
Molar Flow	[kgmole/h]	39860	39590
Mass Flow	[kg/s]	269	266

Appendix O: Heat Exchanger curves Kusmaya Original model

SWHE-1/WMR CWHE

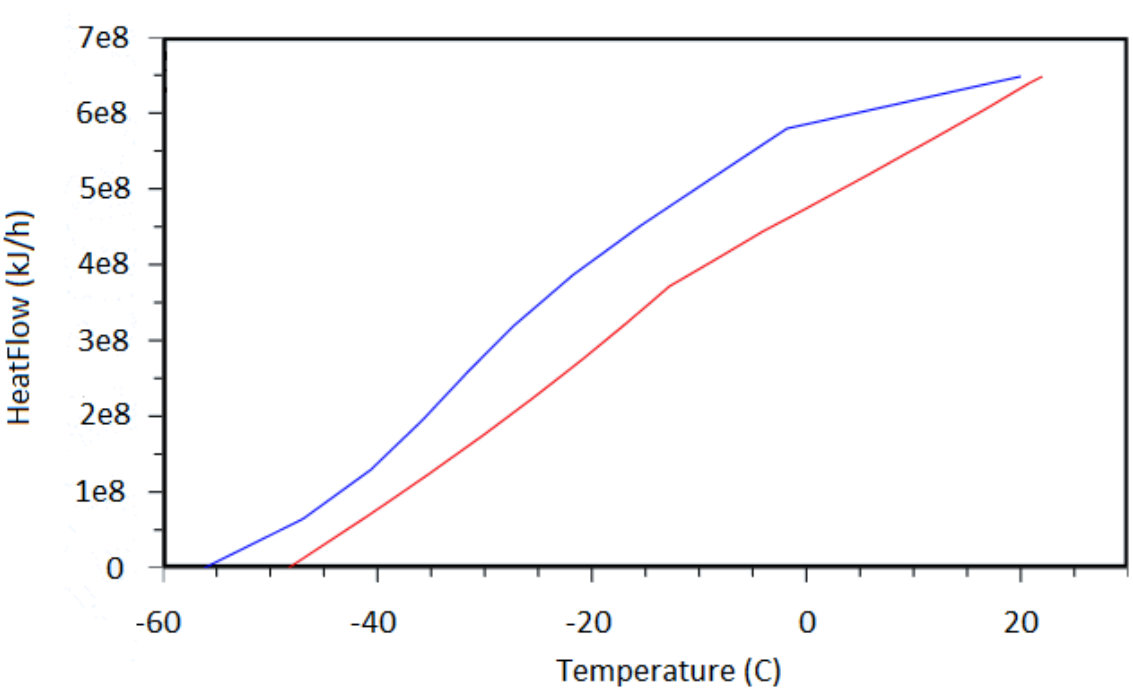

SWHE2-1/CMR CWHE Lower Bundle

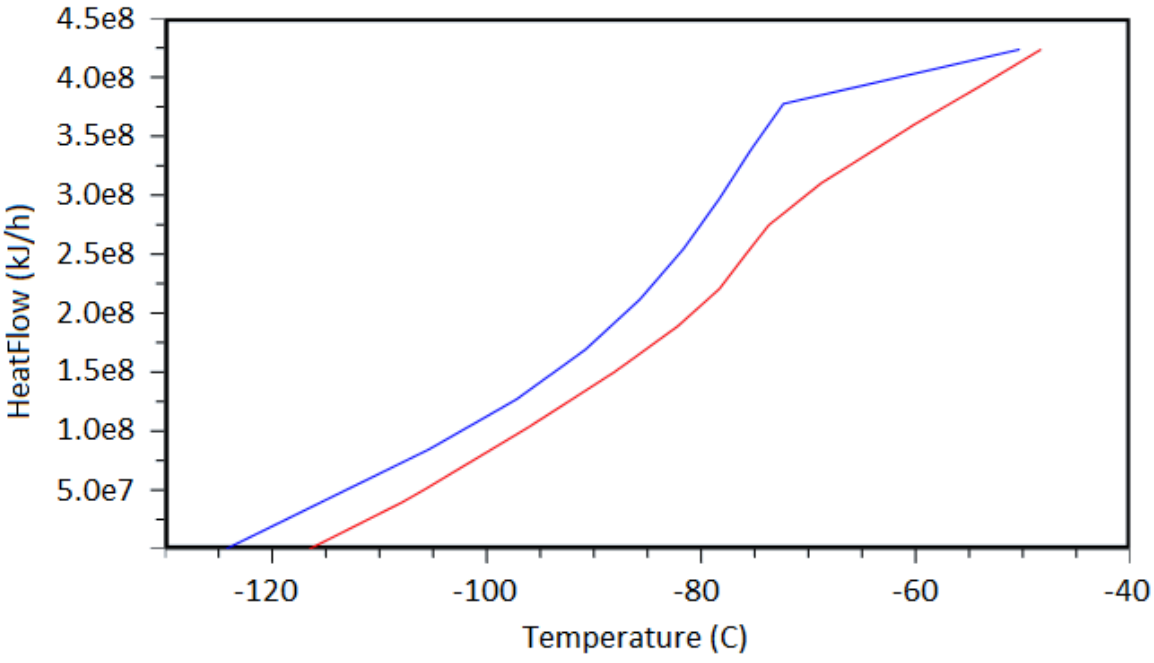

SWHE2-2/CMR CWHE Upper Bundle

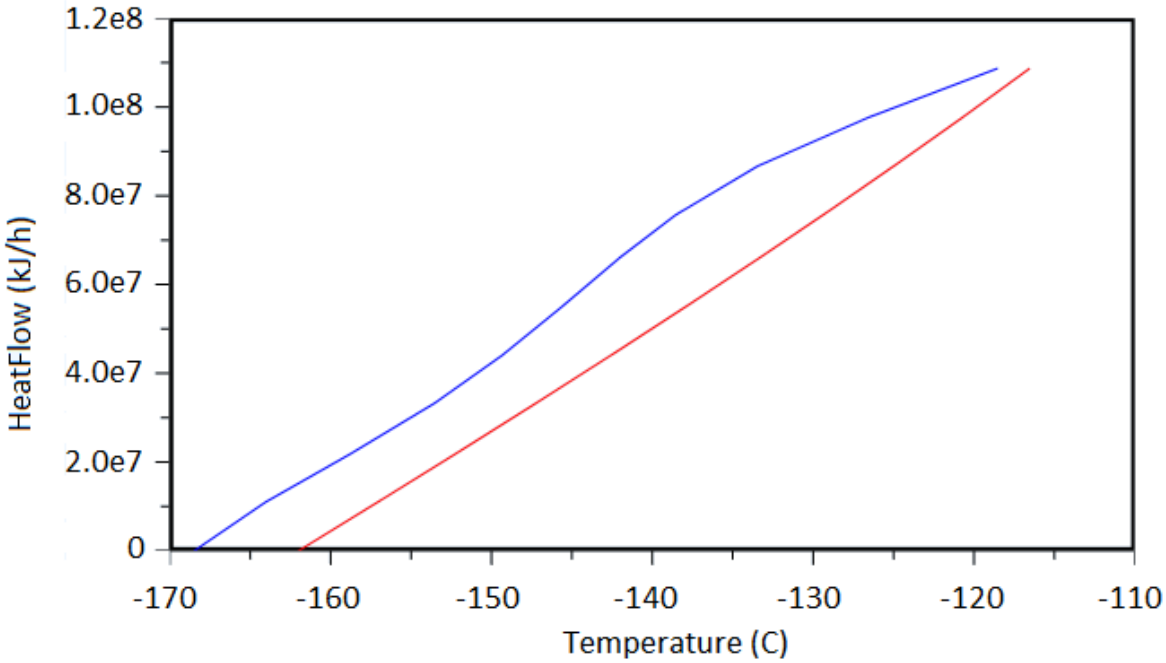

Appendix P: Heat Exchanger curves Kusmaya post optimization

SWHE-1/WMR CWHE

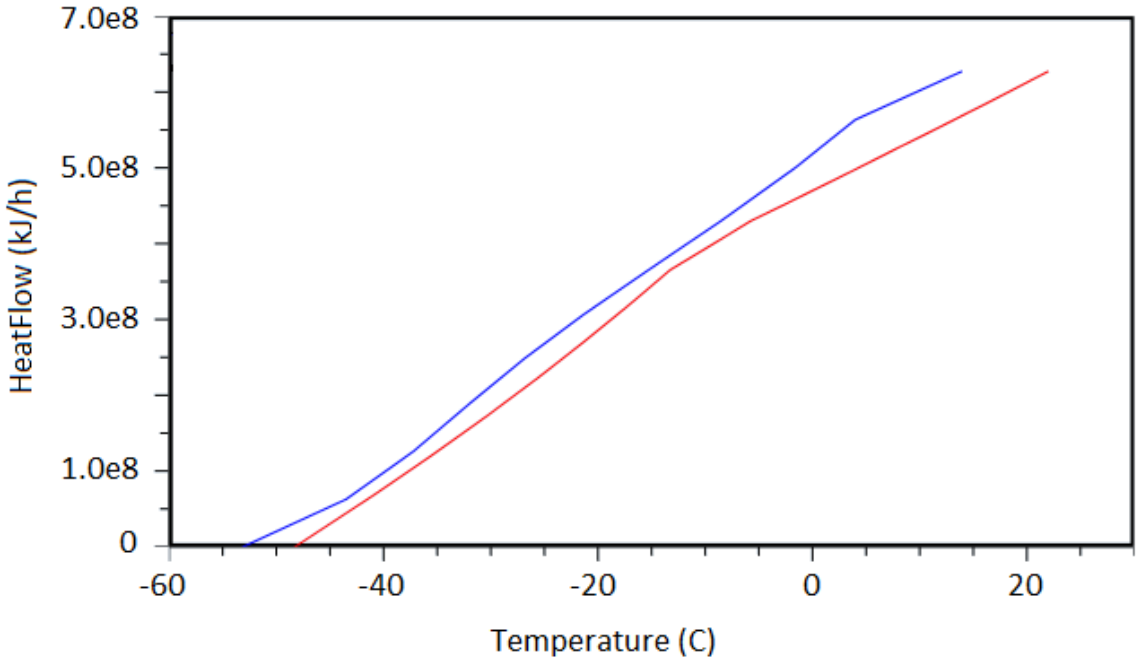

SWHE2-1/CMR CWHE Lower Bundle

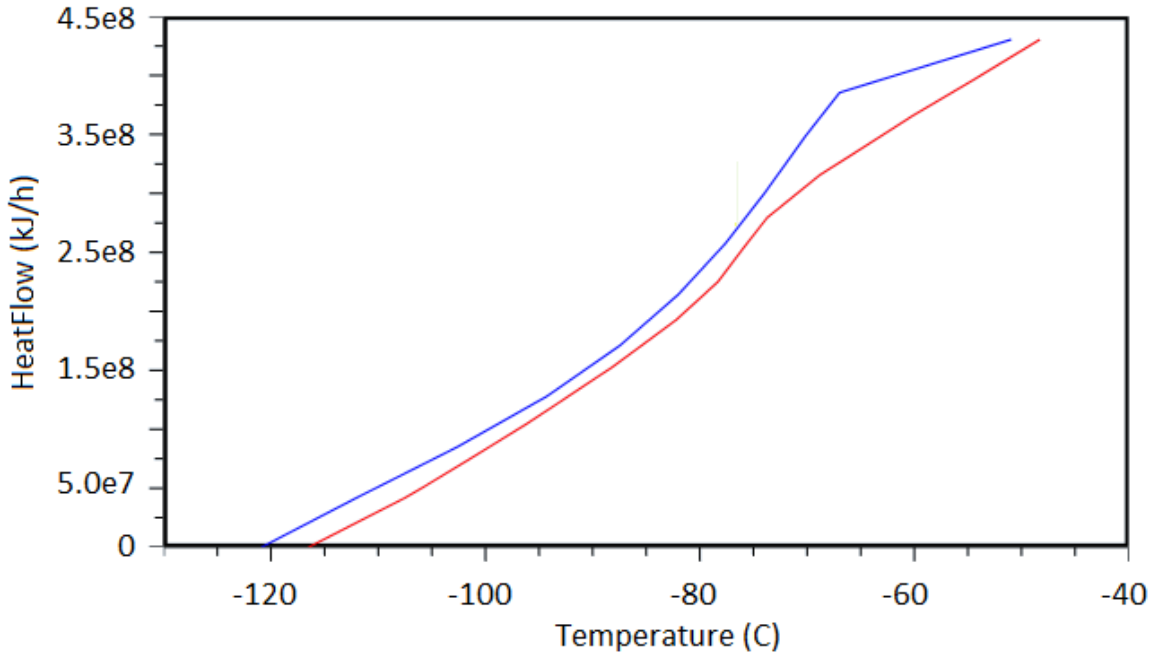

SWHE2-2/CMR CWHE Upper Bundle

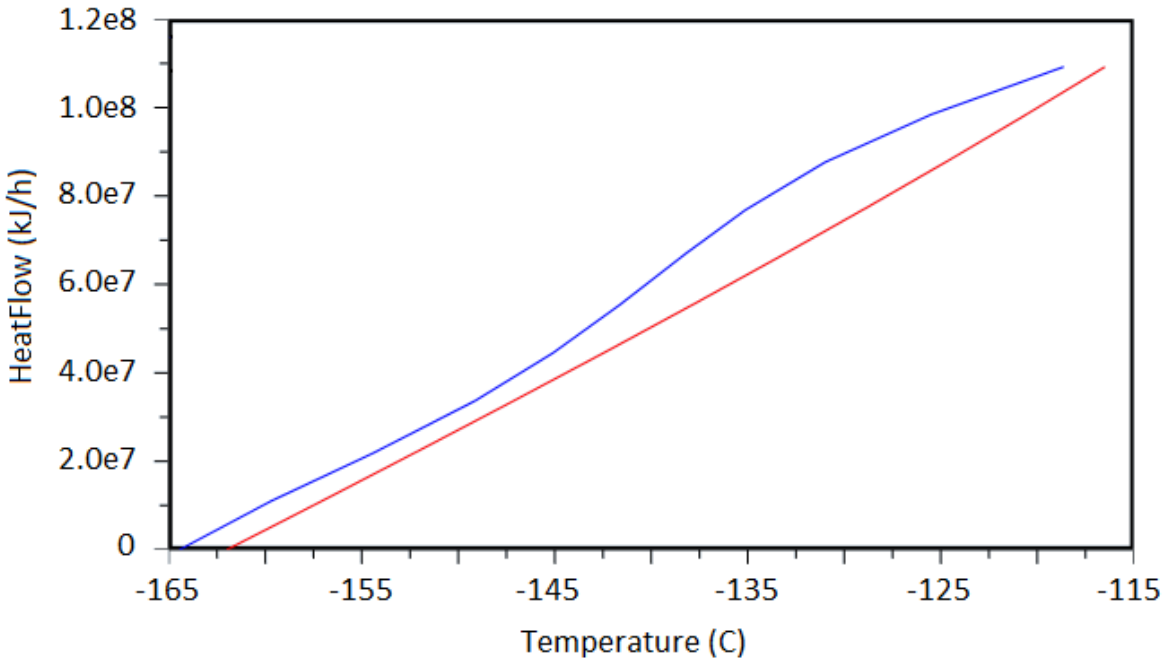

Appendix Q: Comparison between the Kusmaya (2012) and Optimized model by similar UA values from Chapter 8.2

Comparison between the pressure levels according to the optimization in Chapter 8.2 and the Kusmaya (2012) model

Tag Original/Optimized	Property	Unit	Kusmaya Model	Optimized Model
25/WMR3	Pressure	[Bar]	8.60	5.45
12/WMR5	Pressure	[Bar]	19.74	17.05
19/WMRVapor2	Pressure	[Bar]	46.95	30.00
35/CMR4	Pressure	[Bar]	4.68	3.17
40/CMR5	Pressure	[Bar]	14.50	16.47
42/CMR7	Pressure	[Bar]	23.00	25.08
44/CMR9	Pressure	[Bar]	36.00	35.20
30/CMR1	Pressure	[Bar]	55.00	44.94

Comparison between the composition in the WMR stream according to the optimization in Chapter 8.2 and the Kusmaya (2012) model

Property	Unit	WMR Stream Kusmaya Model	WMR Stream Optimized Model
Methane	Mole Fraction	0.1200	0.0350
Ethane	Mole Fraction	0.6850	0.6348
Propane	Mole Fraction	0.0789	0.1111
i-Butane	Mole Fraction	0.0614	0.0604
n-Butane	Mole Fraction	0.0547	0.1587
Molar Flow	[kgmole/h]	38030	31510
Mass Flow	[kg/s]	346	326

Comparison between the composition in the CMR stream according to the optimization in Chapter 8.2 and the Kusmaya (2012) model

Property	Unit	CMR Stream Original Model	CMR Stream Optimized Model
Nitrogen	Mole Fraction	0.1617	0.0868
Methane	Mole Fraction	0.3979	0.4211
Ethane	Mole Fraction	0.4304	0.4371
Propane	Mole Fraction	0.0100	0.0551
Molar Flow	[kgmole/h]	39860	36300
Mass Flow	[kg/s]	269	249.7

Appendix R: Initial Variables and Constraints concerning LNG production utilized to optimize the Kusmaya (2012) model

Initial variables and variable boundaries utilized in order to optimize the Kusmaya (2012) process

Tag	Property	Unit	Minimum	Initial Value	Maximum
Methane-WMR	Molar Flow	[kgmole/h]	750	1500	10000
Ethane-WMR	Molar Flow	[kgmole/h]	20000	27227	35000
Propane-WMR	Molar Flow	[kgmole/h]	3500	9900	15000
i-Butane-WMR	Molar Flow	[kgmole/h]	50	800	5000
n-Butane-WMR	Molar Flow	[kgmole/h]	50	800	5000
Nitrogen-CMR	Molar Flow	[kgmole/h]	2000	11000	15000
Methane-CMR	Molar Flow	[kgmole/h]	8000	15000	20000
Ethane-CMR	Molar Flow	[kgmole/h]	10000	24000	30000
Propane-CMR	Molar Flow	[kgmole/h]	500	1100	2000
WMR3	Pressure	[Bar]	1	6	20
WMR5	Pressure	[Bar]	8	16	25
WMRVapor2	Pressure	[Bar]	30	46	55
CMR4	Pressure	[Bar]	1	6	15
CMR5	Pressure	[Bar]	10	12.56	32
CMR7	Pressure	[Bar]	21	25.23	35
CMR9	Pressure	[Bar]	35.2	39.45	45
CMR1	Pressure	[Bar]	41	54.5	70
NG_Feed	Molar Flow	[kgmole/h]	24500	24670	35000

Process constraints utilized in order to optimize the Kusmaya (2012) process

Tag name	Restriction	Minimum	Initial value	Maximum
WMR1	Vapor Fraction	Empty	0	0
SWHE-1	Temperature approach	2	11.12	Empty
SWHE2-1	Temperature approach	2	5.23	Empty
SWHE2-2	Temperature approach	2	11.55	Empty
WMR4-DP1	Temperature approach	6	23.96	Empty
CMR4-DP2	Temperature approach	6	17.48	Empty
K-108	Power	13000	13036	14000
K-100	Power	26500	37219	27500
K-101	Power	22000	31755	23000
K-102	Power	31500	20549	32500
K-103	Power	16000	33200	17000
K-104	Power	15000	19192	16000